WHOI-2020-02

# Woods Hole Oceanographic Institution

# CALYPSO 2019 Cruise Report: Field Campaign in the Mediterranean

by

A. Mahadevan, E. D'Asaro, J. Allen, P. Almaraz García, E. Alou-Font, H. M. Aravind, P. Balaguer, I. Caballero, N. Calafat, A. Carbornero, B. Casas, C. Castilla, L. Centurioni, M. Conley, G. Cristofano, E. Cutolo, M. Dever, A. Enrique Navarro, F. Falcieri, M. Freilich, E. Goodwin, R. Graham, C. Guigand, B. Hodges, H. Huntley, S. Johnston, M. Lankhorst, P. Lermusiaux, I. Lizaran, C. Mirabito, A. Miralles, B. Mourre, G. Navarro, M. Ohmart, S. Ouala, T. Ozgokmen, A. Pascual, J-M. H. Pou, P.M. Poulain, A. Ren, D. Rodriguez Tarry, D. Rudnick, M. Rubio, S. Ruiz, I. Rypina, J. Tintore, U. Send, A. Shcherbina, M. Torner, G. S. Vieira, N. Wirth, and N. Zarokanellos

January 2020

## Technical Report

Funding was provided by the Office of Naval Research under Contract No. N000141613130.

**WHOI-2020-02**

**CALYPSO 2019 Cruise Report:**
**Field Campaign in the Mediterranean**

by

A. Mahadevan, E. D'Asaro, J. Allen, P. Almaraz García, E. Alou-Font, H. M. Aravind, P. Balaguer, I. Caballero, N. Calafat, A. Carbornero, B. Casas, C. Castilla, L. Centurioni, M. Conley, G. Cristofano, E. Cutolo, M. Dever, A. Enrique Navarro, F. Falcieri, M. Freilich, E. Goodwin, R. Graham, C. Guigand, B. Hodges, H. Huntley, S. Johnston, M. Lankhorst, P. Lermusiaux, I. Lizaran, C. Mirabito, A. Miralles, B. Mourre, G. Navarro, M. Ohmart, S. Ouala, T. Ozgokmen, A. Pascual, J-M. H. Pou, P.M. Poulain, A. Ren, D. Rodriguez Tarry, D. Rudnick, M. Rubio, S. Ruiz, I. Rypina, J. Tintore, U. Send, A. Shcherbina, M. Torner, G. S. Vieira, N. Wirth, and N. Zarokanellos

Woods Hole Oceanographic Institution
Woods Hole, Massachusetts 02543

January 2020

## Technical Report

Funding was provided by the Office of Naval Research under Contract No. N000141613130.



**Approved for Distribution:**

**Amy Bower, Chair**

Department of Physical Oceanography

# CALYPSO 2019 Cruise Report

Field Campaign in the Mediterranean

March 28 - April 11, 2019

A. Mahadevan, E. D'Asaro

J. Allen, P. Almaraz García, E. Alou-Font, H. M. Aravind, P. Balaguer, I. Caballero, N. Calafat, A. Carbornero, B. Casas, C. Castilla, L. Centurioni, M. Conley, G. Cristofano, E. Cutolo, M. Dever, A. Enrique Navarro, F. Falcieri, M. Freilich, E. Goodwin, R. Graham, C. Guigand, B. Hodges, H. Huntley, S. Johnston, M. Lankhorst, P. Lermusiaux, I. Lizarán, C. Mirabito, A. Miralles, B. Mourre, G. Navarro, M. Ohmart, S. Ouala, T. Ozgokmen, A. Pascual, J-M. H. Pou, P.M. Poulain, A. Ren, D. Rodríguez Tarry, D. Rudnick, M. Rubio, S. Ruiz, I. Rypina, J. Tintoré, U. Send, A. Shcherbina, M. Torner, G. S. Vieira, N. Wirth, and N. Zarokanellos

# Contents

Simón Ruiz (IMEDEA) and Ananda Pascual (IMEDEA)
Isabel Caballero (ICMAN-CSIC), Gabriel Navarro (ICMAN-CSIC) and Nikolaos Zarokanellos (SOCIB)

# Chapter 1

# Summary

Amala Mahadevan (WHOI) and Eric D'Asaro (UW)

## 1.1 Overview

This cruise aimed to identify transport pathways from the surface into the interior ocean during the late winter in the Alborán sea between the Strait of Gibraltar (5°40′W) and the prime meridian. Theory and previous observations indicated that these pathways likely originated at strong fronts, such as the one that separates salty Mediterranean water and the fresher water inflowing from the Atlantic. Our goal was to map such pathways and quantify their transport. Since the outcropping isopycnals at the front extend to the deepest depths during the late winter, we planned the cruise at the end of the Spring, prior to the onset of thermal stratification of the surface mixed layer.

More specifically, our strategy was to locate regions roughly 100 km in extent using operational models and satellite data, survey these regions using arrays of surface drifters, the ship's ADCP underway system, and an underway CTD system (UCTD) to locate submesoscale fronts where subduction of surface water into the interior was most likely to occur. We would then measure subduction, as well as the surrounding conditions, at these locations using a suite of specialized tools. These included CTD sections across the fronts measuring biological tracers of surface waters, a towed V-Wing chain making very high resolution (10's of meters) T, S and velocity sections across the front, a freely drifting Wirewalker making similar measurements, small scale surface drifter arrays, and 3 Lagrangian floats designed to follow the three-dimensional trajectories of water parcels.

This strategy was to be implemented 3-4 times during the 14 day cruise, but the full suite of measurements was only deployed once, due to a variety of operational constraints described below. Preliminary results include:

1. The combination of large numbers of drifters with ship surveys proved highly effective in mapping the regional circulation and the location of fronts, with the drifters providing realtime guidance for the ship sections. Figure 1.1 shows an example of a mapped circulation as shown in our realtime display.

2. The measured features were poorly predicted by regional operational models and products, providing an opportunity to make more quantitative comparisons.

3. Small scale ship surveys and drifter arrays resolved temperature and salinity gradients, vorticity, strain and possibly divergence on kilometer scales at the fronts, allowing direct comparison with submesoscale models.

4. Vorticity and strain rate of the order of the planetary vorticity, $f$, occurred frequently, clearly demonstrating the existence of submesoscale dynamics. The mesoscale environment was thoroughly mapped.

5. At fronts, isopycnals commonly extended from the surface to depths of 100 m or more, indicating that subduction along isopycnals to these depths is possible in this season, unlike what was observed in a previous late Spring 2018 cruise.

6. Biogeochemical (oxygen and chlorophyll) and physical (temperature anomaly) tracers measured across these fronts indicated regions of subduction at some fronts. More sophisticated genomic tracers and measurements of oxygen consumption rates may lead to estimates of subduction rates. These data may allow testing of dynamical hypotheses on subduction rates at these fronts.

7. The density contrast across the fronts was largely due to the salinity contrast. Most fronts showed a surface density maximum, near the isopycnal outcrop, forming a dense filament in the 20-50m deep mixed layer.

8. A short deployment of water-following Lagrangian floats showed subduction to the base of the 50 m deep mixed layer beneath a layer of lighter fresher water, confirming that subduction does indeed occur here during this season.

## 1.2 Operational Issues

Despite these successes, the cruise suffered from several operational limitations. We had originally planned to use the NATO ship *Alliance*, as in 2018. However, Alliance suffered mechanical failures and could not be ready in time for the cruise. Instead, we used the IFREMER ship *N/O Pourquoi Pas?* chartered on short notice. The vessel and its crew were very capable, but, we could not send the shipping container with our equipment until very close to the deadline for shipping. The shipment was then unexpectedly delayed due to a change in the container ship's schedule and did not reach Almería, our port, until April 4, halfway through the cruise. Much of our equipment was thus not available for the first half

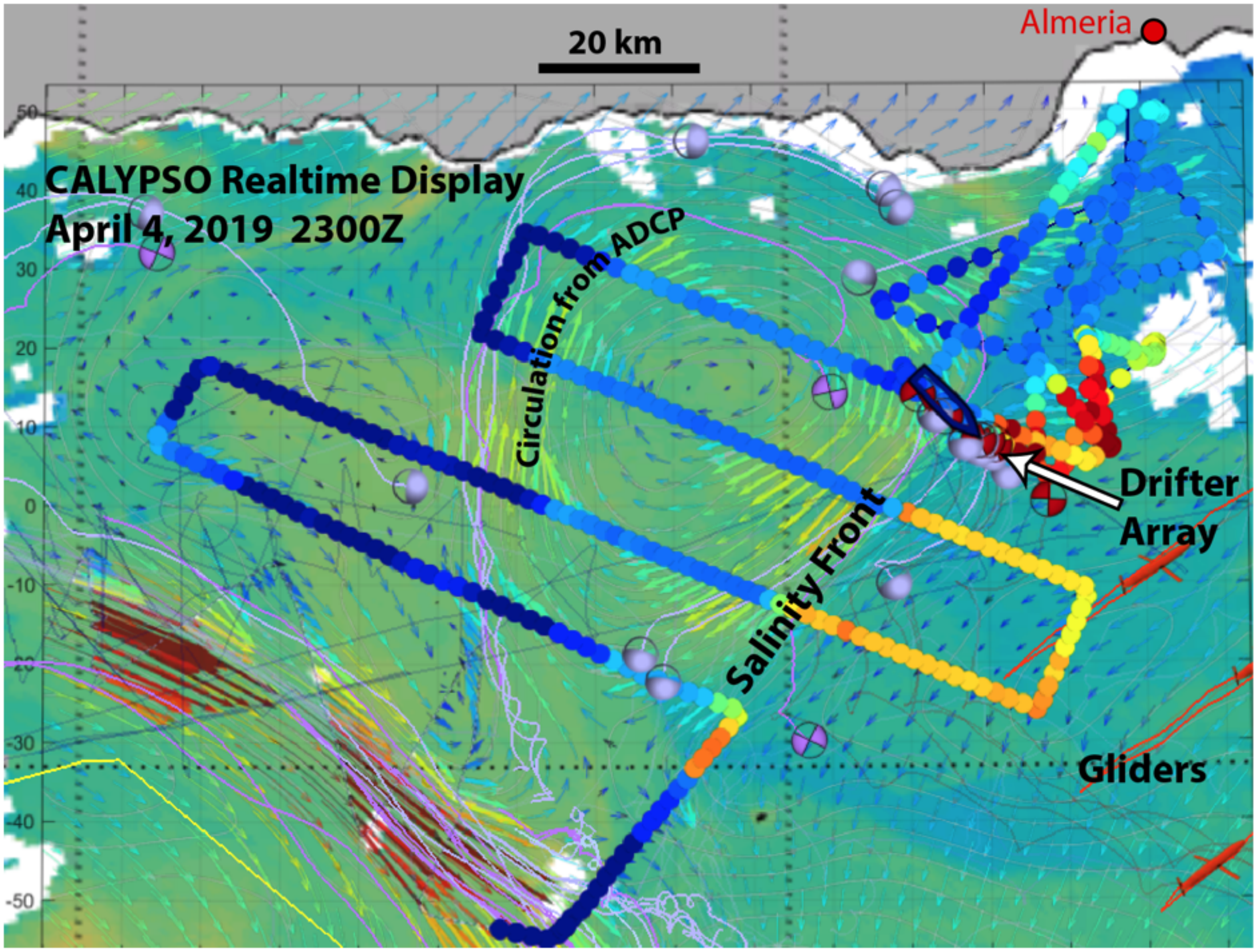


Figure 1.1: CALYPSO realtime display showing a strong salinity front (colored dots are salinity from the ship's flowthrough system) separating saltier Mediterranean water to the east and fresher, Atlantic influenced water to the west as mapped by the ship. The front is formed by the confluence of these two water masses just south of Spain, as shown by the objectively mapped surface circulation (colored arrows) from the ship's ADCP. At this time, a small-scale array of drifters has just been deployed at the front, just to the west of the glider array. A set of drifters (trajectories in grey/lilac) released a few days prior in the west, map the fastest flow on the northeast flank of the Western Alboran Gyre (WAG). The Eastern Alboran Gyre (EAG) is not set set up at this time. The background is an ocean color image from April 4 that also shows the front.

of the cruise. Additionally, we could not apply for diplomatic clearance within the normal 6 month lead time. Clearance was approved for Spain in time for the cruise, but Moroccan clearance only became available for the last few days, too late to be useful. Algeria refused clearance. We were thus limited to operations in Spanish waters. Since most Lagrangian trajectories originating in Spanish waters and within the strong currents associated with fronts enter Moroccan or Algerian waters within a few days, this significantly limited our deployment opportunities. As a result of these constraints, we were only able to make one full deployment of our equipment at a less than optimal site.

Additional problems were caused by unusually strong and persistent winds (Fig. 1.2). Climatologically, winds over 10 m/s occur less than 15% of the time in this season; they occurred about half the time during the cruise. The large size and deep draft of *N/O Pourquoi Pas?* made it an unusually stable platform, allowing underway CTD operations to continue despite these conditions. However, the ship's large freeboard and hull shape made over-the-side recovery of the floats or Wirewalker impractical and small-boat operations were not possible in high winds. This prevented us from deploying these key instruments most of the time.

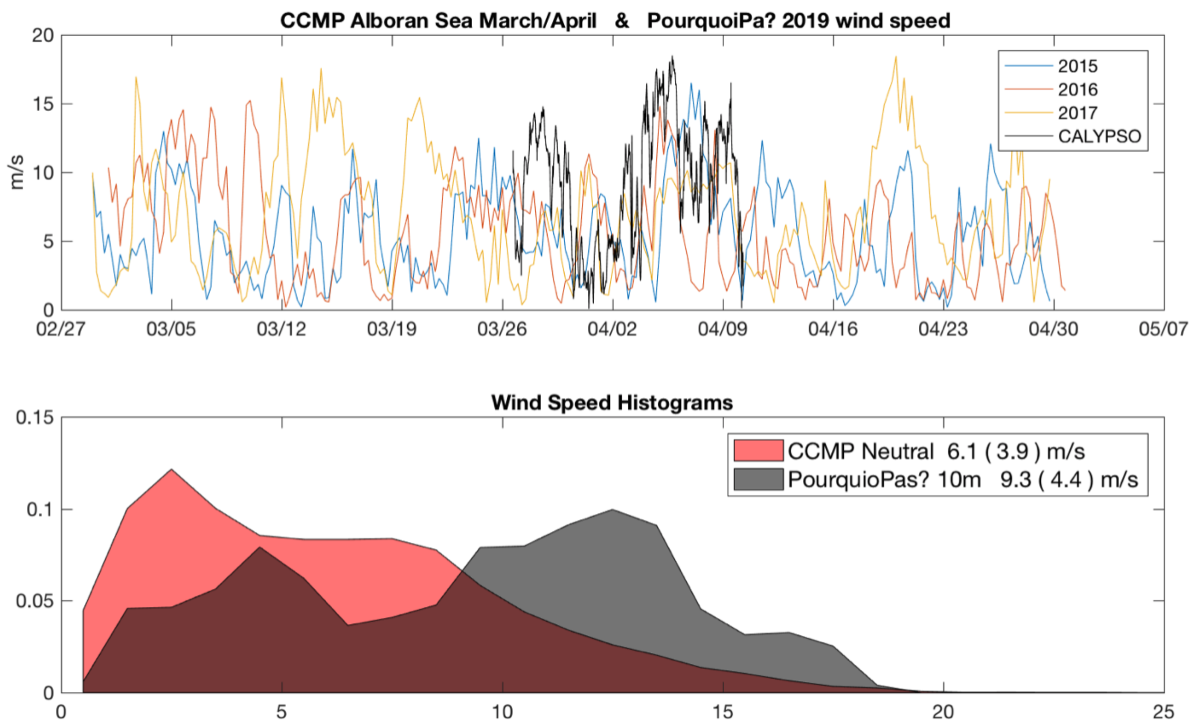


Figure 1.2: Top: Measured wind speed during the 2019 CALYPSO cruise, adjusted from 30 m to 10 m assuming neutral conditions, compared to CCMP winds for the Alboran Sea for 2015, 2016 and 2017. Lower Panel: Histograms of CCMP winds compared with the cruise. Wind speed (m/s) is on the $x$-axis.

## 1.3 Science Crew and Instrumentation

The science crew included the following members:

| | | |
|---|---|---|
| Amala Mahadevan | Woods Hole Oceanographic Institution | amala@whoi.edu |
| Eric D'Asaro | University of Washington, APL | dasaro@apl.washington.edu |
| Michael Ohmart | University of Washington, APL | ohmart@uw.edu |
| Andrey Shcherbina | University of Washington, APL | shcher@uw.edu |
| Tamay Ozgokmen | University of Miami, RSMAS | tozgokmen@rsmas.miami.edu |
| Cedric Guigand | University of Miami, RSMAS | cguigand@rsmas.miami.edu |
| Raymond Graham | Woods Hole Oceanographic Institution | rgraham@whoi.edu |
| Benjamin Hodges | Woods Hole Oceanographic Institution | bhodges@whoi.edu |
| Mara Freilich | MIT/Woods Hole Oceanographic Institution | mfreilich@whoi.edu |
| Mathieu Dever | Woods Hole Oceanographic Institution | mdever@whoi.edu |
| Margaret Conley | Woods Hole Oceanographic Institution | conlemar@oregonstate.edu |
| Eugenio Cutolo | IMEDEA - CSIC | e.cutolo@imedea.uib-csic.edu |
| Daniel Rodríguez Tarry | IMEDEA - CSIC | drtarry@imedea.uib-csic.edu |
| Said Ouala | IMT-Atlantique | said.ouala@imt-atlantique.fr |
| Benjamín Casas | IMEDEA - CSIC | benjamin.casas@csic.edu |
| Noemi Calafat | IMEDEA | noemi.calafat101@alu.ulpgc.es |
| Joan Horrach Pou | IMEDEA | - |
| Eva Alou-Font | SOCIB | ealou@socib.es |
| Andrea Cabornero | SOCIB | acabornero@socib.es |
| Nikolaus Wirth | SOCIB | nwirth@socib.es |
| Isabel Caballero | ICMAN - CSIC | isabel.caballero@icman.csic.es |
| Angélica Enrique Navarro | ICMAN - CSIC | angelica.enrique@csic.es |
| Pablo Almaraz García | ICMAN - CSIC | pablo.almaraz@csic.es |
| Pierre-Marie Poulain | CMRE | Pierre-Marie.Poulain@cmre.nato.int |
| Gino Cristofano | OGS | gcristofano@inogs.it |
| Alice Ren | Scripps Institution of Oceanography, UCSD | aren@ucsd.edu |
| Evan Goodwin | Scripps Institution of Oceanography, UCSD | emrandallgoodwin@ucsd.edu |
| Shaun Johnston | Scripps Institution of Oceanography, UCSD | tmsjohnston@uscd.edu |
| Francesco Falcieri | CNR - ISMAR | francesco.falcieri@ve.ismar.cnr.it |
| José-Miguel Moll Kraft | EMS | ems@ems-sistemas.com |
| Josep-María Erta Montejo | EMS | ems@ems-sistemas.com |
| Mauro Puig | EMS | ems@ems-sistemas.com |
| Aravind Harilal Meenambika | Northeastern University | a.harilalmeenambika@northeastern.edu |
| Guilherme Salvador-Vieira | Northeastern University | g.salvadorvieira@northeastern.edu |

The following list provides contact information for the chief scientists and scientists who provided instrumentation:


| | | |
|---|---|---|
| Chief Scientists | Eric D'Asaro, | dasaro@apl.washington.edu, |
| | Amala Mahadevan | amala@whoi.edu |
| UCTD | Shaun Johnston (Leg 1), | tmsjohnston@uscd.edu, |
| | Tom Farrar (Leg 2) | jfarrar@whoi.edu |
| EcoCTD | Amala Mahadevan | amala@whoi.edu |
| Water Samples | Joaquin Tintore/John Allen, | jtintore@socib.es/jallen@socib.es, |
| | Amala Mahadevan | amala@whoi.edu |
| Drifters: | | |
| SVP | Luca Centurioni | lcenturioni@ucsd.edu |
| Code | Pierre-Marie Poulain | Pierre-Marie.Poulain@cmre.nato.int |
| Carthe | Tamay Ozgokmen | tozgokmen@rsmas.miami.edu |
| Layered | Irina Rypina | irypina@whoi.edu |
| Profiling floats | Pierre-Marie Poulain | Pierre-Marie.Poulain@cmre.nato.int |
| V-Wing | Tom Farrar | jfarrar@whoi.edu |
| Wirewalker | Melissa Omand | momand@uri.edu |
| Lagrangian Float | Eric D'Asaro | dasaro@apl.washington.edu |


## 1.4 Cruise Narrative

The cruise was organized into 2 legs, the first without the equipment in the container and the second, with the equipment after the container was picked up in Almería.

### Leg 1

For leg 1, only the ship's ADCP and surface drifters were available. To make detailed surveys of the mesoscale and submesoscale circulation, Shaun Johnston and the Scripps science party moved their UCTD operations from R/V SOCIB to the *N/O Pourquoi Pas?* Eva Alou from SOCIB was able to provide much of what was needed to carry out the water sampling for flow cytometry and DNA sequencing. The CSIC lab in Almería provided necessary consumables. With this equipment, we were able to make detailed surveys of the mesoscale and submesoscale circulation using the UCTD, the ship's ADCP and the drifters that were already on the ship. We placed CTD sections at strategic places within this context as planned. Thus, Leg 1 emphasized biological sampling of the fronts along with the mapping of the circulation field, based on which we planned to choose the subduction experiment sites in Leg 2. Figure 1.3 shows the circulation and surface density during Leg 1.

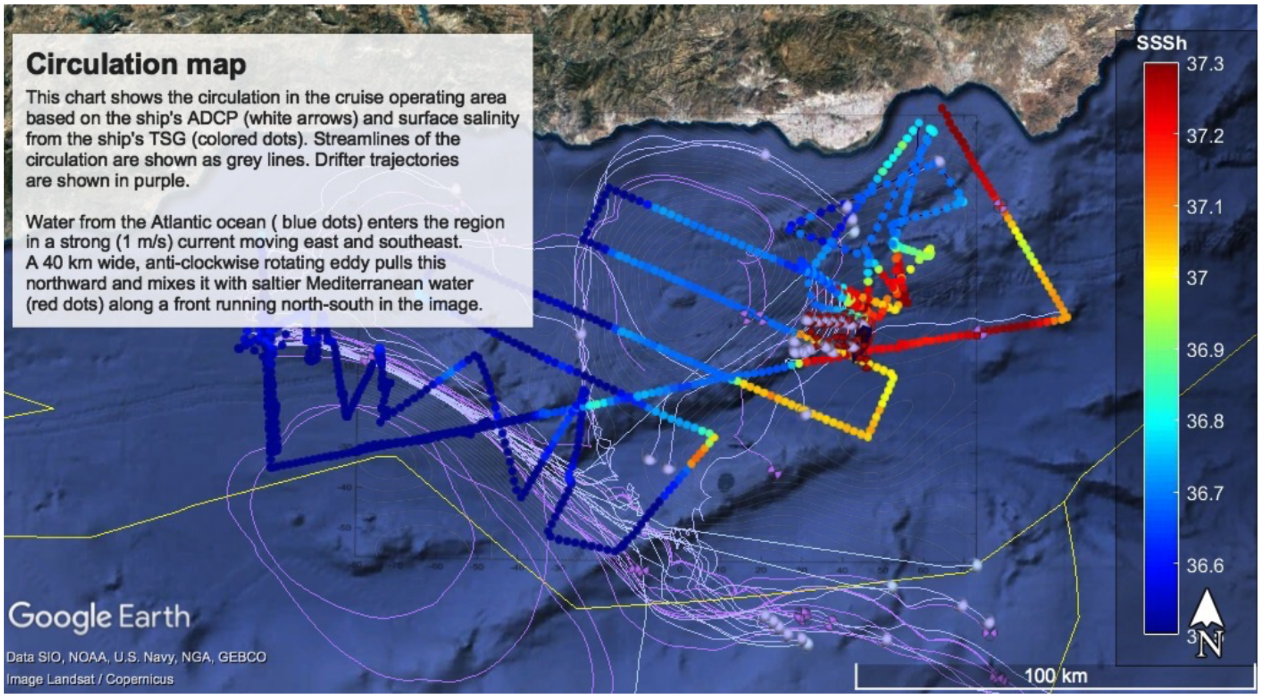


Figure 1.3: Surface salinity (colors) along ship track and drifter trajectories during Leg 1. The Western Alboran Gyre (WAG) is in the lower left quadrant of the figure. The country EEZ boundaries are shown in yellow. Ship operations were restricted to the Spanish EEZ.

***March 28***: We left Almería and surveyed eastward to check for the existence of an Almería-Oran front. Consistent with altimetry, no front was found, so we surveyed westward to check for the existence of an Eastern Gyre feeding the front. This was not found, so we proceeded westward deploying drifters. A strong eastward current was found on the northern edge of the Western Alboran Gyre (WAG) as expected from altimetry. A salinity front formed the northern boundary of the fresher Atlantic water in the WAG.

***March 29-April 1***: We surveyed the eastward WAG jet as shown in Figure 1.4. A line of drifters was released across the jet at the western edge. The ship followed the drifters as they advected eastward, making two CTD sections across the front. The front showed deep diving isopycnals (Figure 1.5) and a density maximum at the isopycnal outcrop.

***April 1-4***: Drifters released on the initial survey suggested a gyre north of the WAG and the E-W section and a satellite color image showed a stronger front here, which was close to Almería and far from the Moroccan and Algerian EEZ. We thus surveyed this region with a lawnmower pattern and then did a more detailed survey in the southward flowing jet (Figure 1.6). This showed a clear salinity front formed by the convergence of two water masses at the northern end. The overall pattern of the WAG eddy to the southwest, a northern eddy south of Almería and a coastal flow from the east formed an interesting pattern of mixing and frontogenesis. The CTD and UCTD sections showed evidence of subduction across the front, with high variability in temperature along outcropping isopycnals. This eddy seemed to be a well-formed and well-surveyed structure by the time we returned to Almería and we

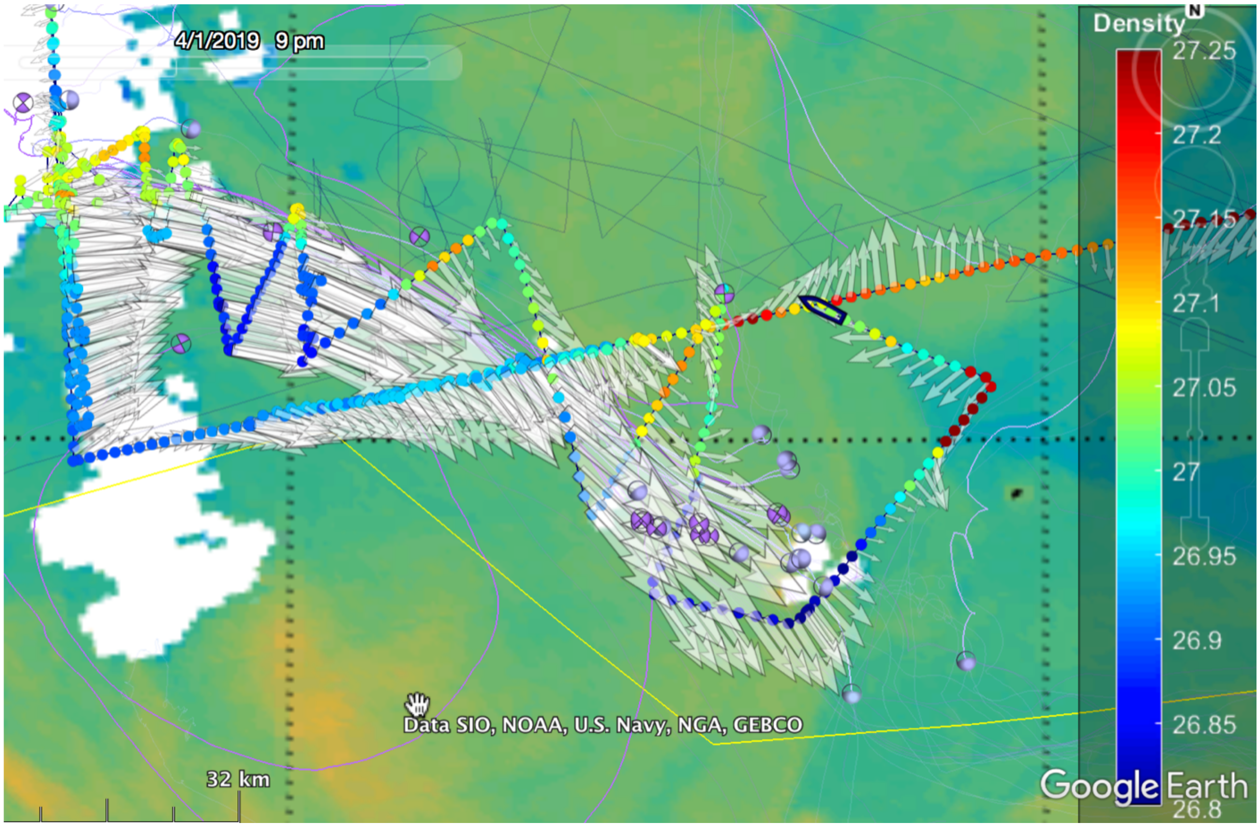


Figure 1.4: Leg 1. March 29-April 1. Colors show density from the TSG along the ship track. Arrows show the velocity from the ship's ADCP at ∼8 m depth. Circles show drifter locations with thin lines showing drifter trajectories.

planned to work in this region for Leg 2.

During this leg, strong winds from the east persisted until March 31, followed by 2 days of relative calm (April 1-2). April 1 was a beautiful day and we flew the drone and took pictures.

***April 4 – Port call***: We set for Almería on April 3, but the container was delayed until April 4, so we did a few more hours of surveying. We docked at 8am on April 4. The Scripps UCTD was moved to the R/V SOCIB along with the Scripps team and two Spanish students joined us. The container was unpacked and the equipment set up. We left Almería at 2pm.

## Leg 2

***April 5-6***: We returned to make detailed studies of the region that we had just surveyed starting with a small-scale drifter line (Figure 1.7). The wind increased from the west (having entirely switched direction), at times exceeding 15 m/s and exciting strong near-inertial oscillations. We were not able to put any equipment out because the weather conditions would not allow us to retrieve them. At times, the weather was so severe that even UCTD

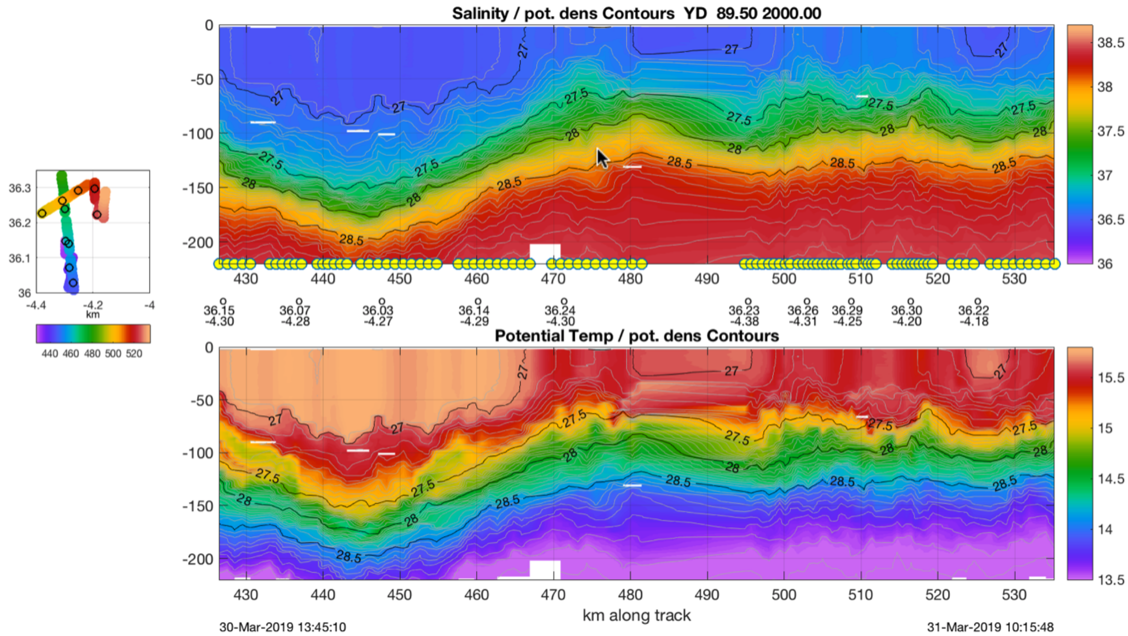


Figure 1.5: A UCTD section across the northern flank of the WAG. The 27 kg m$^{-3}$ isopycnal outcrops on the dense side of the front and extends to a depth of 70 m within on the light side of the front, providing a potential pathway from the surface to depth.

operations had to stop. The forecast showed no change in this pattern for the remainder of the cruise, but the forecast for the Western Alboran looked much better in comparison, so we decided to move our operations there.

***April 6-8***: We first resurveyed the northern edge of the WAG (Fig. 1.8) with the goal of finding a good location to make subduction measurements. The strong inertial currents significantly contaminated the ADCP currents, so many drifters were released along the track (Fig. 1.8). These showed an eastward coastal current, probably associated with separation from a nearby cape (which we ignored), and the northern edge of the WAG, slightly displaced from what we saw previously (e.g. Fig. 1.3 and 1.4). A strong front appeared to form on the northeastern side of this jet, but deployment in this region was hazardous, as the strong currents would advect into the Moroccan EEZ within a day. We thus chose to deploy 1-2 days upstream from here, with the hope of seeing subduction associated with the frontogenesis in this region.

Science measurements were stopped at 9am on April 10 and the assets recovered. We arrived in Almería on the morning of April 11.

***April 8-10***: After an initial CTD section, we deployed the Wirewalker, the multi-layered WHOI drifter array and two Lagrangian floats and a drifter array. Shortly after the deployment, we received permission to enter the Moroccan EEZ. The ship surveyed across this array following one of the drifters, pausing for a second CTD line and a final drifter deployment (Figure 1.9).

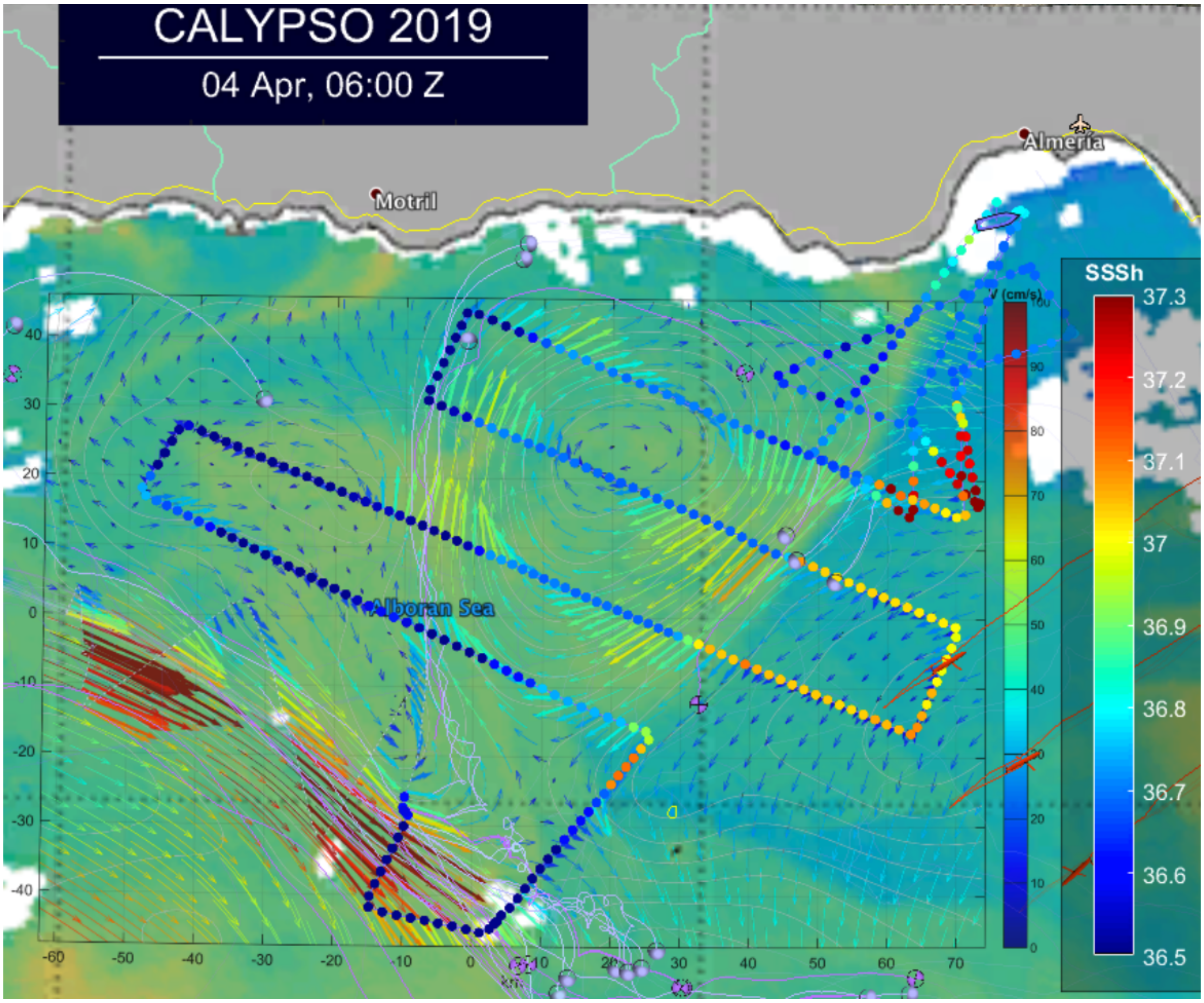


Figure 1.6: Surveys April 1-4. Colored dots are sea surface salinity using right color bar. Arrows show mapped near-surface ADCP velocity with color indicating speed using smaller color bar. Circles show drifter positions with lines showing trajectories. Background is ocean color image. A salinity front runs SW to NE across the image formed by a confluence of saltier and fresher water at the northern end and a diffluence at the southern end. This is supported by the pattern of three mesoscale eddies.

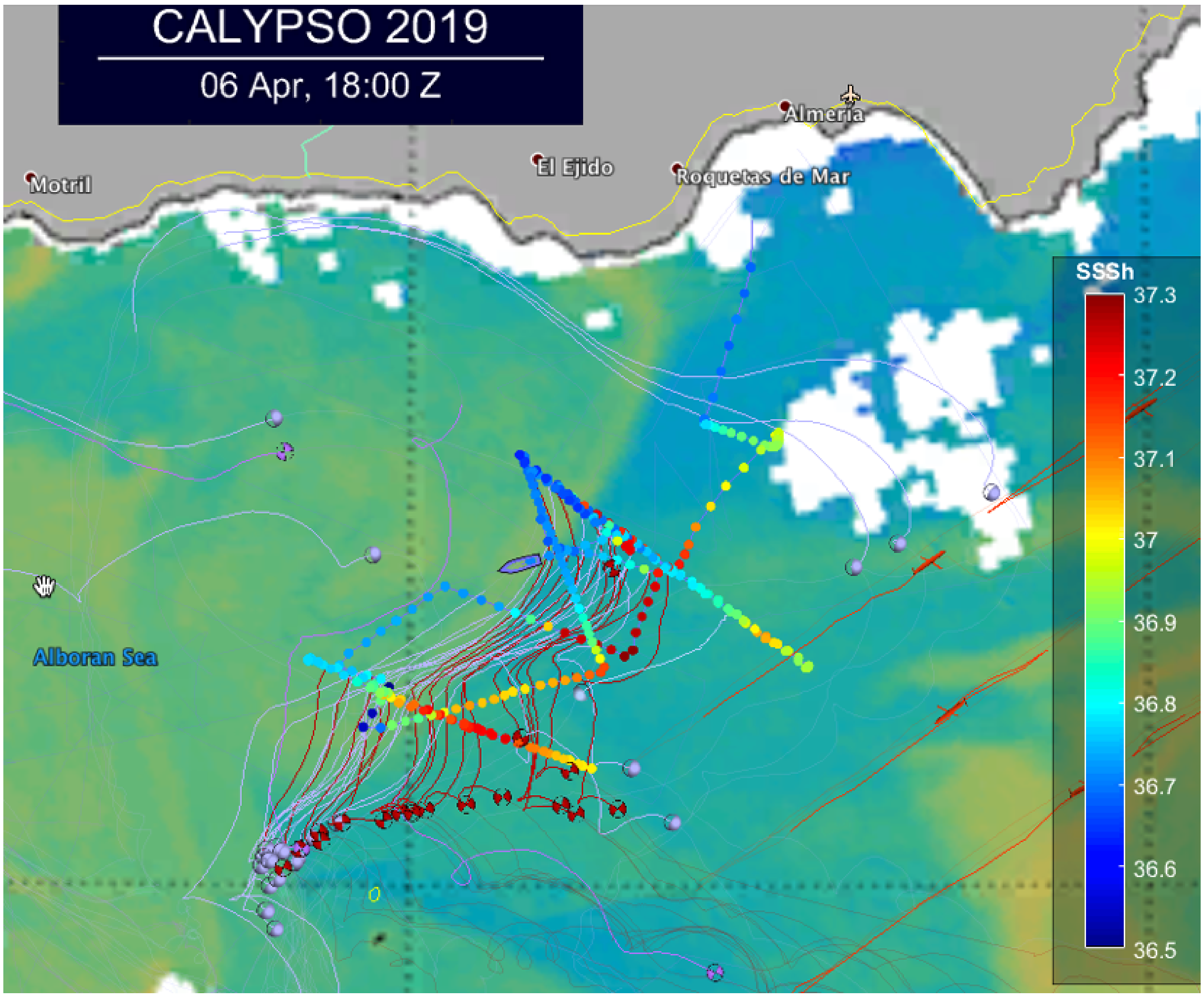


Figure 1.7: Operations on April 5-6. A drifter array moved southward along the front, showing strong near-inertial oscillations. Ship surveys were limited by high winds.

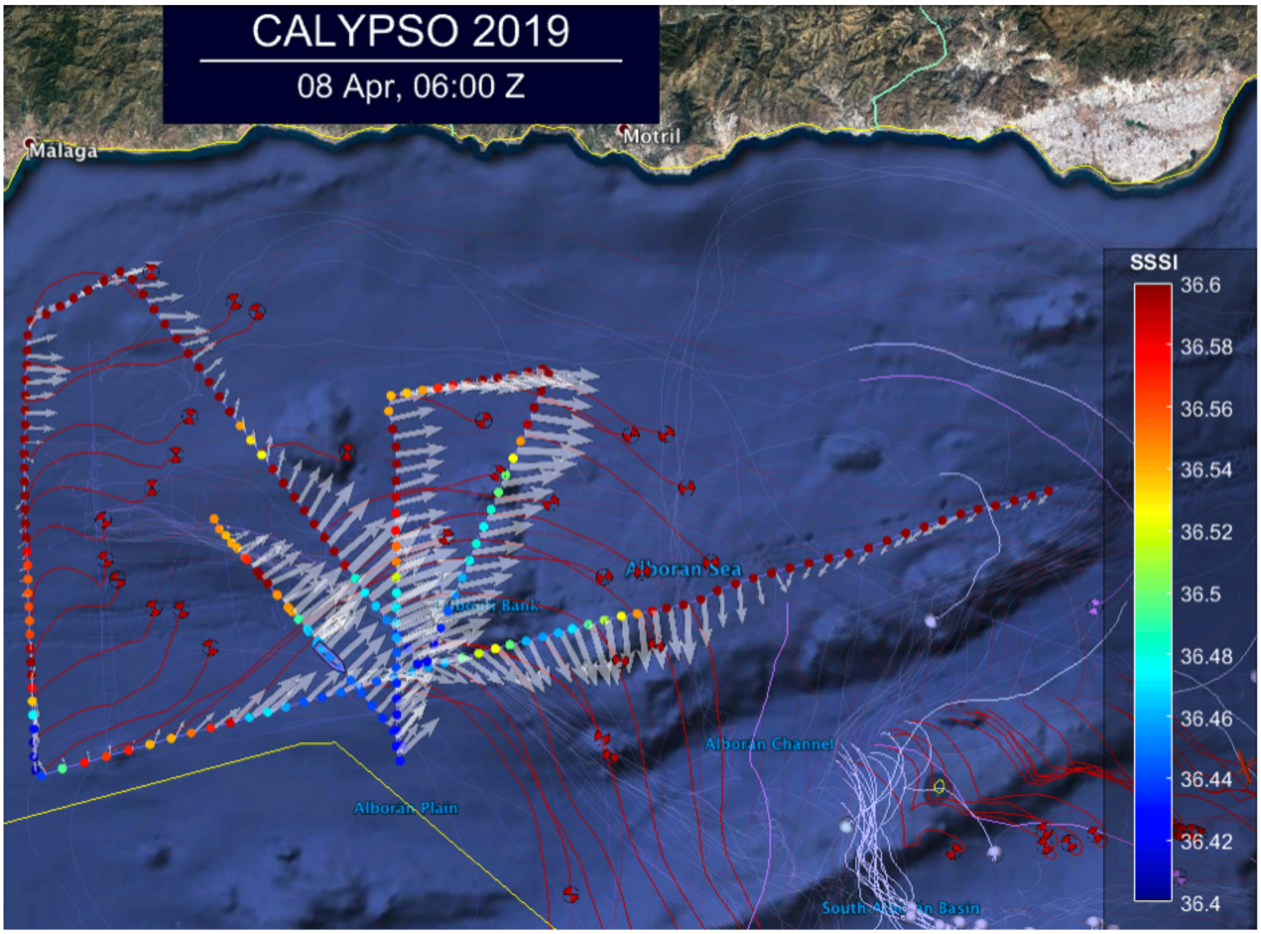


Figure 1.8: April 5-8 survey showing surface salinity, near-surface ADCP velocity and drifter trajectories. Yellow line is the Moroccan EEZ boundary.

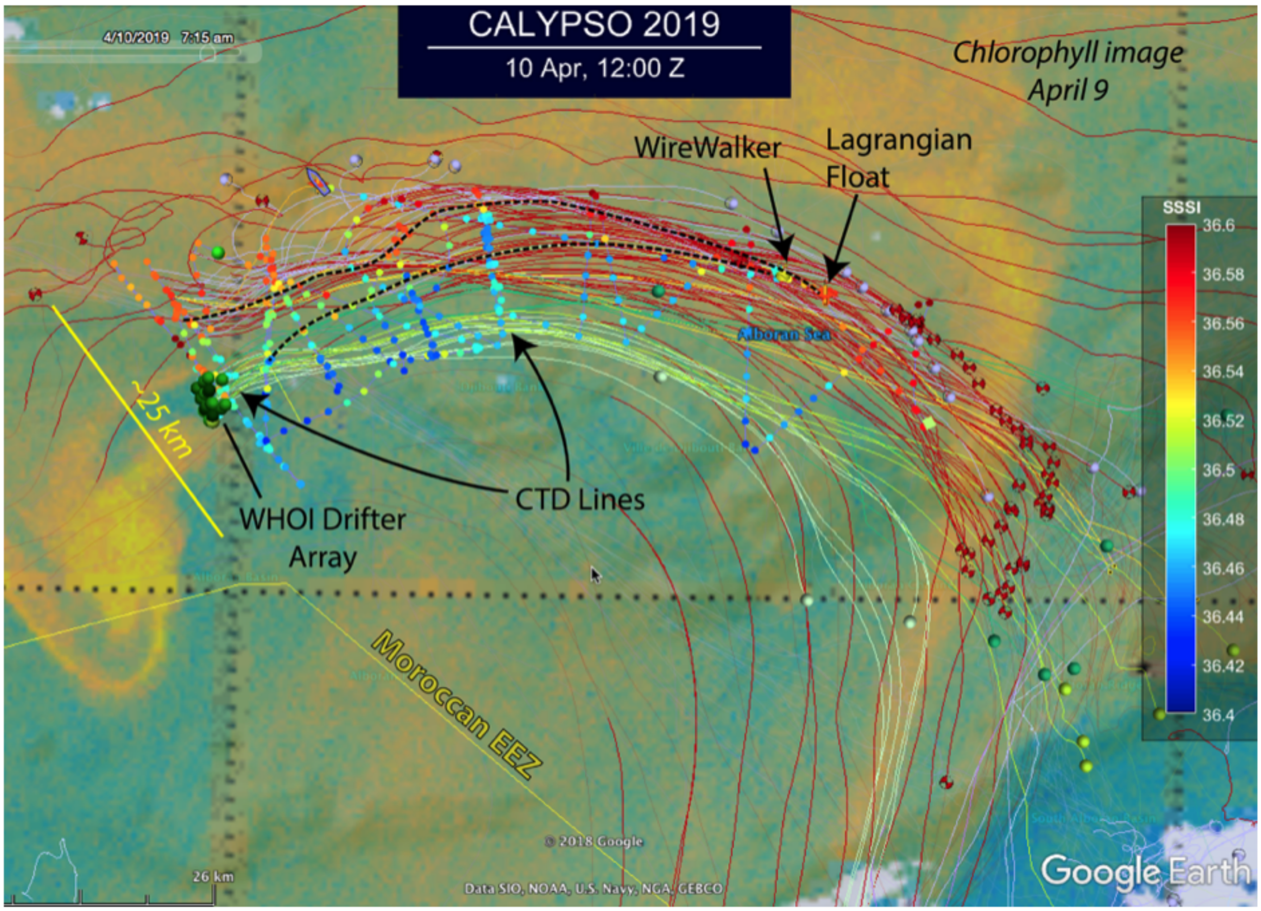


Figure 1.9: Subduction deployment April 8-10. Multiple drifter arrays, a drifting Wirewalker mooring, two Lagrangian floats and CTD and UCTD surveys across these arrays were used to study subduction along a density front.

# Chapter 2

# UCTD and EcoCTD operations

Mathieu Dever (WHOI)

The cruise was divided into two legs: Leg 1 spanned the time period from March 28, 2019 to April 4th, while Leg 2 covered the time period between April 4th and April 11th. The two legs were separated by a port call in Almería (Spain) to pick up a delayed container that carried both the EcoCTD and UCTD equipment. Shaun Johnston (Scripps) transferred UCTD operations from R/V SOCIB to N/O Pourquoi Pas ? for leg 1. A metal plate to secure the UCTD winch to the deck of the *N/O Pourquoi Pas?* was ordered in Almería and delivered on mobilization day (March 27th). This UCTD system was returned to the R/V SOCIB on April 4th, once the container was picked up in Almería. For the second leg of the cruise, the UCTD system lent by Tom Farrar (WHOI) was then mounted onto the deck of the *N/O Pourquoi Pas?* for the remainder of the cruise. The same UCTD winch was used for EcoCTD operations. Combining UCTD and EcoCTD operations, 1,810 profiles were collected along 72 transects (see Table 2.2).

## 2.1 UCTD operations

### Modus operandi

The UCTD winch was operated in tow-yo mode, where no line is spooled around the UCTD tail spool [*Rudnick and Klinke*, 2007]. The UCTD probe was first allowed to free-fall for 90 seconds, which corresponds to a depth ranging between 200 and 250 dbar, depending on the profile. The probe was then reeled back to the ship using a winch. Once close to the ship's stern, the probe was released again for another 90 seconds. Each profiling cycle took about 5 min, which corresponds to a horizontal resolution of about 1 km at a ship speed of 6 knots.

After 10 profiles (about 1 hour), or at the end of a section, the probe was recovered and swapped for another UCTD probe, to allow for data download. Data download took about 40 min, and data was made available to the science party immediately afterwards to inform the sampling plan.

## First leg

The UCTD winch was mounted in the middle of the ship's fan tail, and operated around-the-clock by 3 watches: (1) Shaun Johnston (Watch Leader), Ray Graham, and Joan Horrac; (2) Ben Hodges (Watch Leader) and Alice Sonya; (3) Evan Goodwin (Watch Leader), Nikolaus Wirth, and Noemi Calafat. The UCTD was used whenever the ship was underway. A total of 1082 profiles over 30 sections were collected over the first leg (Figure 2.1). Three different probes provided by Shaun Johnston were used alternatively (see Table 2.1).

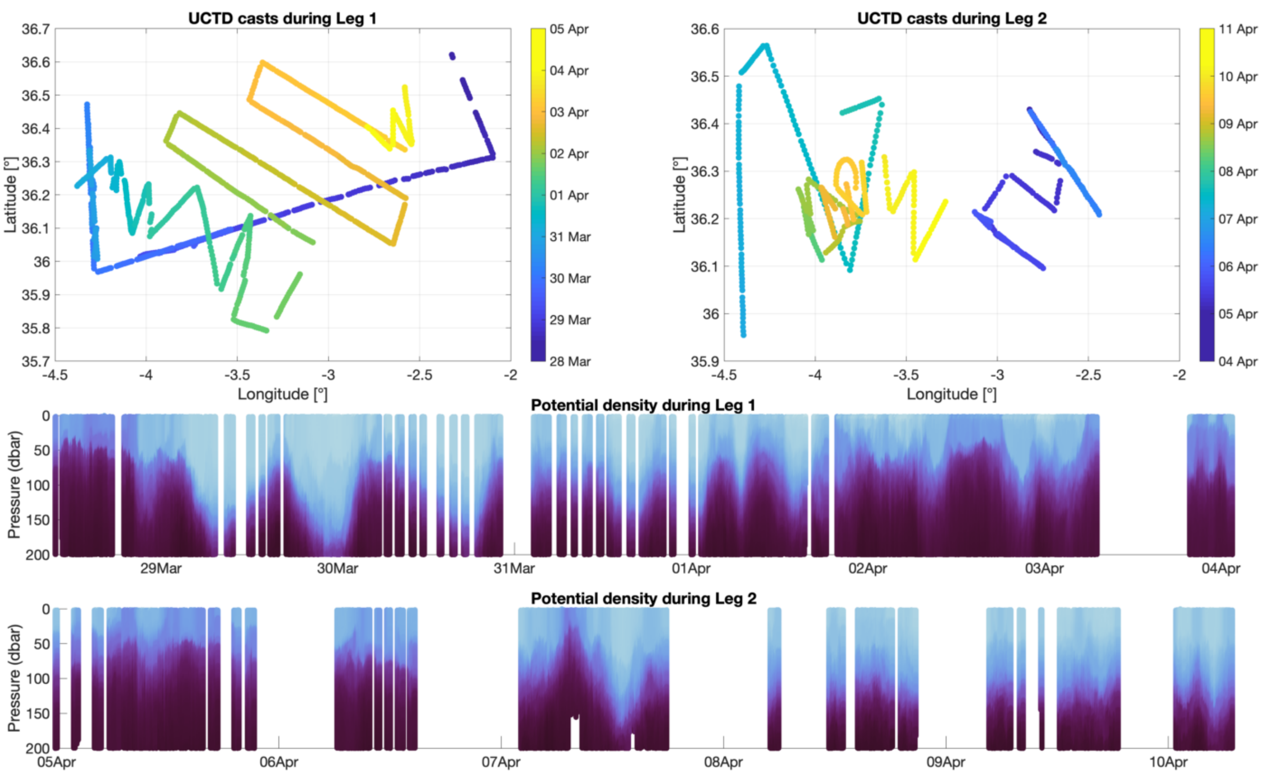


Figure 2.1: [Top] Location of UCTD casts during cruise legs 1 and 2. [Bottom] Time series of potential density as measured from the UCTD probe during cruise legs 1 and 2.

## Second leg

The UCTD winch was mounted in the middle of the port side of the ship's fan tail, to accommodate the V-Wing installed on the starboard side of the fan tail. The objective was

Table 2.1: Serial numbers and last calibration of UCTD probes used during the cruise.

| | Probe Number | Last Calibration |
|---|---|---|
| **Leg 1** | 70200275 | Nov 2018 |
| | 70200276 | Nov 2018 |
| | 70200280 | Nov 2018 |
| **Leg 2** | 70200010 | Sep 2018 |
| | 70200027 | Sep 2018 |
| | 70200029 | Sep 2018 |

to operate the UCTD while the V-Wing was deployed. Within the first few UCTD profiles, the UCTD spectra line seemed to get tangled with the rope used to deploy the V-Wing. Some blue color rubbed off of the V-Wing rope and was observed on the UCTD spectra line. The decision was made to not simultaneously deploy the UCTD and V-Wing from thereon.

Similarly to leg 1, the UCTD was operated around-the-clock by 3 watches: (1) Ray Graham (Watch Leader), Said Ouala, and Pablo Almaraz García; (2) Mathieu Dever (Watch Leader), Aravind Harilal, and Daniel Tarry (3) Nikolaus Wirth (Watch Leader), Noemi Calafat, and Benjamín Casas. The UCTD was used whenever the ship was underway. A total of 606 profiles over 12 sections were collected over the second leg (Figure 2.1). Three different probes provided by Tom Farrar's group were used alternatively (see Table 2.1).

## 2.2 EcoCTD operations

### Modus operandi

The EcoCTD was operated in the same way as the UCTD, except for the drop time: To account for the larger fall rate of the EcoCTD, it was allowed to free-fall for 70 s, instead of 90 s for the UCTD. Just like for the UCTD, each profiling cycle took about 5 min, which corresponds to a horizontal resolution of about 1 km at a ship speed of 6 knots. After 10 profiles (about 1 hour), or at the end of a section, the EcoCTD was recovered, the data was downloaded, and the EcoCTD was immediately redeployed if necessary. Recovery, download, and redeployment took less than 5 min, essentially sacrificing the equivalent of 1 profile for 10 profiles collected. Data was immediately available for visualization to the rest of the science team.

## First leg

The EcoCTD was not operated during the first leg of the cruise, due to the delayed arrival of the container carrying the EcoCTD.

## Second leg

The EcoCTD was used instead of the UCTD for four different transects during the second leg of the Cruise (see Figure 2.2). EcoCTD operations were supervised by the same watches as the UCTD. Ship speed was limited to 8 knots during EcoCTD operations, to limit the load on the winch's motor. A total of 112 profiles were collected, starting with 3 test profiles where the probe was allowed to free-fall for 55, 60, and 65 s to evaluate a proper free-fall time to sample the upper 200 m of the water column. A calibration cast was also performed, for which the EcoCTD was strapped to the CTD rosette for a cast down to 320 m for cross-calibration purposes. On April 9, around 05:30, the spectra line connecting the EcoCTD to the winch was sectioned for an unknown reason, and the probe was lost to the sea.

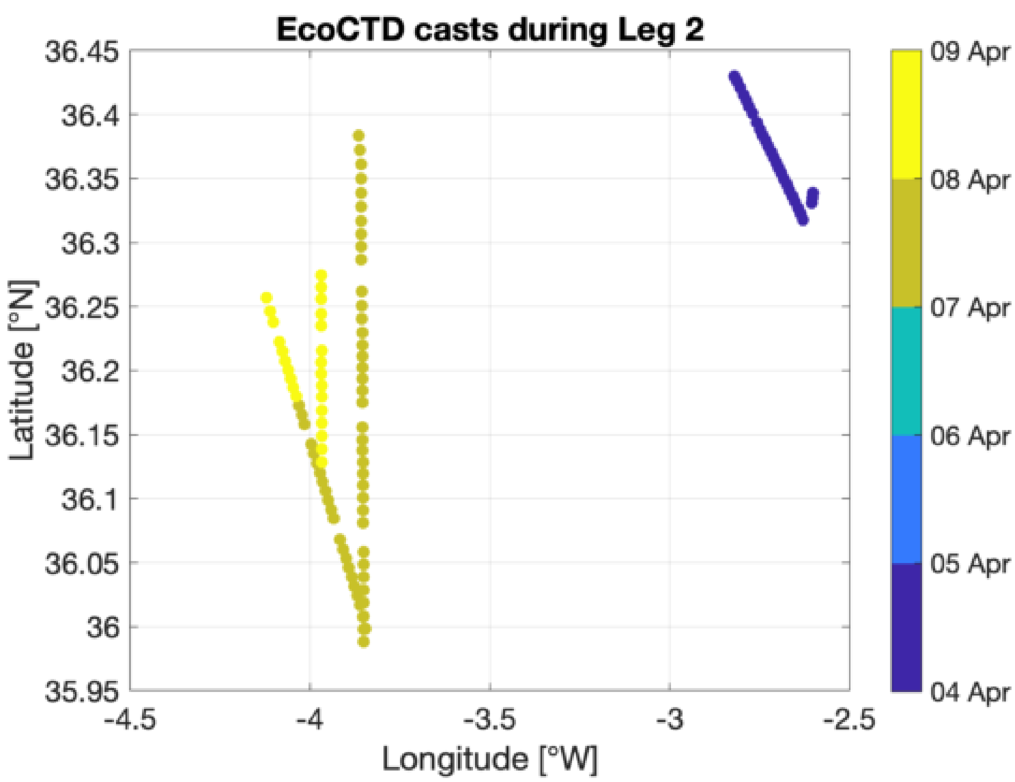


Figure 2.2: Location of EcoCTD casts during cruise leg 2.

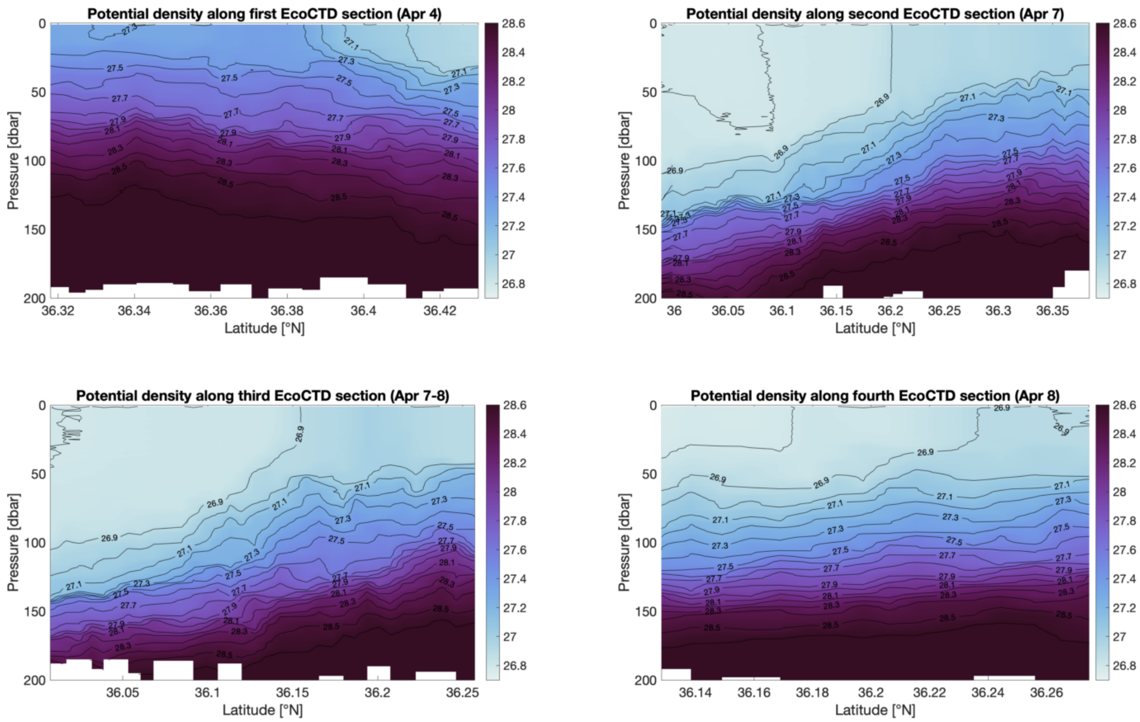


Figure 2.3: Potential density measured by the EcoCTD along the four transects completed during Leg 2 of the cruise (see Figure 2.2).

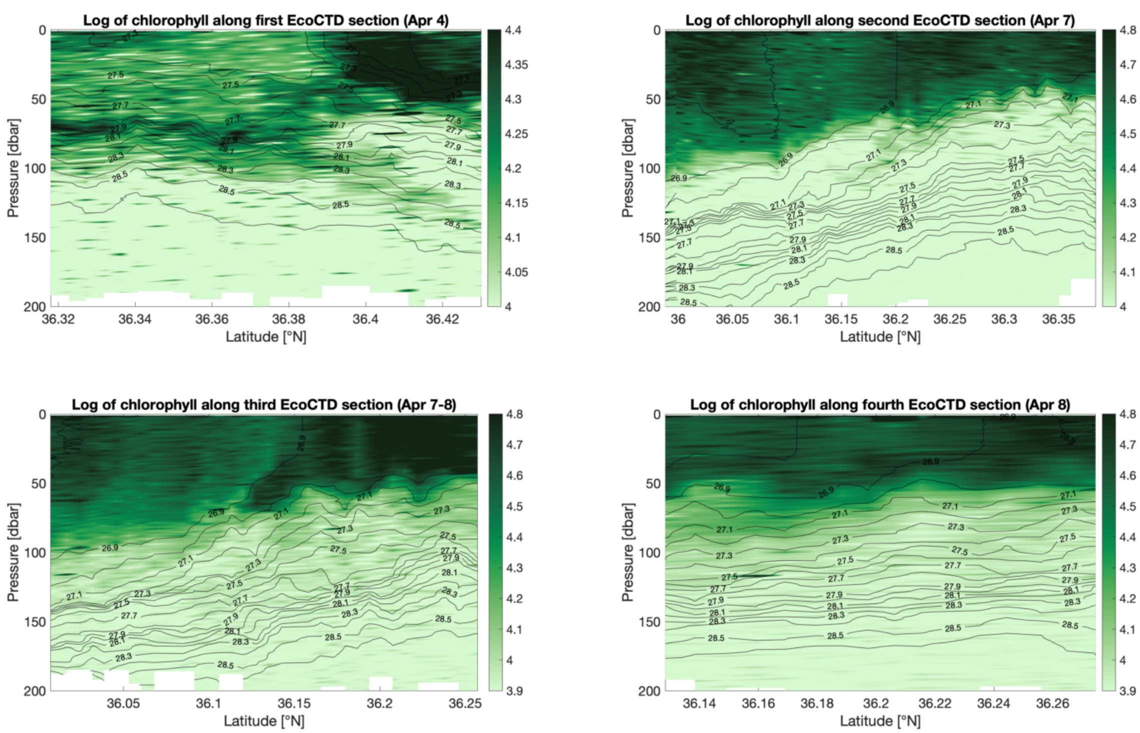


Figure 2.4: Logarithm of the chlorophyll concentration measured by the EcoCTD along the four transects completed during Leg 2 of the cruise (see Figure 2.2). Density contours are superimposed.

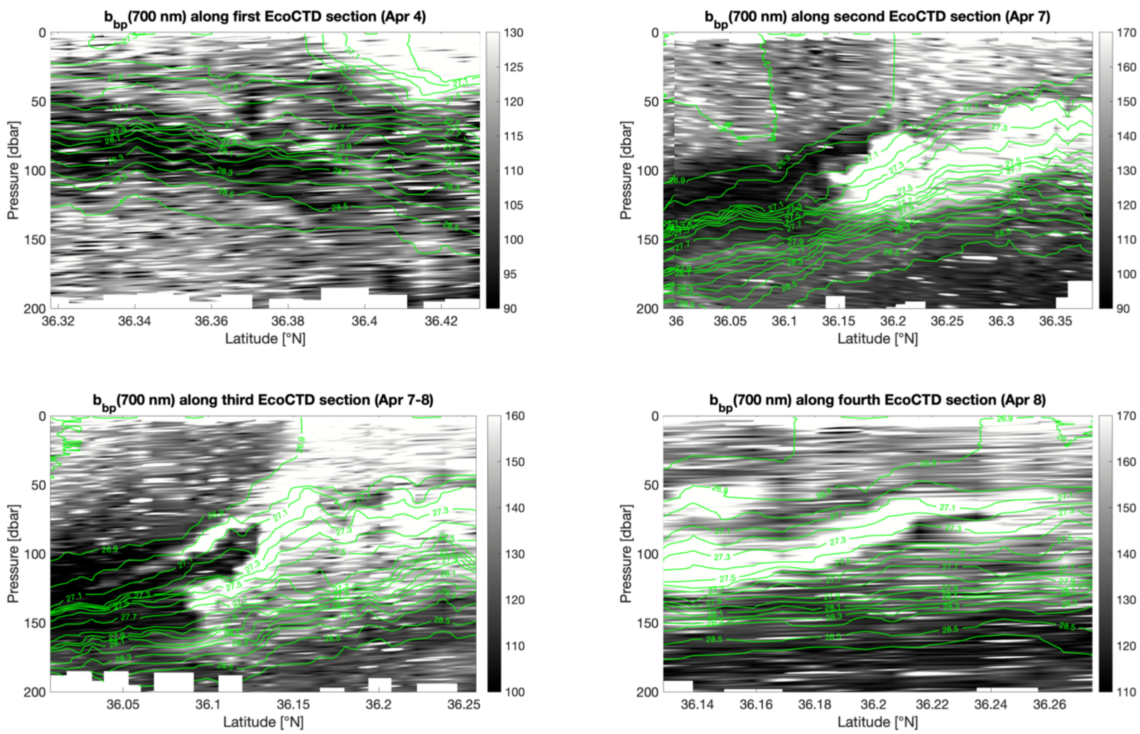


Figure 2.5: Backscatter at 700 nm measured by the EcoCTD along the four transects completed during Leg 2 of the cruise (see Figure 2.2). Density contours are superimposed.

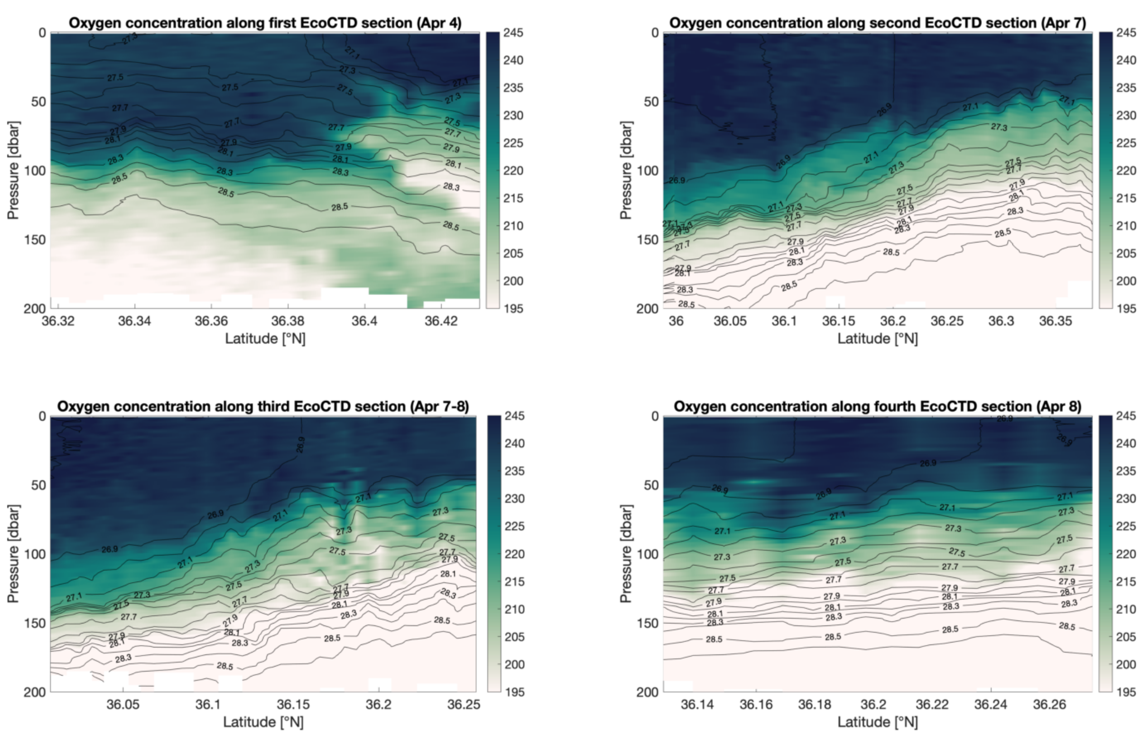


Figure 2.6: Oxygen concentration measured by the EcoCTD along the four transects completed during Leg 2 of the cruise (see Figure 2.2). Density contours are superimposed.

Table 2.2: List of transects sampled during the two legs of the 2019 cruise. The two legs are separated by a horizontal line between transects 43 and 47. Transects are numbered based on the ship track.

| Transect number | Number of profiles | Instrument | Start date | End date |
|---|---|---|---|---|
| 1 | 27 | UCTD | 27-March-2019 16:27:34 | 28-March-2019 13:17:48 |
| 2 | 144 | UCTD | 28-March-2019 13:17:49 | 29-March-2019 07:38:30 |
| 3 | 35 | UCTD | 29-March-2019 07:38:31 | 29-March-2019 16:41:51 |
| 4 | 71 | UCTD | 29-March-2019 16:41:52 | 30-March-2019 00:33:13 |
| 5 | 49 | UCTD | 30-March-2019 00:33:14 | 30-March-2019 05:49:33 |
| 6 | 38 | UCTD | 30-March-2019 05:49:34 | 30-March-2019 18:22:58 |
| 7 | 31 | UCTD | 30-March-2019 18:22:59 | 30-March-2019 22:20:16 |
| 15 | 26 | UCTD | 31-March-2019 02:31:00 | 31-March-2019 05:02:51 |
| 16 | 14 | UCTD | 31-March-2019 05:02:52 | 31-March-2019 08:59:01 |
| 17 | 9 | UCTD | 31-March-2019 08:59:02 | 31-March-2019 10:49:37 |
| 18 | 31 | UCTD | 31-March-2019 10:49:38 | 31-March-2019 16:45:01 |
| 19 | 27 | UCTD | 31-March-2019 16:45:02 | 31-March-2019 19:45:29 |
| 20 | 16 | UCTD | 31-March-2019 19:45:30 | 01-April-2019 01:35:53 |
| 21 | 27 | UCTD | 01-April-2019 01:35:54 | 01-April-2019 04:09:52 |
| 22 | 30 | UCTD | 01-April-2019 04:09:53 | 01-April-2019 07:03:59 |
| 23 | 27 | UCTD | 01-April-2019 07:04:00 | 01-April-2019 10:03:30 |
| 24 | 35 | UCTD | 01-April-2019 10:03:31 | 01-April-2019 14:10:16 |
| 25 | 17 | UCTD | 01-April-2019 14:10:17 | 01-April-2019 15:38:21 |
| 26 | 20 | UCTD | 01-April-2019 15:38:22 | 01-April-2019 19:37:55 |
| 27 | 70 | UCTD | 01-April-2019 19:37:56 | 02-April-2019 02:47:54 |
| 28 | 10 | UCTD | 02-April-2019 02:47:55 | 02-April-2019 03:48:23 |
| 29 | 109 | UCTD | 02-April-2019 03:48:24 | 02-April-2019 14:36:19 |
| 30 | 16 | UCTD | 02-April-2019 14:36:20 | 02-April-2019 16:10:41 |
| 31 | 76 | UCTD | 02-April-2019 16:10:42 | 02-April-2019 23:35:38 |
| 32 | 11 | UCTD | 02-April-2019 23:35:39 | 03-April-2019 00:46:29 |
| 33 | 67 | UCTD | 03-April-2019 00:46:30 | 03-April-2019 07:20:43 |
| 40 | 17 | UCTD | 03-April-2019 19:41:01 | 03-April-2019 21:28:42 |
| 41 | 13 | UCTD | 03-April-2019 21:28:43 | 03-April-2019 23:01:48 |
| 42 | 10 | UCTD | 03-April-2019 23:01:49 | 04-April-2019 00:10:21 |
| 43 | 12 | UCTD | 04-April-2019 00:10:22 | 04-April-2019 01:42:59 |
| 47 | 3 | EcoCTD | 04-April-2019 17:03:08 | 04-April-2019 20:51:23 |
| 48 | 26 | EcoCTD | 04-April-2019 20:51:24 | 04-April-2019 23:06:45 |
| 49 | 11 | UCTD | 04-April-2019 23:06:46 | 05-April-2019 03:09:31 |
| 50 | 10 | UCTD | 05-April-2019 03:09:32 | 05-April-2019 05:05:48 |
| 52 | 11 | UCTD | 05-April-2019 05:39:46 | 05-April-2019 06:58:34 |
| 53 | 6 | UCTD | 05-April-2019 06:58:35 | 05-April-2019 07:52:12 |
| 54 | 20 | UCTD | 05-April-2019 07:52:13 | 05-April-2019 09:49:25 |
| 55 | 10 | UCTD | 05-April-2019 09:49:26 | 05-April-2019 10:56:14 |
| 56 | 29 | UCTD | 05-April-2019 10:56:15 | 05-April-2019 14:20:55 |
| 57 | 33 | UCTD | 05-April-2019 14:20:56 | 05-April-2019 20:32:42 |
| 58 | 9 | UCTD | 05-April-2019 20:32:43 | 05-April-2019 21:33:07 |
| 62 | 39 | UCTD | 06-April-2019 05:45:52 | 06-April-2019 10:05:16 |
| 63 | 28 | UCTD | 06-April-2019 10:05:17 | 06-April-2019 15:14:41 |
| 65 | 58 | UCTD | 07-April-2019 01:59:18 | 07-April-2019 07:24:57 |
| 66 | 17 | UCTD | 07-April-2019 07:24:58 | 07-April-2019 08:31:36 |
| 67 | 47 | UCTD | 07-April-2019 08:31:37 | 07-April-2019 13:11:56 |
| 68 | 32 | UCTD | 07-April-2019 13:11:57 | 07-April-2019 16:10:33 |
| 69 | 15 | UCTD | 07-April-2019 16:10:34 | 07-April-2019 18:00:24 |
| 70 | 37 | EcoCTD | 07-April-2019 18:00:25 | 07-April-2019 21:48:06 |
| 71 | 32 | EcoCTD | 07-April-2019 21:48:07 | 08-April-2019 01:00:02 |
| 73 | 12 | UCTD | 08-April-2019 03:48:18 | 08-April-2019 06:06:28 |
| 78 | 8 | UCTD | 08-April-2019 09:34:54 | 08-April-2019 12:09:55 |
| 79 | 9 | UCTD | 08-April-2019 12:09:56 | 08-April-2019 13:04:00 |
| 80 | 3 | UCTD | 08-April-2019 13:04:01 | 08-April-2019 14:49:28 |
| 81 | 7 | UCTD | 08-April-2019 14:49:29 | 08-April-2019 15:41:47 |
| 82 | 8 | UCTD | 08-April-2019 15:41:48 | 08-April-2019 16:35:14 |
| 83 | 16 | UCTD | 08-April-2019 16:35:15 | 08-April-2019 18:52:41 |
| 84 | 19 | UCTD | 08-April-2019 18:52:42 | 08-April-2019 20:57:48 |
| 85 | 15 | EcoCTD | 08-April-2019 20:57:49 | 08-April-2019 22:30:46 |
| 89 | 16 | UCTD | 09-April-2019 04:32:47 | 09-April-2019 06:07:34 |
| 90 | 10 | UCTD | 09-April-2019 06:07:35 | 09-April-2019 07:47:28 |
| 91 | 6 | UCTD | 09-April-2019 07:47:29 | 09-April-2019 09:44:39 |
| 92 | 12 | UCTD | 09-April-2019 09:44:40 | 09-April-2019 11:53:43 |
| 93 | 8 | UCTD | 09-April-2019 11:53:44 | 09-April-2019 13:01:51 |
| 94 | 2 | UCTD | 09-April-2019 13:01:52 | 09-April-2019 13:20:07 |
| 95 | 20 | UCTD | 09-April-2019 13:20:08 | 09-April-2019 15:35:38 |
| 96 | 13 | UCTD | 09-April-2019 15:35:39 | 09-April-2019 16:58:52 |
| 97 | 17 | UCTD | 09-April-2019 16:58:53 | 09-April-2019 18:50:56 |
| 101 | 11 | UCTD | 10-April-2019 00:42:45 | 10-April-2019 01:58:10 |
| 102 | 13 | UCTD | 10-April-2019 01:58:11 | 10-April-2019 03:18:12 |
| 103 | 17 | UCTD | 10-April-2019 03:18:13 | 10-April-2019 05:02:14 |
| 104 | 20 | UCTD | 10-April-2019 05:02:15 | 10-April-2019 07:03:30 |

# Chapter 3

# CTD and water sampling

Eva Alou-Font (SOCIB), Andrea Cabornero (SOCIB), and Mara Freilich (WHOI)

## 3.1 Overview

There were a total of 49 CTD stations during the cruise (Figure 3.1). Most of these casts are arranged in lines of 3 or more sequential casts. The position of casts in CTD lines was determined based on UCTD or EcoCTD sections immediately prior to the CTD line. The CTD casts that are not part of the CTD lines, with the exception of the first CTD cast, are calibration casts. During the calibration casts, water was sampled only for chlorophyll-a concentration, oxygen concentration, and salinity. Samples were taken for these calibrations during almost all CTD casts. The distinction of calibration cast signifies that samples were not taken for phytoplankton community composition or physiology.

All CTD casts used a CTD lowered from a winch on the starboard side of the ship. All water samples were taken from 5L Niskin water samplers. The CTD was rented from EMS Sistemas de Monitorización Medio Ambiental, S.L.U. The CTD was operated by technicians from EMS and the ship's crew. Once the CTD was in the water, it was lowered to 10 meters to allow the Seabird pumps to prime. Once ready for sampling, the CTD was raised to 5 meters and then data recording began.

The CTD casts typically went to 300 meters depth. The calibration casts sometimes went to 600 meters on leg 1 and 500 meters on leg 2 for calibration purposes.

The scientific party determined the depths at which to fire bottles. There were 12 Niskin bottles on the CTD rosette. The locations of the bottles were targeted to sample high

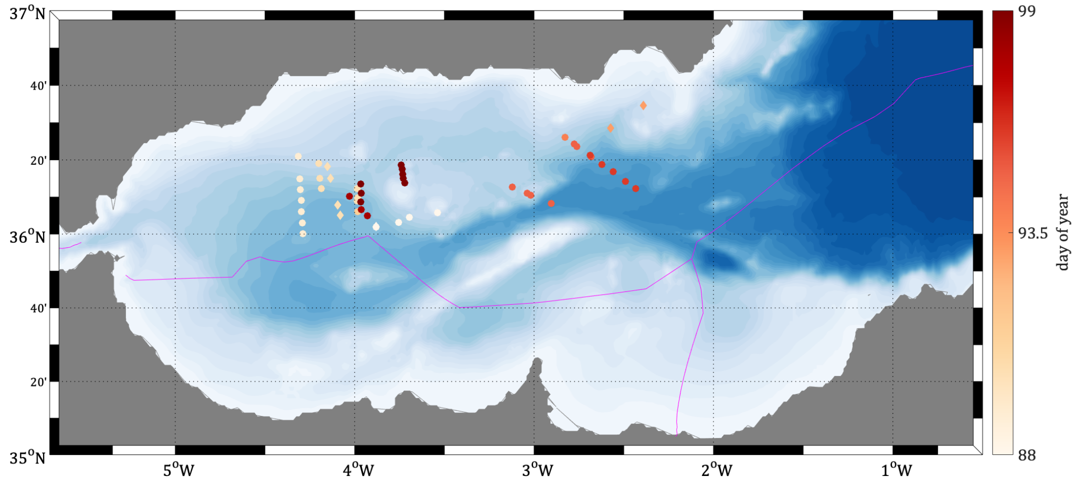


Figure 3.1: CTD cast locations colored by day of year. The diamonds are calibration casts. The background color is topography with the darkest blue being 3000 meters depth and the lightest white 0 meters. The pink lines show the exclusive economic zone boundaries.

chlorophyll surface layers, whether this was a DCM or the whole mixed layer, subducted features, or the presumed source water of subducted features. The samples for phytoplankton community composition were generally chosen using this template:

1. Surface (5m - fixed)
2. Mixed layer (~25 meters)
3. Deep chlorophyll maximum or lower mixed layer
4. Lower deep chlorophyll maximum
5. Secondary chlorophyll maximum or other intrusion. If not present, fixed depth at 120 meters.

## 3.2 Objectives

1. Complete hydrographic survey of the CALYPSO19 cruise study area through deployment of a CTD instrument frame (SeaBird SBE911*plus*) with extra mounted sensors and rosette equipped with 12 5l Niskin bottles.

2. Discrete water sample collection at various depths for the purpose of:
   - 2.1 Sensor field correction with the *in situ* discrete water samples for salinity, dissolved oxygen and chlorophyll a (Chl *a*) concentration
   - 2.2 Biogeochemical sampling of nutrients, phytoplankton community (through pigments and microscopic post-cruise analyses) and photo-physiological algal state (through photosystem II efficiency or increase in degradation pigments)
3. High spatial resolution, depth resolution, and spatial coverage of casts in order to
   - 3.1 Inform the use of biophysical tracers to infer the timescales of vertical tracer fluxes
   - 3.2 Understand the importance of physical oceanographic processes including vertical advection, horizontal advection, and mixing on changes in community composition.

A ship activity log detailing the parameters sampled was completed during the cruise and will be updated after the cruise (see Table 3.1 for detailed biogeochemical sampled parameters).

## 3.3 Sensors used

During leg 2, a SUNA V2 nitrate sensor was mounted with the sensor package. The SUNA was powered by an external battery pack and data was downloaded between CTD lines. Each time the data was downloaded, the SUNA clock was synced with the ship's time server.

## 3.4 Filenames

The CTD casts are named following two conventions, indicating the water samples that were taken during those casts. The CTD casts during which water samples were taken for phytoplankton community composition, pigments, cell physiology, and calibration of chlorophyll, oxygen, and salinity are named "cast###" and are numbered sequentially from 001 to 043. The casts during which samples were only taken for calibration of chlorophyll, oxygen, and salinity are named "cal###" and are numbered sequentially from 001 to 006.

There is an irregularity in the file names for CTD station 2. Three casts were performed at this station because many of the Niskin bottles misfired during the first two casts. The first cast file is named "Cast002-BAD.hex". The second cast file is named "Cast002.hex". The final cast file is named "Cast002B.hex" for the downcast data and "Cast002BU.hex" for the upcast data. This is the cast during which water samples were taken.


Figure 3.2: The CTD rosette with the SUNA nitrate sensor and battery pack.

## 3.5 On board personnel

**Leg 1 - biogeochemical sampling**

Eva Alou Font (SOCIB)

Andrea Cabornero (SOCIB)

Isabel Caballero (ICMAN)

Daniel Rodríguez (IMEDEA)

Eugenio Cutolo (IMEDEA)

Said Ouala

**Leg 1 - phytoplankton sampling**

Margaret Conley (WHOI)

Mara Freilich (WHOI)

Aravind Harilal Meenambika (Northeastern)

Guilherme Salvador Vieira (Northeastern)

**Leg 2 - biogeochemical sampling**

Eva Alou Font (SOCIB)

Andrea Cabornero (SOCIB)

Isabel Caballero (ICMAN)

Eugenio Cutolo (IMEDEA)

Angelica Enrique (ICMAN)

**Leg 2 - phytoplankton sampling**

Margaret Conley (WHOI)

Mara Freilich (WHOI)

Guilherme Salvador Vieira (Northeastern)

## 3.6 Post-cruise calibration and biogeochemical sample processing

### Salinity

Post cruise processing will involve the correction of the salinity data based on calibration with in situ water samples analyzed in the lab with a Guildline Portasal model 8410A salinometer.

### Biogeochemical parameters

As mentioned in the general objectives, the primary objective of the biogeochemical data collection during this cruise is to compare the CTD oxygen (SBE-43) and fluorescence (Cyclops and Eco) sensors against the *in situ* discrete water samples of these parameters.

Secondary field objectives are:

1. To estimate chl *a* concentration and distribution (as a proxy for phytoplankton biomass).

2. To assess nutrient concentration distribution: Nitrate ($NO_3^-$), nitrite ($NO_2^-$), silicate ($SiO_4^{2-}$) and phosphate ($PO_4^{3-}$).

3. To study phytoplankton community composition and physiological state.

## Dissolved Oxygen

Discrete water samples (Winkler's method, *Langdon* [2010]) for comparison were taken at each station at a maximum of 3 depths. We chose depths of varying oxygen concentrations in order to sample the full spectrum of oxygen concentrations (see logbook generated during the cruise for more details on sampling depths, replicates and parameters sampled at each station).

Samples were analyzed on board after an 8-24 h period in darkness with a titration procedure with potentiometric endpoint detection (Metrohm 888 Titrator).

The final dissolved oxygen dataset will be produced post-cruise following the analysis of the data.

## Chl *a* concentration

Samples for chl *a* concentration were taken at all stations at 4 depths (see logbook for details). For each sample, a volume of 500 ml was filtered through 45 mm Whatman GF/F filters and immediately placed in plastic vials and stored in a freezer onboard (-20°C). Chl *a* determination will be carried out at the IMEDEA by fluorimetry (using a Turner 10-AU fluorometer).

## Nutrients

Samples for inorganic nutrient concentrations were taken at all stations at a maximum of 6 depths (see logbook for detailed information on sampling depths and protocols). Samples will be sent to ICMAN for analyses right after the cruise and one replicate will be kept frozen at -20°C at the IMEDEA as a backup.

## Phytoplankton pigments

Samples were taken on some stations at the deep chlorophyll maximum (DCM) for general cell identification (cells fixed in Lugol's solution, *Utermöhl* [1958]). Samples for microscopy will be analyzed post-cruise at the IMEDEA.

Samples for High Performance Liquid Chromatography (HPLC) analyses were taken at each station at 2 depths (surface and DCM). The total fraction was collected and a volume of 1l filtered through a GF/F filter (retaining microorganisms larger than the nominal pore size of 0.7 $\mu$m). Samples were stored on board in a liquid nitrogen dry-shipper.

## Photosystem II efficiency

The photosynthetic performance of algae was assessed by examining the changes in chlorophyll fluorescence with the electron transport inhibitor 3.(3,4-dichlorophenyl)-1,1-dimethylurea (DCMU) that blocks electron transport at the electron acceptor Q in PSII. Minimum and maximum fluorescence were measured after 30 min of dark adaptation using a Turner Designs 10-AU fluorometer on board.

## Preliminary results

The final biogeochemical dataset will be produced in due course following post-cruise analyses of the data. Below we present some preliminary results obtained with the CTD sensors for dissolved oxygen (Sea-Bird SBE43) in leg 1, Fig. 3.3. Note that no QC has been applied yet to the data.

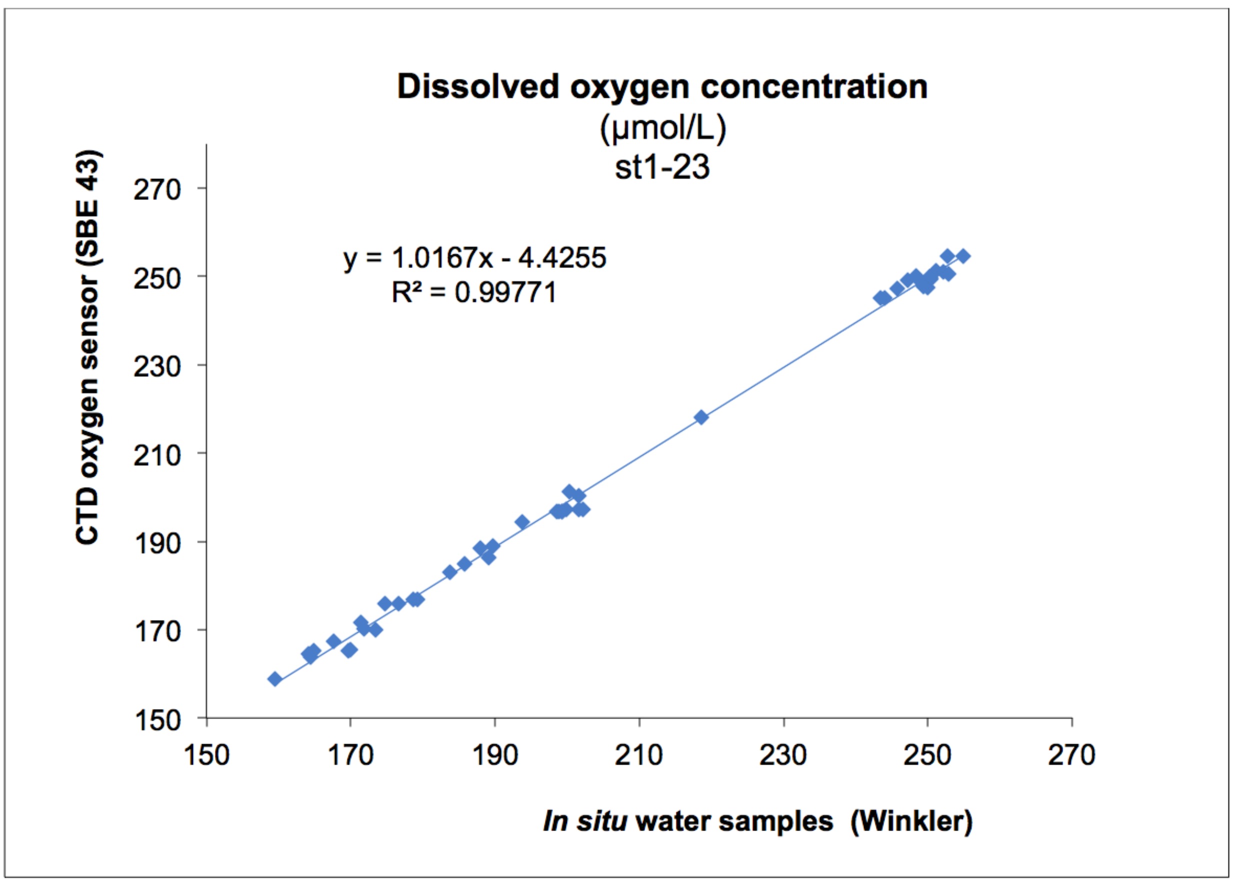


Figure 3.3: Comparison between the dissolved oxygen measured using a SBE-911*plus* CTD probe (Sea-Bird Electronics, SBE 43) and the dissolved concentration of *in situ* water samples (Winkler titration) for leg 1 of the CALYPSO 19 cruise.

## 3.7 Respiration measurements

We quantified biological oxygen demand (BOD) in order to better interpret changes in AOU along- and across-fronts. We sampled BOD at a maximum of two depths in each CTD cast. The samples were taken below the euphotic depth and within and outside of subducted filaments (AOU anomalies). We also measured the BOD at one sample in the inferred source waters of a subducted filament (this sample may be from the euphotic zone, but was incubated in the dark). Incubations took place at 14°C in the dark in the temperature controlled room of the Pourquoi Pas?. The BOD measurements took place using the autoBOD, a device that measures oxygen continuously using an oxygen optode [*Collins et al.*, 2018]. There are 12 bottles on the autoBOD. When using the autoBOD, we took 4 replicates for each sample, giving us the capacity to measure BOD for 3 distinct samples simultaneously. We had a total of 24 bottles for the autoBOD and at times we had some samples incubating in drawers in the temperature controlled room where the autoBOD was operating, but not being measured.

## 3.8 Phytoplankton community composition

All samples for phytoplankton community composition were processed immediately after the CTD cast was complete. All samples were in storage within 45 minutes of the completion of the cast.

### Metagenomics

We preserved samples for metagenomic analysis from five depths on each CTD cast that was not a calibration cast. In order to preserve samples, we filtered 500 ml of seawater onto 0.2 $\mu$m Supor filters (47 mm). We filtered two replicates for each sample. After filtering, samples were stored in the -80°C freezer on deck 4. The extraction of the DNA will take place at the Monterey Bay Aquarium Research Institute in Alexandra Worden's lab. During leg 1 of the cruise we took water for the samples into acid washed 1 L water bottles covered in black tape. Bottles were rinsed with distilled water, MilliQ water, and seawater before sampling. The filtering for the DNA took place on the filtration rig owned by Socib after the filtration of samples for chlorophyll-a and HPLC was completed. During leg 2, samples were taken in 1 L

| | N | Oxygen | Nutrients | Chl *a* | HPLC | Phyto | Fv/Fm | Salinity |
|---|---|---|---|---|---|---|---|---|
| ST_Cal | 6 | 18 (2 depths) | 0 | 24 (4 depths) | | | | 18 (1-2 depths) |
| ST_Biogeo | 43 | 95 (2-3 depths) | 774 (6 depths) | 172 (4 depths) | 126 (2 depths) | 43 (1 depth) | 44 (3 depths) | 65 (2 depths) |

Table 3.1: List of sampled stations, variables sampled and number of depths.

amber bottles which had been previously acid washed. Samples were filtered on the filtration rig shipped from Woods Hole, but the pump shipped from Woods Hole did not work on the European power system. Instead, the pump owned by Socib was used for filtering the DNA samples after filtration for chlorophyll-a and HPLC samples was completed.

## Cell quantification

We preserved samples for quantification by flow cytometry using the Worden lab protocol from the same Niskin bottles from which we took the samples for DNA extraction. The preservation was done in the dry lab on deck 3, using the fume hood on that deck. During leg 1 of the cruise, samples were flash frozen in the -80°C freezer on deck 4. During leg 2 of the cruise, samples were flash frozen in liquid nitrogen, where they remained for at least 2 hours. Samples were then stored in the -80°C freezer on deck 4. We took 3 replicates of each sample. Six replicates were taken for cast 34. Of these, 3 were flash frozen at -80°C and 3 were flash frozen in liquid nitrogen for comparison of the two methods. Quantification will take place in the Worden lab at the Monterey Bay Aquarium Research Institute.

### Flow cytometry protocol

1. Use a pipette helper (LIVE) and a 5 ml serological pipette (10 ml during leg 1) to take 3 ml of seawater from the amber bottle.

2. Add the 3 ml of seawater to a 5 ml conical tube (15 ml during leg 1) (not in chemical hood).

3. In chemical hood: add 30 $\mu$l of EM grade 25% Glutaraldehyde to 3 ml of seawater (use a P200 and P200 tips to add Glut [P100 during leg 1]) and screw cap on.

4. Vortex tube gently (but so that you see a vortex), twice, and start timer for 20 min.

5. Aliquot the 3 ml to 3 cryovials (∼1 ml of sample in each tube), tighten all caps.

6. Fill canes with cryotubes, protect with a cryosleeve, and place in dark to finish the 20 minutes of fixation.

7. When fixation time is over, put cane into liquid nitrogen dewar (-80°C freezer during leg 1).

# Chapter 4

# Lagrangian Drifter and Float Deployments

Pierre-Marie Poulain (OGS), Tamay Ozgokmen (RSMAS/UM),
Cedric Guigand (RSMAS/UM)
Gino Cristofano (OGS), and Luca Centurioni (SIO/UCSD)
Irina Rypina (WHOI)

## 4.1 Introduction

This chapter provides information on the deployments of the drifters and floats provided by OGS, (Italy), RSMAS (Florida) and SIO (California). After a brief description of the Lagrangian instruments (section 4.2), details on the deployments are given in sections 4.3 and 4.4. Preliminary results can be found in section 4.6. Conclusions and recommendations for future CALYPSO experiments in the same area are in the last section, 4.7.

This chapter is a summary of the full technical report published by OGS. See *Poulain et al.* [2019] for the full report and references.

## 4.2 Lagrangian instruments

1. **SVP-type drifters**

   **Standard Surface Velocity Program (SVP) drifter**: A spherical surface buoy tethered to a weighted nylon drogue that allows it to track the horizontal motion of water at a nominal depth of 15 m. The drifter has a satellite Iridium transmitter and a thermistor to measure Sea Surface Temperature (SST), set to sample at a frequency of 1 Hz. The 53 SVP drifters used during the CALYPSO 2019 campaign were manufactured by the Lagrangian Drifter Laboratory (LDL) at SIO/UCSD in La Jolla, California.

**The Directional Wave Spectra (DWS) drifter**: Essentially the surface buoy of an SVP drifter for which the drogue was replaced by a small ($\sim$50 cm) stabilizing chain. It is equipped with a high-performance GPS engine paired with in-house developed software algorithms for onboard computation of the Directional Wave Spectrum (DWS). Location, SST, voltage and wave parameters are transmitted to Iridium satellite at hourly intervals. The 6 DWS drifters used here were designed and produced by the LDL in La Jolla, California.

2. **CODE-type drifters**
The Coastal Ocean Dynamics Experiment (CODE) drifter was designed to measure the currents within the top meter of the water column. The CODE drifter used in the CALYPSO 2019 campaign is similar to the design manufactured by Technocean/DBi. It was constructed by MAXO, an Italian company, and was equipped with a SPOT/-GlobalStar TRACE module, which includes a GPS receiver to measure position with high accuracy (<10 m) and high frequency (every 10 min). Additional external batteries have been fitted to the TRACE modules in order to increase the autonomy of the drifters to a few months, using a 10 min sampling period. A total of 50 CODE drifters were planned for the CALYPSO 2019 experiment.
A prototype drifter similar to the CODE drifter was fitted with a Nortek Aquadopp acoustic velocimeter and Acoustic Doppler Current Profiler (ADCP) to measure the horizontal relative flow around and below the drifter, respectively. The Aquadopp ADCP was set up with 20 vertical cells of 1 m, a blanking distance of 0.41 m and average interval of 1 s, and transmitted acoustic signals at 2 MHz. The radial velocities obtained from each beam are combined to estimate the currents in the upper layer of the sea below the drifter with an accuracy of about 1 cm/s.

3. **CARTHE drifter**
CARTHE drifters were developed to be compact, easy to transport and assemble, and 85% biodegradable. A total of 100 of these drifters were used in the CALYPSO 2019 experiment. They were set to transmit their GPS positions every 5 min via the GlobalStar satellite system.

4. **Arvor profiling float**
An ARVOR profiling float is an Argo float manufactured by NKE in Hennebont, France. Three Arvor-I floats were used, one standard and two with additional Aandeera Optode to measure dissolved oxygen concentration. They were programmed to profile every 3 h down to about 200 m, after their first surfacing. Their parking depth was set to 350 m and their vertical resolution was 1 m. These floats are part of the Argo-Italy program, the Italian contribution to the global Argo array. After the experiment, the floats will be programmed with the standard MedArgo parameters.

5. **WHOI multi-layer drifter array**
   WHOI multi-layer drifter array consisted of 48 drogued drifters, 8 drifters at 6 layers - 1, 10, 30, 50, 75, and 100m. Drifters were built at WHOI using eco-friendly all-natural materials such as cotton and metal, and, like CARTHE drifters, were transmitting their GPS positions every 5 min via the GlobalStar system. Unfortunately, the lower 3 layers of drifters stopped transmitting GPS positions shortly after deployment.

## 4.3 Drifter deployments

The drifter and float deployments were conducted between 28 March and 9 April 2019. They are described hereafter in chronological order. All deployments were conducted from *N/O Pourquoi Pas?* In total, **185 drifters have been deployed**. One DWS was recovered and redeployed. The CODE with Nortek velocimeters and ADCP (hereafter called CODE ADCP) was deployed 3 times and recovered safely each time. See the full report for details, including deployment coordinates for each drifter.

a. **28-29 March 2019**
   A total of 11 drifters were deployed along an almost zonal transect connecting Almería to the West Alboran Gyre (WAG), including 3 DWS and 7 CODE drifters. All drifters were deployed from the stern on the starboard side, in ship speeds of 0-8 kts.

   Unfortunately, two CODE drifters sank upon deployment due to excess weight (12.4 kg instead of 10.4 kg). It appeared that all the 50 CODE units had been weighted incorrectly at production level by the MAXO company. To minimize the impact of this problem on the CALYPSO 2019 experiment, two quick fix solutions were envisaged:

   - the first one was to attach 2 plastic bottles with air and some water to the upper end of the CODE tubular body, in order to increase its buoyancy by about 2 kg, using duck tape. This was done for 5 CODE drifters.
   - the second one was to remove all the sand in the tubular body by poking holes in it, and flushing it with water. Then, the concrete tap located in the middle of the tube was pushed to the bottom part, using compressed air and/or by banging the drifter on the floor. This operation was executed on 18 drifters.

   It was decided to use only half of the CODE drifters available onboard for the CALYPSO 2019 experiment and to return 25 units back to the MAXO manufacturing company for repair or substitution. This had some impact on the original drifter deployment planning of the cruise.

b. **30-31 March 2019**
   In total, 36 drifters were deployed in a tight cluster (with minimum drifter separation distance of 1.5 km) near the northern limb of the WAG. The CODE and SVP were deployed in pairs (same positions).

c. **3-4 April 2019**
On our way back to Almería, the CODE ADCP, one DWS and later 3 SVP drifters were deployed.

d. **4-5 April 2019**
A cluster of 14 SVP and 16 CARTHE drifters were deployed in a cluster (with distance between the drifters of about 1 km) along 2 transects across a front in the southern part of an anticyclonic eddy located south of Almería.

e. **5 April 2019**
Additional SVP (5) and CARTHE (6) drifters were released downstream of the previous cluster to "fill the gaps" and try to obtain a more isotropic array of drifters (most drifters released on 4-5 April ended up on a zonal line).

f. **6-7 April 2019**
Thirty-six CARTHE drifters were released along a zonal transect reaching the WAG and a meridional line extending to its northern edge. They were deployed every 30 min with the ship sailing at about 6 kts.

g. **8 April 2019**
A V-shaped cluster of 14 SVP and 14 CARTHE drifters was released in the front near the northern edge of the WAG. Separation distance between the drifters was about 1 km (every 5-6 min with ship speed near 6 kts). One DWS was also released at the northernmost position.

h. **9 April 2019**
The CODE ADCP drifter was deployed (and recovered) for the third time, along with a DWS drifter. A total of 25 CARTHE drifters were released along an almost complete circle in the front, downstream of the cluster released on 8 April. They were deployed every 4-5 min with ship speed at 6 kts.

## 4.4 Float deployments

Three Argo floats were deployed during the CALYPSO 2019 campaign, one regular ARVOR with CTD and 2 ARVORs with CTD and dissolved oxygen sensor. Using the Iridium downlink, commands were sent to program them to cycle every 3 h. Doing so, they were able to profile between the surface and about 200 m. See the full report for deployment details. Unfortunately float WMO 6903265 performed anomalously short profiles since its deployment and the data collected by this float are useless. It drifted in the southern part of the Alboran Sea into Moroccan waters and could not be recovered. In addition to these 3 floats, one ARVOR float (WMO 3901974) deployed in the Alboran Sea in May 2018 during the CALYPSO PILOT experiment happened to be in the northwestern Alboran Sea (off Málaga). Using the iridium downlink, it was set back to high-frequency sampling (3 h). It drifted offshore and provided data in the WAG.

## 4.5 Real time processing and displaying

The drifter and float data were processed in real time by several systems at OGS, RSMAS/UM and SIO/UCSD. The status of the instruments, along with their trajectories, was monitored using web-based systems reachable with the internet connection onboard *N/O Pourquoi Pas?* In addition, all the drifter and float data were inserted into Google Earth for display with the measurements of other instruments (ship ADCP and underway, gliders, etc.).

## 4.6 Preliminary results

During the period 28 March – 3 April, the drifters initially revealed a well defined WAG centered at its usual location and a weaker anticyclonic feature located more to the northeast in the direction of Almería. During the second leg of the cruise (4–10 April), the WAG was displaced to the northeast and the Almería anticyclone disappeared. In contrast, an anticyclonic vortex appeared off the African coast southeast of the WAG. The drifters were entrained in the above-mentioned circulation features with speeds sometimes reaching 1 m/s, before approaching the Algerian coast near Oran and joining the Algerian Current. Fig. 4.1 shows all the drifter trajectories between 28 March and 10 April 2019. A zoom on the Alboran Sea and the drifter tracks between 9 and 10 April is depicted in Fig. 4.2. The cluster released on 8–9 April in the northern limb of the WAG is evident. The drifters released before have dispersed and joined the northern part of an anticyclonic feature off the African coast, before joining the Algerian Current. Some of them got trapped in an area located just south of the bathymetric feature including the Alboran Island (near 35N45' 3W00') where the water was quite stagnant for some days. High frequency currents (mostly inertial) are ubiquitous in all the drifter trajectories, as expected since the winds remained rather sustained (10-30 kts) during the experiment.

Two of the ARVOR floats moved anticyclonically in the WAG. Their tracks between 30 March and 10 April are shown in Fig. 4.3. Float WMO 6903264 collected interesting data in the WAG, including a remarkable signature of internal waves of tens of meters in amplitude at the interface between the Atlantic Water (on top) and the Mediterranean Water (below) between 100 and 200 m depth. Fig. 4.5 shows, as an example, the contour diagram of salinity versus depth and time for float WMO 6903264 from its deployment until 24 April, and the corresponding trajectory in the WAG. Float WMO 3901974 left the coastal Spanish waters off Marbella and drifted to the south and east, but it was not captured by the WAG, moving instead cyclonically in the central western Alboran Sea (Fig. 4.3). Finally, float WMO 6903266 which was deployed later (on 5 April) during the cruise, moved to the south and then to the east, turning cyclonically around the Alboran Island (Fig. 4.3)

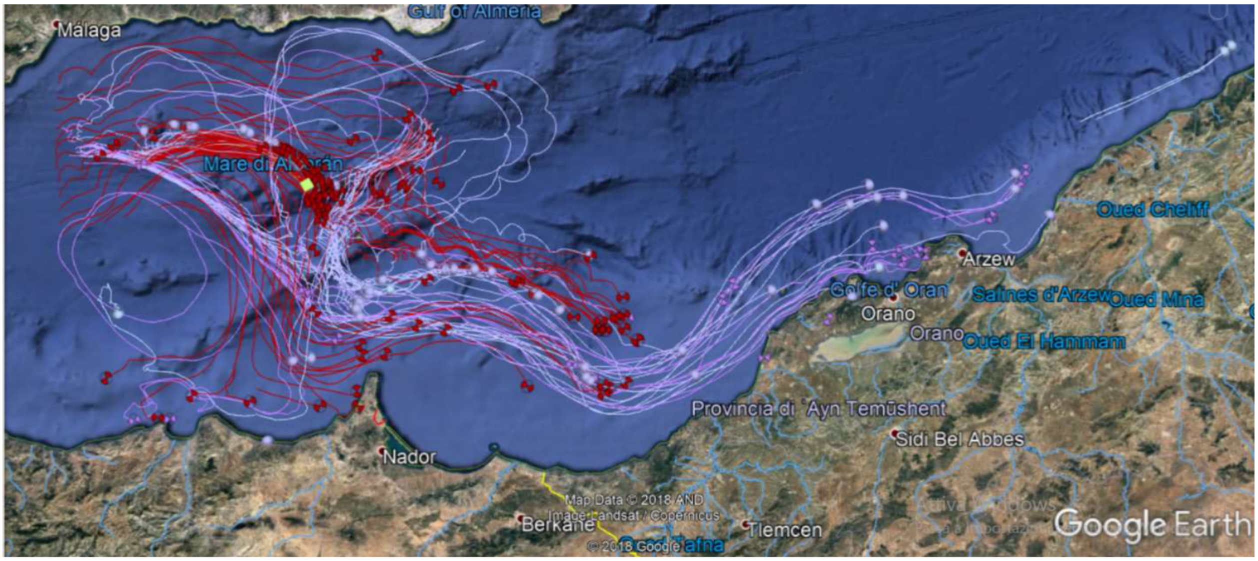


Figure 4.1: Trajectories and last positions on 10 April 2019 of all CODE (magenta), CARTHE (red) and SVP (white) drifters.

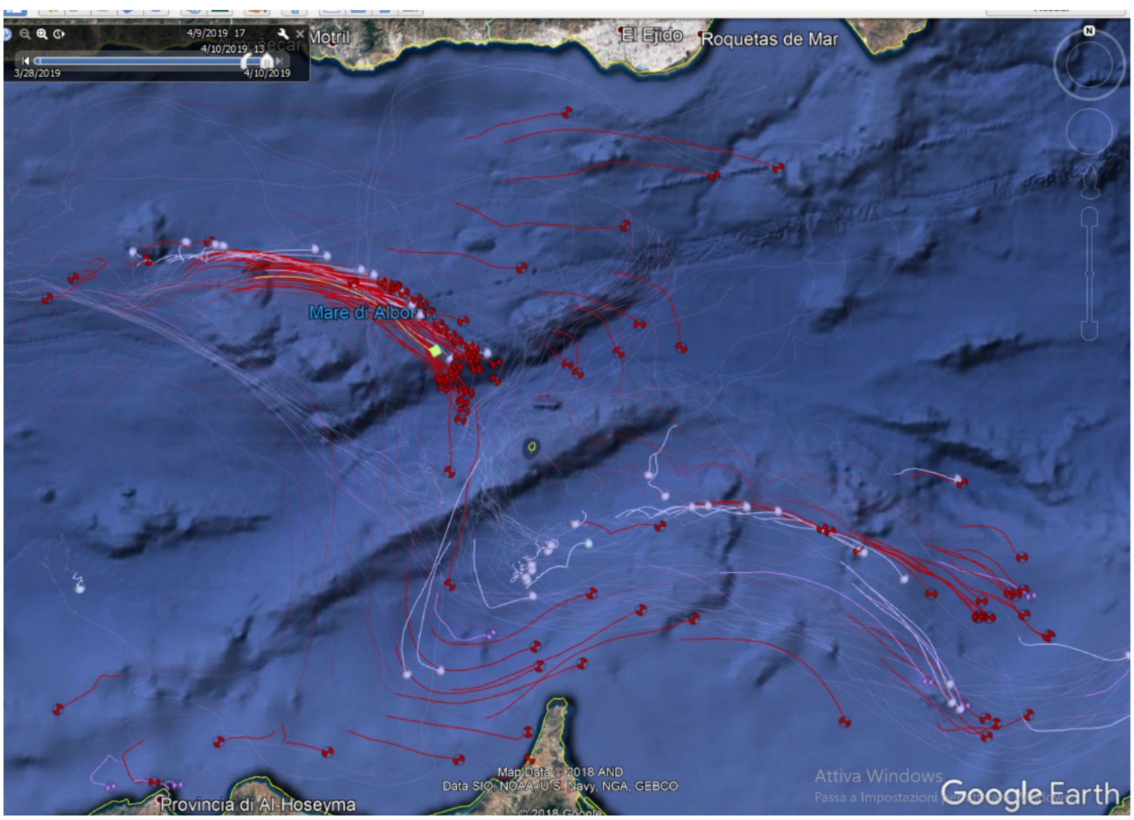


Figure 4.2: Trajectories between 9 and 10 April 2019 of all CODE (magenta), CARTHE (red) and SVP (white) drifters. Symbols represent the last locations. The last position of the CODE ADCP drifter is shown with a yellow dot.

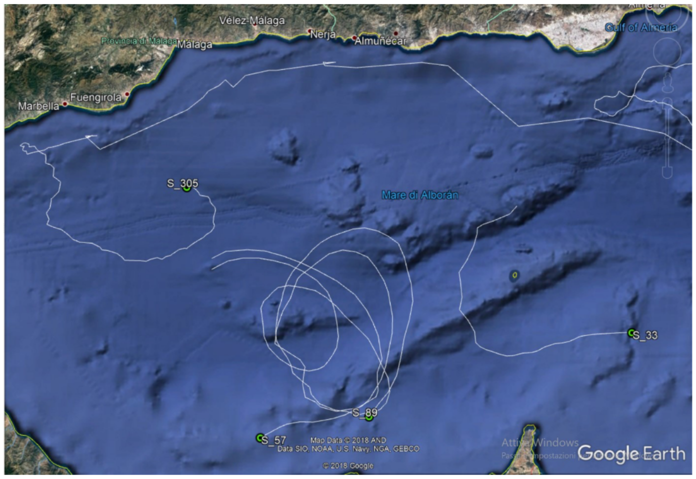


Figure 4.3: Trajectories the Argo floats operating in the Alboran Sea during the CALYPSO 2019 campaign. Symbols and numbers correspond to their locations on 10 April 2019 (S_305 = WMO 3901974, S_89 = WMO 6903264, S_57 = WMO 6903265 and S_33 = WMO 6903266).

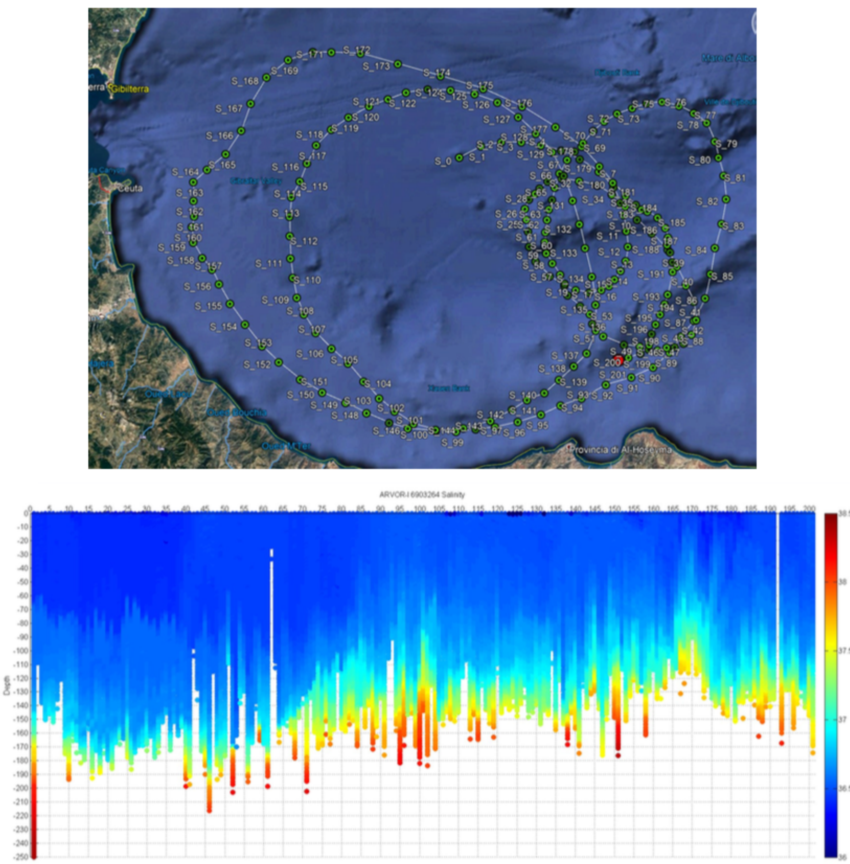


Figure 4.4: Trajectory and profile locations (top) and salinity versus depth and profile number (or time, bottom) for ARVOR float WMO 6903264 between 30 March and 24 April 2019.

All WHOI drifters initially followed anticyclonic circulation around the outer part of the WAG, later transitioning into the anticyclonic flow around the outer perimeter of the smaller EAG. Initially, deeper drifters veered northward, on average, compared to shallower layers, but the drifter tracks at different layers converged back together near the southern part of EAG.

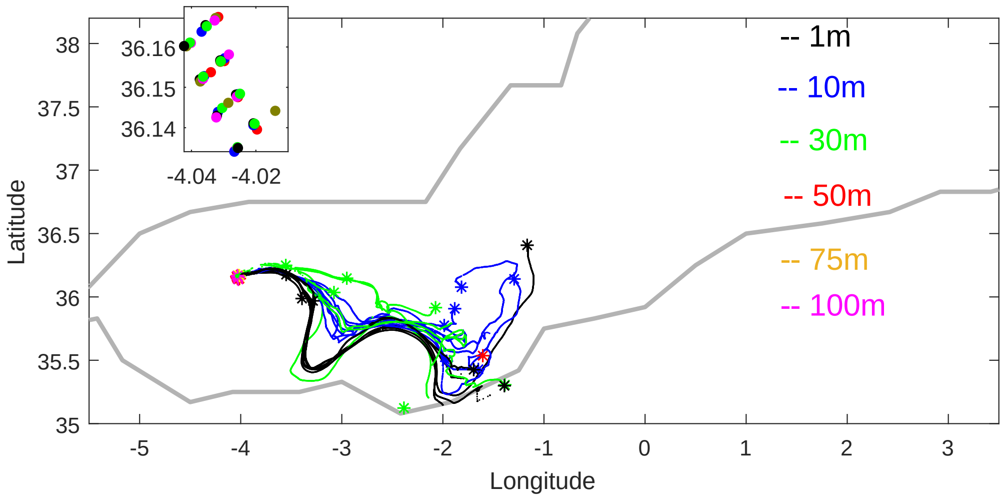


Figure 4.5: Trajectories of WHOI layered drifters color-coded by drogue depth. Asterisks mark last obtained GPS position. Small inset shows deployment locations.

## 4.7 Conclusions and recommendations

Overall the drifter and float operations carried on during the CALYPSO 2019 Experiment on 28 March – 10 April 2019 went well, despite problems with CODE drifters. The deployment operations were performed by the various teams onboard *N/O Pourquoi Pas?* in a coordinated and efficient way. The data collected by the Lagrangian instruments during and after the campaign are of good quality and will provide new and interesting results on the dynamics and circulation in the Alboran Sea and Western Mediterranean.

A few recommendations for the future CALYPSO experiments in the Alboran Sea are:

1. Drifters can be deployed safely at ship speeds as high as 12 kts. This will allow for deployment of arrays of a large number of drifters quasi-synoptically.

2. Given the size of *N/O Pourquoi Pas?* GPS fixes should be made near the deployment locations with hand-held GPS. The bridge GPS is different because the ship is long (∼110 m).

# Chapter 5

# Shipboard ADCP

Andrey Shcherbina (UW)

## 5.1 Overview

PQP has two hull-mounted Ocean Surveyor RDI ADCPs - 150 and 38 kHz.

They were operated by *N/O Pourquoi Pas?*s electronics technician team. They handled the configuration of the instruments, with some input from the science team.

The ADCPs are operated in the VmDAS framework. Data files are also restarted daily.

The standard procedure was to switch from "shallow water/petit fond" (typically broadband with bottom tracking) to "deep water/grand fond" (typically narrowband without bottom tracking). The science team requested to keep OS150 in broadband mode through most of the cruise. We also tried to keep OS38 in bottom-tracking mode, but it interfered with OS150, so we switched back to the "deep water" config at 09:33UTC on 30 March 2019. OS38 had a short break in sampling on 28 March 2019 (from 15:07 to 15:20) due to mis-configured synchronization.

## 5.2 Configuration

Heading source was inertial navigation (PHINS), no pitch/roll input, calculated speed of sound (using a fixed salinity of 35 ppt).

Ping intervals were quite irregular. The typical ping interval was 0.8-2 s for OS150 and 3-8 s for OS38, depending on bottom tracking settings.

Configuration changes and data file rotations were recorded in the "changement_fichier*.doc" files and summarized in Tables 5.1 and 5.2. OS150 configuration was custom-tuned to allow better resolution and lower noise levels (bin size reduced to 4 m, ambiguity velocity [WV] reduced to 1.7-2 m/s). OS38 used default shallow-/deep-water configurations.

Table 5.1: OS150 configuration

| Date/Time | Config file | Data file # | Bot. track? | Broad-band? | # of bins | Bin size (m) | $1^{st}$ bin (m) | Ambiguity vel. (m/s) |
|---|---|---|---|---|---|---|---|---|
| 28/03/19 07:26 | pp150ptfd_1.5.txt | 1 | Y | Y | 50 | 4 | 8.24 | 3.9 |
| 28/03/19 11:58 | pp150gdfdNB_1.5.txt | 2 | N | N | 55 | 8 | 11.9 | 3.9 |
| 28/03/19 13:33 | pp150ptfd_1.5.txt | 3 | Y | Y | 50 | 4 | 8.2 | 3.9 |
| 28/03/19 15:07 | pp150gdfdBB_CALYPSO.txt | 4-9 | N | Y | 50 | 4 | 8.6 | 1.7 |
| 01/04/19 07:44 | pp150gdfdBB_CALYPSO_2.txt | 10-18 | N | Y | 65 | 4 | 8.2 | 2.0 |

Table 5.2: OS38 configuration

| Date/Time | Config file | Data file # | Bot. track? | Broad-band? | # of bins | Bin size (m) | $1^{st}$ bin (m) | Ambiguity vel. (m/s) |
|---|---|---|---|---|---|---|---|---|
| 28/03/19 07:26 | pp38ptfd_SynchroExterne_V1_4.txt | 1 | Y | Y | 80 | 16 | 27 | 3.9 |
| 28/03/19 12:00 | pp38gdfdNB_SynchroExterne_V1_4.txt | 2 | N | N | 62 | 24 | 48 | 3.9 |
| 28/03/19 13:33 | pp38ptfd_SynchroExterne_V1_4.txt | 3-7 | Y | Y | 80 | 16 | 27 | 3.9 |
| 30/03/19 09:33 | pp38gdfdNB_SynchroExterne_V1_4.txt | 8-19 | N | N | 62 | 24 | 48 | 3.9 |

# 5.3 Initial Assessment

## Alignment

Both ADCPs appear well aligned (Fig. 5.1). Perhaps 1% amplitude correction in OS150 is worth looking into (3 cm/s bias at 6 kts).

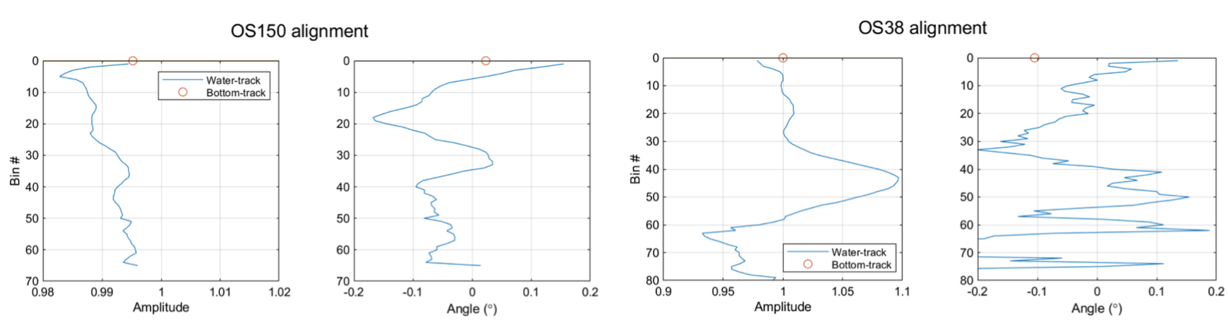


Figure 5.1: ADCP alignment.

## Navigation lag

Navigation seems to be lagging by about 10 s during the turns (Fig. 5.2).

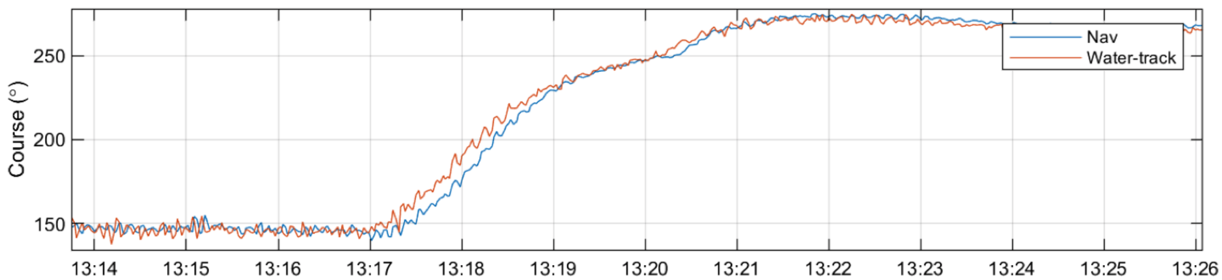


Figure 5.2: Course over time for the water-track and the navigation system, demonstrating the navigation lag.

This is somewhat unexpected: I could understand if it were the other way around, the inertial heading (and therefore water-track course) lagging. Can it be due to a lateral offset between the GPS and the ADCP? Or some data stream delays?

Whatever is the cause, there was occasionally up to 10° error in the ship's course during the turns, which resulted in noticeable velocity bias (up to ±50 cm/s!) (Fig. 5.3).

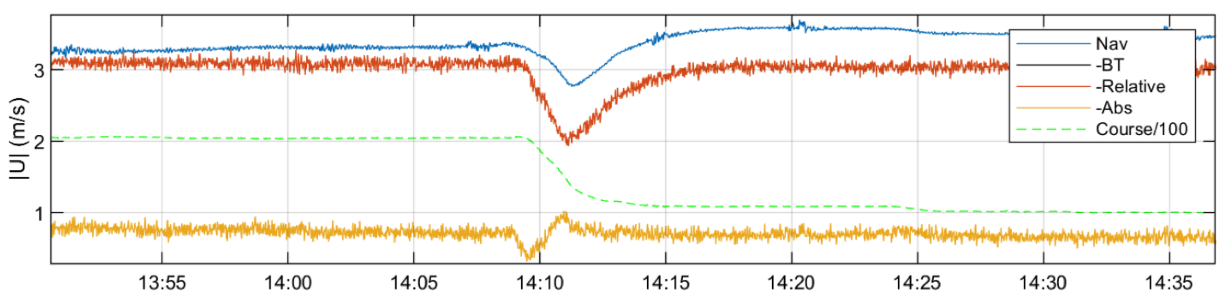


Figure 5.3: Velocity bias caused by navigation lag during turns.

**Further investigation of the navigation lag is recommended. For now, all sampling during turns should be considered unreliable.**

## Data quality, QC

Automatic QC based on signal correlation was applied in-instrument, using the default threshold of 120 counts (for broadband signals). Velocity values with lower correlations were blanked.

Reliable range (90% good data) was approximately 120 m for OS150 and 900 m for OS38 on average. At night, reliable data could be obtained by OS150 down to 200-250 m due to better concentration of scatterers.

## Interference

There seems to be some interference from OS38 in OS150 data. Figure 5.4 shows an example of OS150 echo amplitude (bin 50); OS38 was off from 15:07 to 15:20.

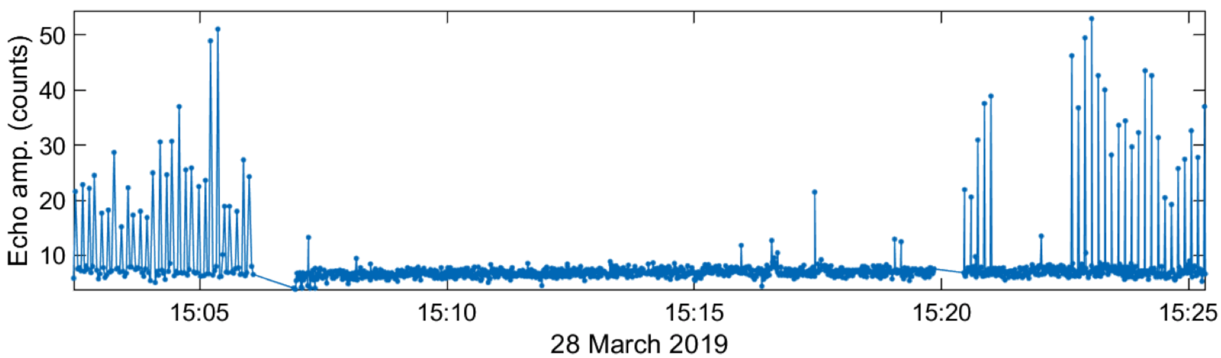


Figure 5.4: Echo amplitude for OS150 showing potential interference from OS38.

Interference was marked with high amplitude and low correlation (but not low enough to be a useful metric or trigger the automatic QC filtering).

It was suspected that the interference was due to OS38's bottom tracking (BT). Interference spikes did line up with OS38 ping timing, but they came and went (probably depending on the BT auto-tune). OS38 BT was turned off at 09:33UTC on 30 March 2019, and the interference was eliminated.

Velocity data are expected to be severely affected by this interference, especially towards the far reaches of the range where SNR was lower. Relative velocity measurements affected by the bias could be reduced by factors of 2-10 (based on quick look), which translated to absolute velocity errors of a few m/s. Short- and long-term averaged data files (STA, LTA) are affected by this bias, even though it may not be apparent. **For OS150 observations prior to 30 March, additional QC of single-ping data is recommended.**

Some other high-amplitude, low-correlation interference signal was commonly seen (Fig. 5.5). Most of it was flagged by the automatic QC. What remains is of less concern, since this interference is too intermittent to affect averages.

Patches of low-amplitude, low-correlation returns were commonly seen (Fig. 5.6). They

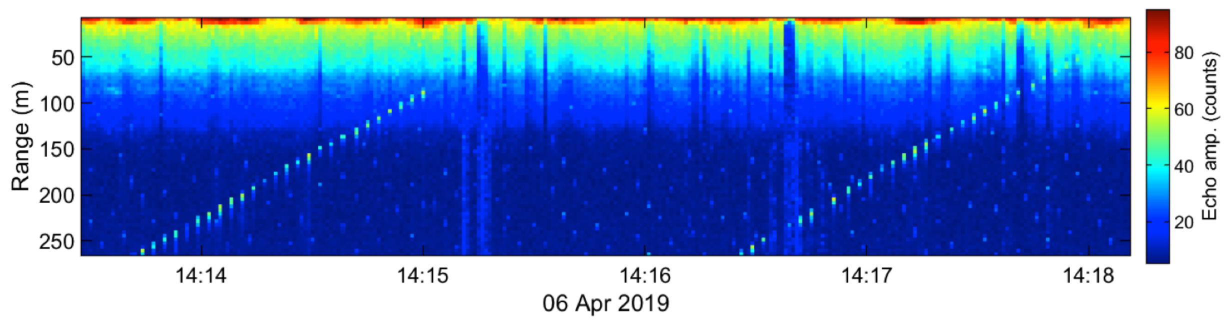


Figure 5.5: Echo amplitude over time showing high-amplitude, low-correlation interference.

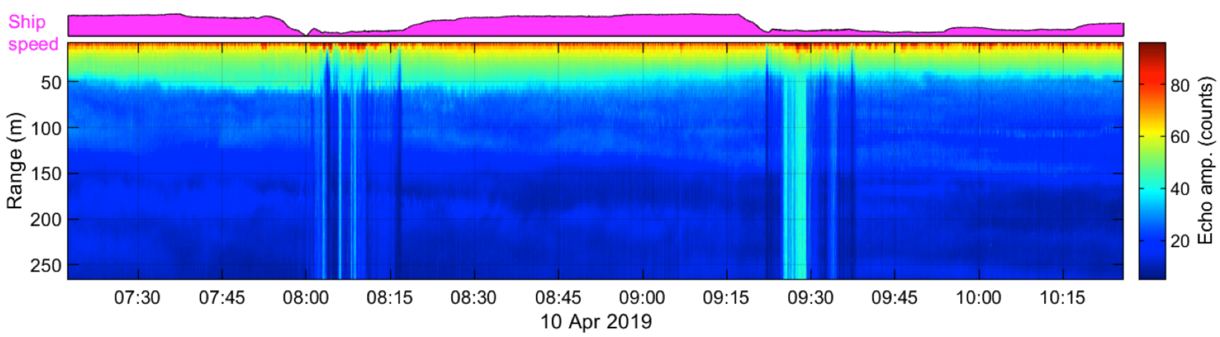


Figure 5.6: Echo amplitude over time showing low-amplitude, low-correlation interference.

mostly occurred at stations, but also occasionally underway. Bubble plumes from the lateral thrusters (on-station) and heavy seas (underway) may have been the cause. Note that there are also patches of high amplitude, but still low correlation (e.g., @09:30); I have no explanation for those. Automatic QC filters out most of them.

There were some other (unidentified) sources of low-amplitude, low-correlation interference (Fig. 5.7). This pattern of interference went away on 1 Apr 2019, coincident with the configuration change (but it is not clear which parameter made it go away). Due to its low correlation, this particular mode of interference was also filtered by the automatic QC.

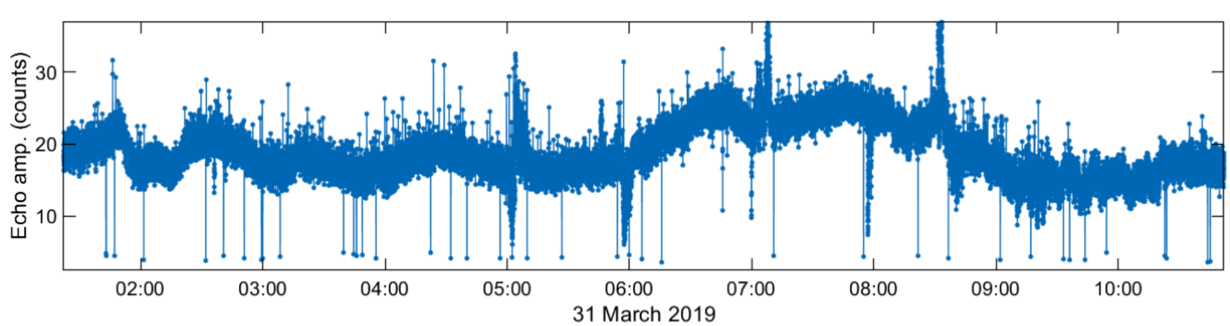


Figure 5.7: Echo amplitude over time showing unidentified low-amplitude, low-correlation interference.

# Chapter 6

# Microstructure Observations

Francesco M. Falcieri (CNR-ISMAR)

## 6.1 Introduction

### Instrumentation

During the CALYPSO 2019 cruise on *N/O Pourquoi Pas?*March 28$^{\mathrm{th}}$ to April 3$^{\mathrm{rd}}$), microstructure observations were collected with a modified version of the MSS90L (serial number 069, operated by CNR-ISMAR) produced by Sea & Sun Technology GmbH; its general characteristics can be found in detail in *Prandke et al.* [2000]. In order to cope with the transmitting cable length (approximately 1300 m), a signal booster has been integrated to the standard RS 485 data telemetry to increase the signal strength of the binary data transmission. Furthermore, an internal averaging over two data samples has been implemented into the profiler electronics to reduce the rate of data samples transmitted to 512 Hz (instead of 1024 Hz). The profiler dimensions are: housing length 1.25 m, diameter 90 mm, weight outside water 16 kg. The maximum depth of operation is 1300 m.

The MSS 90L profiler main features are:

- standard CTD:
  - Pressure
  - Temperature
  - Electrical conductivity
- microstructure/turbulence:

  - 2 microstructure shear sensors
  - Microstructure temperature sensor

- Optical measurements:
  - Turbidity (light scattering) sensor (Seapoint)
  - Chlorophyll fluorescence Cyclops 7 (Turner)

- Control sensors:
  - Vibration
  - 2 axis tilt sensor

- 1300m cable

- electric winch

All sensors, apart from pressure, are mounted on the lower end of the MSS chase. The microstructure sensors are placed on the top of a 150 mm shaft in front of the CTD sensors so as to collect microstructure observations in a field undisturbed by the passage of the probe (figure 6.1).

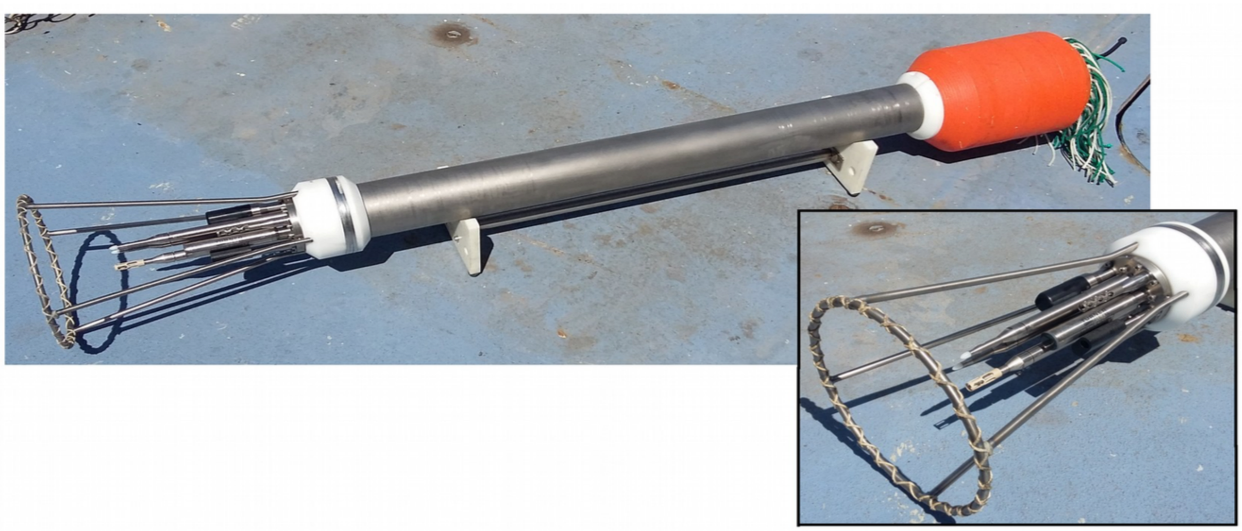

Figure 6.1: The MSS90L No. 069 used during the CALYPSO 2019 cruise. Insert shows the sensor head.

## 6.2 CALYPSO 2019

### Measurements strategy and system set up

The aim of the microstrucure measurements during CALYPSO 2019 was to study the vertical mixing across the frontal zone of a gyre, located in the western side of the Alboran Sea, and integrate other observations collected with CTD and UCTD. MSS measurements were done after each CTD station of Leg 1 with two casts per station repeated in sequence. This permits us to average observations between casts and obtain more statistically sound values. In line with the focus of the cruise, profiles were done up to 200 m depth. For vertical sinking measurements, the profiler was balanced to present a negative buoyancy which resulted in a sinking velocity between 0.6 and 0.8 m/s. The profiler was operated using a dedicated winch for microstructure profilers (Microstructure ship winch type SWM1000, see figure 6.2). The winch was mounted on a steal stend located at the stern of the *N/O Pourquoi Pas?*nd secured to the deck through an anchoring plate and several straps (figure 6.2). During the MSS measurements, the ship was sailing at the lowest possible speed (between 0.5 and 1.2 knots) in order to move away from the cable and from the sinking profiler. Disturbing effects on turbulence measurements caused by cable tension (vibrations) and the ship's movement were prevented by a cable release faster than the sinking velocity so as to create a significant slack in the cable between the ship and the profiler.

Figure 6.2: The winch set up at the stern of *N/O Pourquoi Pas?*

During the CALYPSO 2019 cruise a total of 43 microstructure profiles were collected.

## 6.3 Data processing

For each cast, data logging was stopped at the beginning of the recovery at 200 m depth, since only the downcast is used for processing and the upcast data are removed. After conversion into physical data, a de-spiking routine was applied by checking for values outside a given error range calculated as 2.7 times the standard deviation over intervals of 40 observations. Data that fall outside the valid range are removed and substituted by interpolation. To suppress high frequency noise in the pressure signal, and consequently in the computed sinking velocity, the pressure channel was low pass filtered. This was done using a moving average with a window width of approx. 1.5 m. The first 18 m of each cast were excluded for the turbulence parameters computation to account for the ship wake. The wake depth was defined as three times the 6 m draft of the *N/O Pourquoi Pas?*

At the end of data processing three type of files were produced for each station:

- MSS_ext_CTD: 1 m averages starting from the 1.5 m depth of the CTD parameters (temperature, salinity and pressure), chlorophyll and turbidity;
- MSS_espi_1m: 1 m averages of all the parameters observed and computed in data processing;
- MSS_espi_5m: 5 m averages of all the parameters observed and computed in data processing.

In the files loaded on the *N/O Pourquoi Pas?* erver the chlorophyll and turbidity observations have not been processed and filtered for spikes.

## 6.4 Preliminary analysis on Transect #2 stations 006-012

The second transect done on March 30 from the coast in front of Málaga to the center of the gyre will be shown. The transect started on CTD station 006 (MSS_014, figure 6.3) located outside the gyre toward the Spanish coast. In the microstructure profiles a 70 m mixed layer is visible with high TKE values in the surface layer and near the pycnocline. Below the mixed layer several peaks in TKE can be seen in the correspondence of small steps in the pycnocline (110 m and 130 m).

The second (CTD 007, MSS015/016, figure 6.4) and third (CTD 008, MSS017/018) stations are located in the frontal area and show similar behavior, hence just CTD007 will be shown (figure 6.4). A deep (150 m) mixed layer is present with several TKE peaks over $10^{-7}$ W/kg,

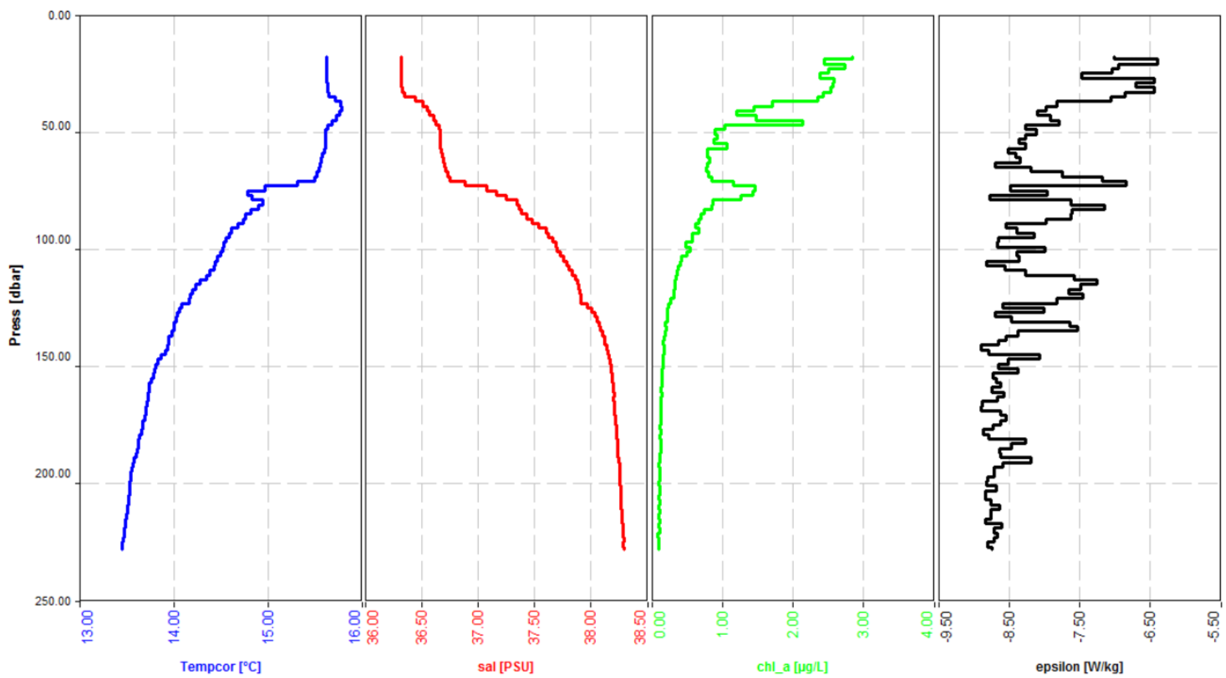


Figure 6.3: Microstructure observations at station CTD 006 averaged over 5 m bins. Plots show temperature (blue), salinity (red), Chlorophyll (green) and the average of the turbulent kinetic energy dissipation rate (black) computed from the two shear sensors.

pointing to intense mixing. A deepening of high values in chlorophyll can be seen between 50 and 115 m. Below the mixed layer TKE presents low values around $10^{-9}$ W/kg.

The last 4 stations of the transect are located inside the gyre. CTD009 (MSS019/020, figure 6.5) shows a slightly colder water intrusion around 80 m depth and an area between 80 and 130 m with high chlorophyll concentrations delimited by dissipation rates up to $10^{-6.5}$ W/kg. This same chlorophyll signal is visible at the innermost station (CTD012, MSS025/026, figure 6.6) at depths between 150 and 200 m, whereas it is not present in the temperature and salinity profiles. It is of interest to note that TKE values at the upper and lower limit of the signal are high, about $10^{-6.5}$ W/kg, considering the depth. This points to the presence of strong shear or internal waves at the interface that cause an increase in turbulence dissipation.

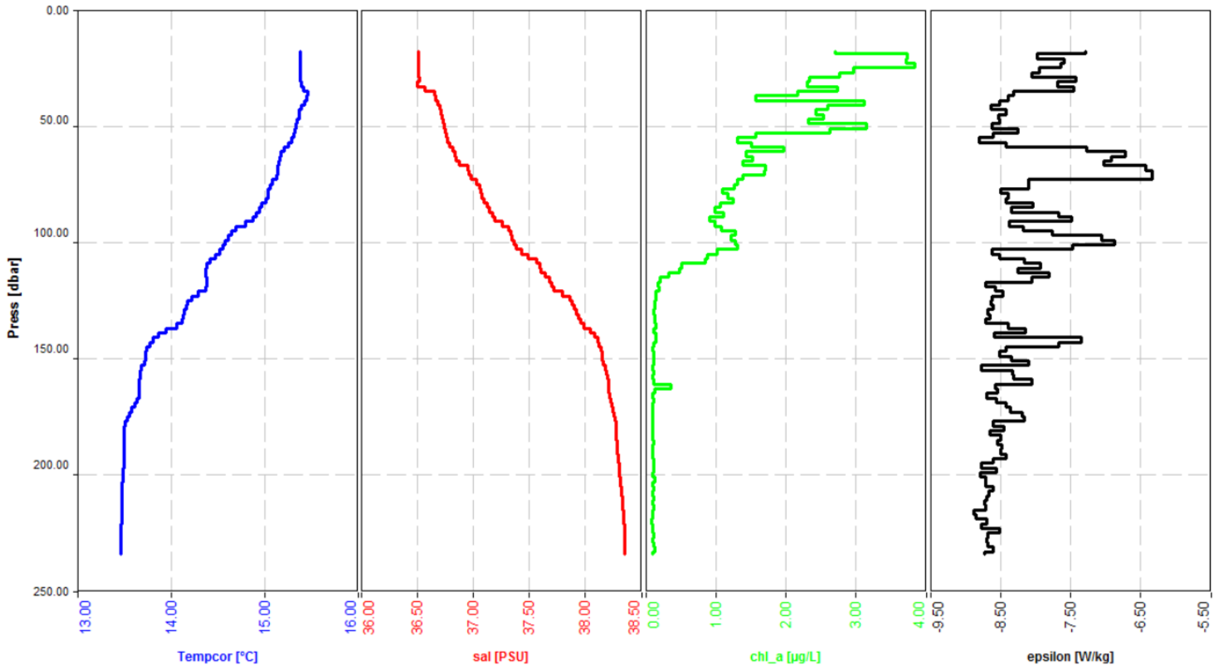


Figure 6.4: Microstructure observations at station CTD 007 averaged over 5 m bins. Plots show temperature (blue), salinity (red), Chlorophyll (green) and the average of the turbulent kinetic energy dissipation rate (black) computed from the two shear sensors.

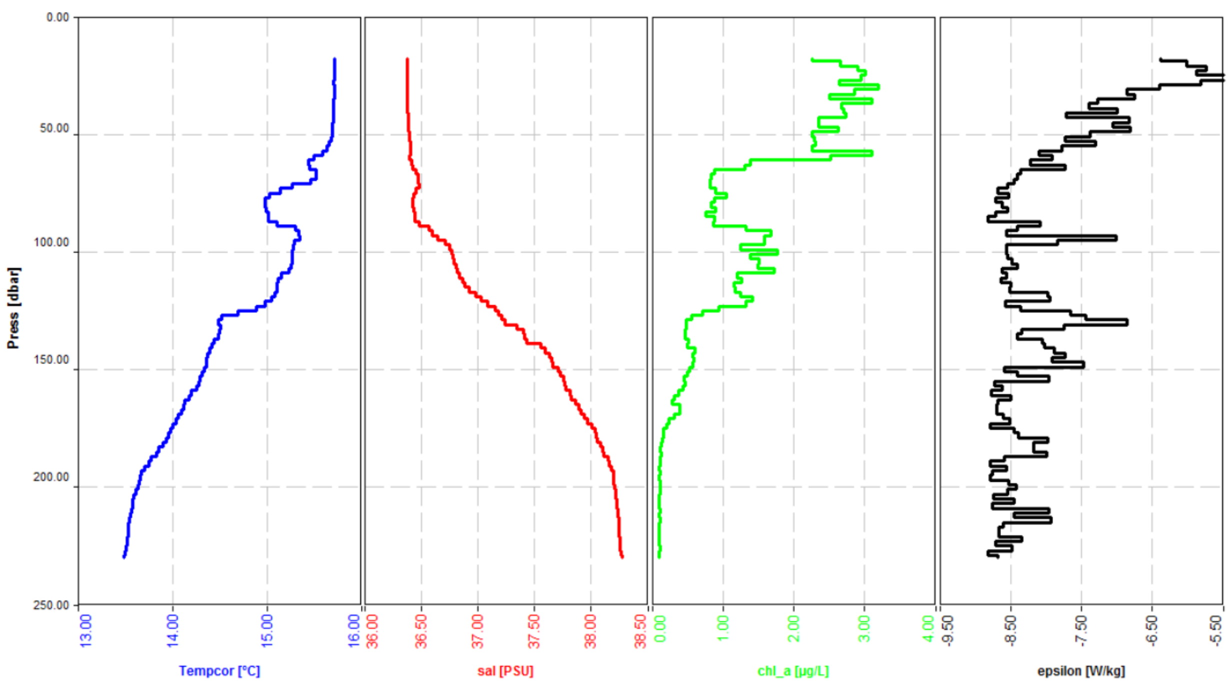


Figure 6.5: Microstructure observations at station CTD 009 averaged over 5 m bins. Plots show temperature (blue), salinity (red), Chlorophyll (green) and the average of the turbulent kinetic energy dissipation rate (black) computed from the two shear sensors.

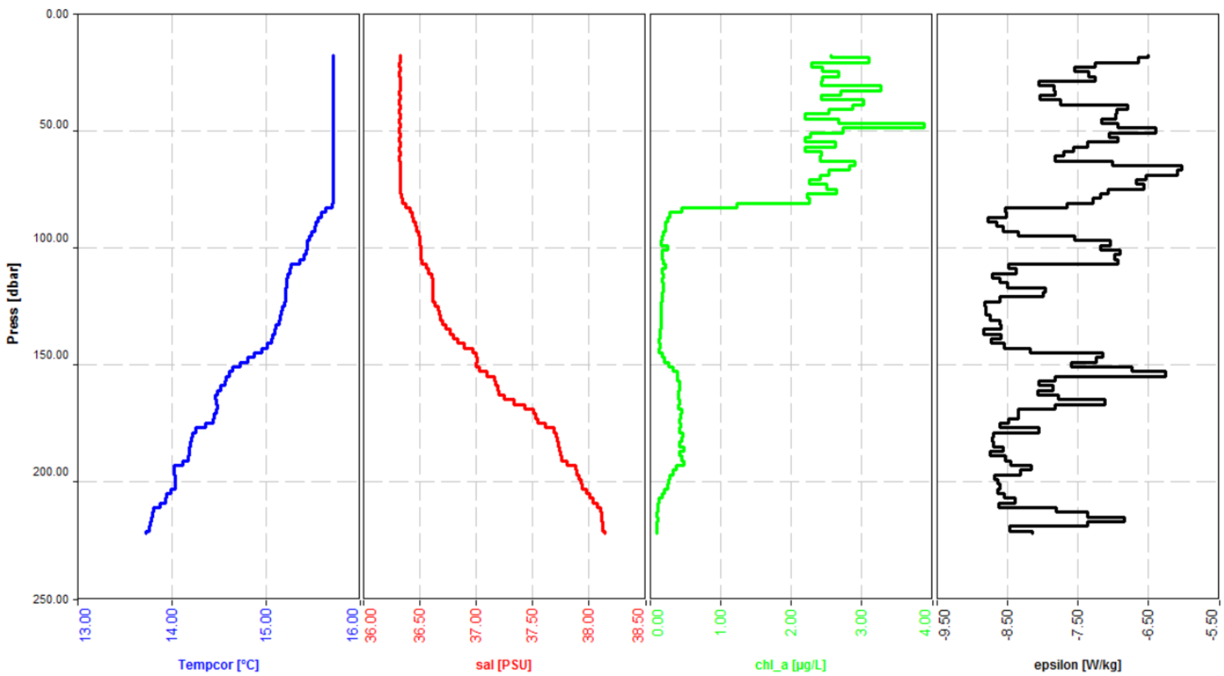


Figure 6.6: Microstructure observations at station CTD 0012 averaged over 5 m bins. Plots show temperature (blue), salinity (red), Chlorophyll (green) and the average of the turbulent kinetic energy dissipation rate (black) computed from the two shear sensors.

# Chapter 7

# V-Wing Operations

Ben Hodges (WHOI)

The V-Wing arrived onboard the *N/O Pourquoi Pas?*n April 4, and a shakedown deployment was carried out under the direction of Ben Hodges and Ray Graham that same day. The configuration for the test exactly repeated that used during the deeper tests from the *Tioga* in December 2018, except that instruments without pressure sensors were omitted; instrument placements are listed in Table 7.1. At the request of the crew, who were concerned about the lack of a bale, a 7-meter-long tagline was fixed to the V-Wing at the tow cable mount point, and secured every foot or so to the tow cable by a wrap of electrical tape, so that, if required during recovery, the end of the line could be accessed with the V-Wing still below the surface. This line, and the higher towpoint (roughly 6 meters above the surface) were the only significant differences from the earlier test. The sheave hung on a cable that ran to a winch mounted on the starboard side of the A-frame, so could be raised or lowered as desired. The deployment began at 15:25Z, and a 4-knot tow commenced at 15:45Z. At 16:15Z, the speed was increased to 6 knots, at 16:45Z we began the recovery, and everything was back on board by 17:00Z. The lateral excursions seemed smaller at 4 knots than 6, and it was decided that the science deployments would be carried out at that speed. The catenary shape was plotted, and was very similar to that obtained from the earlier *Tioga* test. Andrey Shcherbina set up the Nortek Signature 500, and configured it to log data in beam coordinates.

| *Position on line (m from V-Wing)* | *S/N* | *Instrument* |
|---|---|---|
| 0 | 100253 | Signature 500 |
| 20 | 17263 | XR420 TCP |
| 35 | 13249 | XR420 TCP |
| 50 | 66098 | Concerto |
| 65 | 82991 | duet |
| 80 | 82990 | duet |

Table 7.1: April 4 test: Instrument positions along towline.

The sole science deployment took place on April 9. We aimed to tow the V-Wing at a depth of approximately 50 meters so that it would be able to return current velocities all the way to the surface. On the recommendation of biologists on board, we targeted a depth of 20 meters with the Concerto (which provides the only observations of chlorophyll fluorescence and oxygen concentration). Other instruments were arranged along the line in an attempt to avoid large gaps between pressure and conductivity observations. All the available loops over the chosen length of cable were occupied by multi-sensor instruments, so no solo-T's were deployed. The placements are listed in Table 7.2. The deployment began at 09:30Z, and by 10:00Z the ship, near 36°17'N, 3°50'W, had settled into a 4-knot tow along a course of 158°. This was a repeat of a transect that had recently been sampled by the UCTD, and was known to cross a (weakish) front. Line tension, measured over a 5-minute period during the tow, varied from 220 to 250 lb. The UCTD was deployed during the tow, from a point just inside the A-frame on the port side, perhaps 10 meters from the V-Wing tow line. There was suspicion that the lines were interfering by the personnel manning the UCTD winch, and on inspection, blue fibers matching the V-Wing Amsteel tow line were found on the UCTD line near the probe, so after two tow-yos, UCTD operations were suspended. No damage to either system was noted. Recovery commenced shortly after 11:30Z, and was completed by 12:00Z.

| *Position on line (m from V-Wing)* | *S/N* | *Instrument* |
|---|---|---|
| 0 | 100253 | Signature 500 |
| 5 | 15246 | XR420 TC |
| 12.5 | 17562 | XR420 TC |
| 20 | 13249 | XR420 TCP |
| 27.5 | 17560 | XR420 TC |
| 35 | 82991 | duet |
| 42.5 | 66098 | Concerto |
| 50 | 17559 | XR420 TC |
| 65 | 17263 | XR420 TCP |
| 80 | 82990 | duet |

Table 7.2: April 9 deployment: Instrument positions along towline.

The CTD on the 20-meter loop (SN 13249) was mistakenly set to begin sampling at a PM hour rather than AM, and so did not record data. The CT instrument on the 12.5 meter loop also did not record data, although it was configured correctly (screen shots of the configuration screen for each instrument were taken before the deployment).

The ADCP, again set up by Andrey Shcherbina, was this time configured to return data in earth coordinates, with 30 2 meter bins, 8 Hz sampling, and 1.5 meter blanking. I (BH) have no expertise in ADCP data, so the following figure and description are to be taken with a large grain of salt. That said, it appears that there are coherent structures in velocity resolved by the instrument, and the front that can be seen near the 6 km mark in the T and S observations also appears in the current velocity.

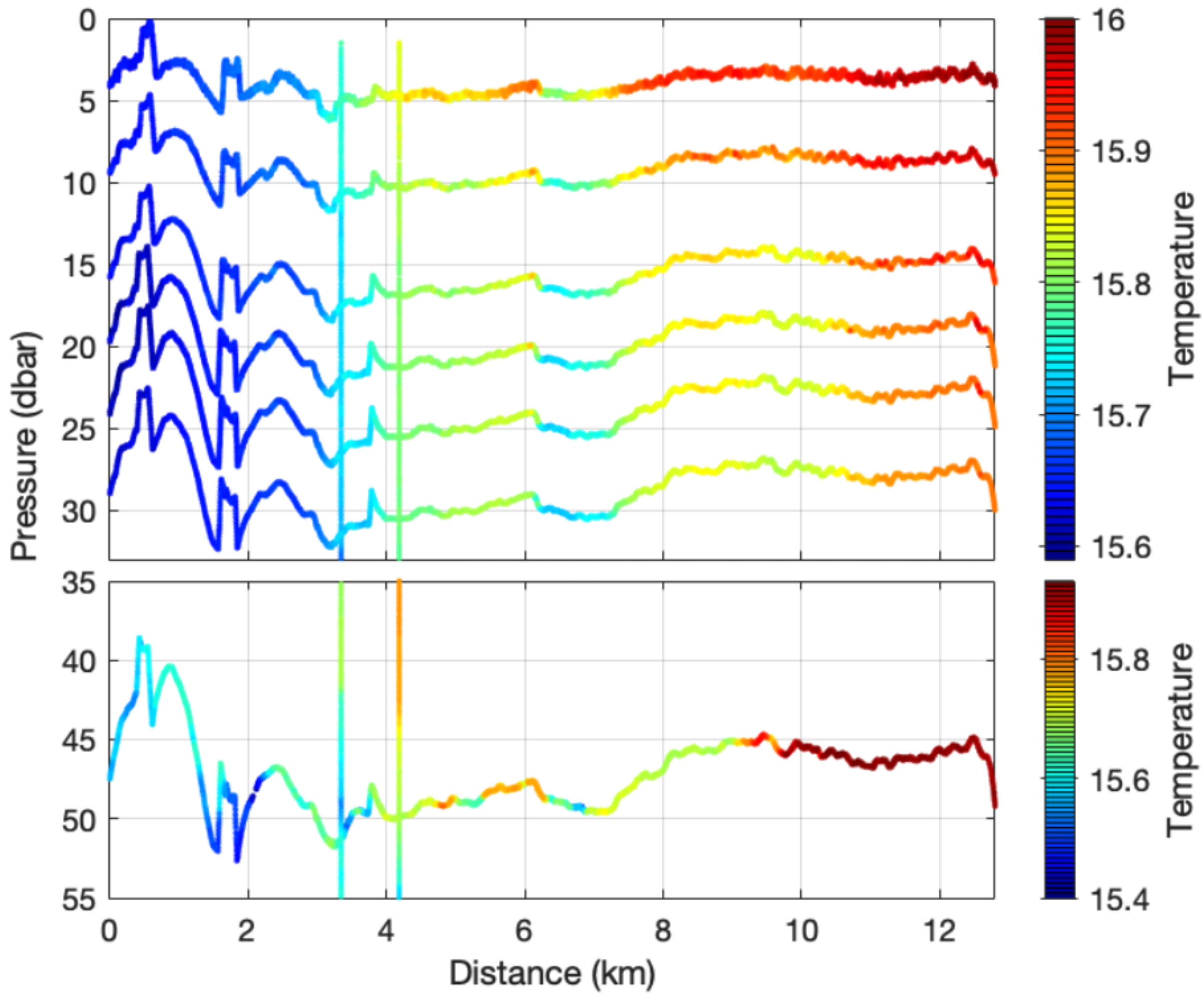


Figure 7.1: Temperature observations from the line-mounted sensors. Also shown is temperature from the two UCTD profiles made during the tow. The deepest sensor is located in the pycnocline, and so is shown with a different colorbar than the rest of the observations to more clearly show structure.

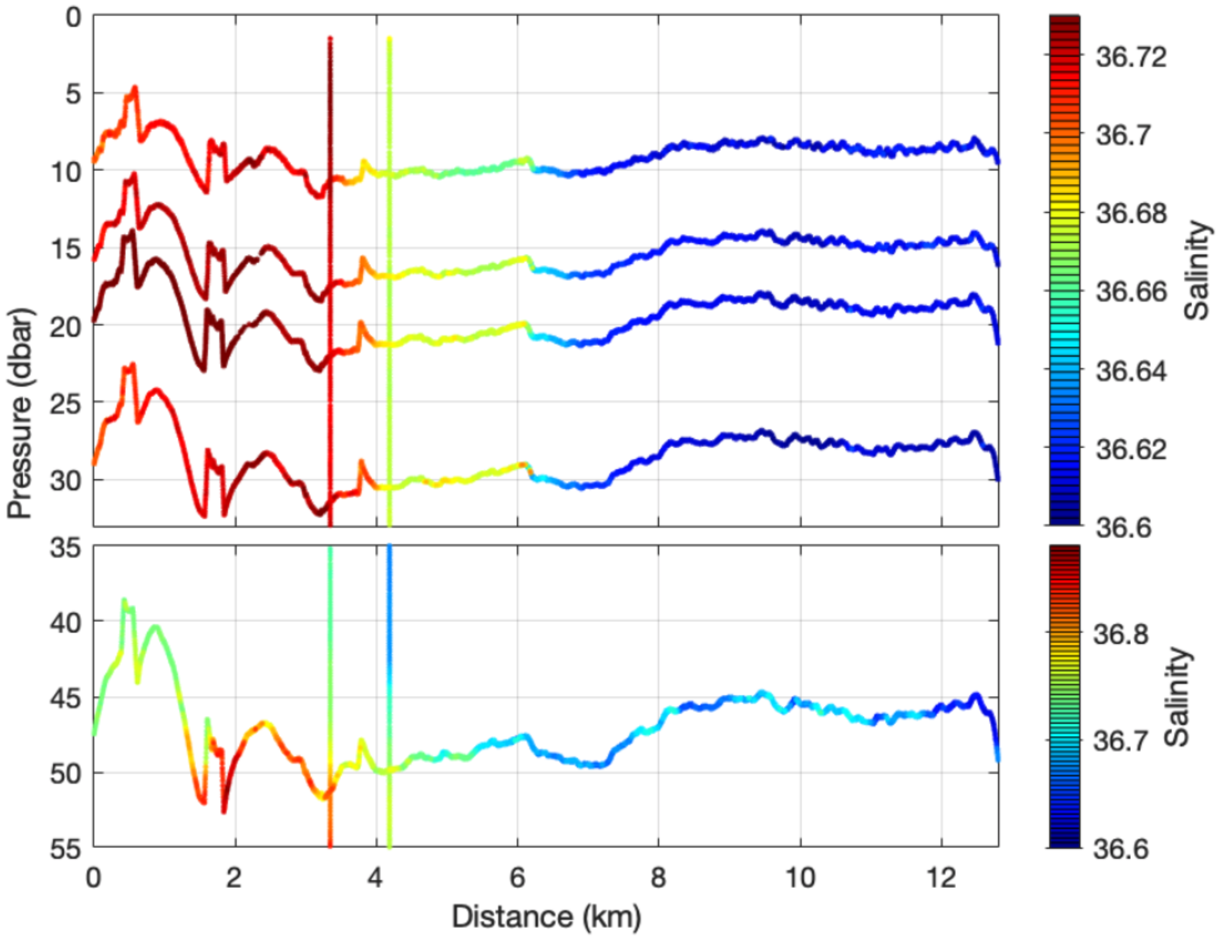


Figure 7.2: Salinity, presented in the same manner as temperature (see Fig. 7.1). For the purposes of this report the conductivities have been shifted to roughly minimize discrepancies, but there are offsets amounting to about 0.15 psu in the raw salinity output by the various instruments which will require careful treatment.

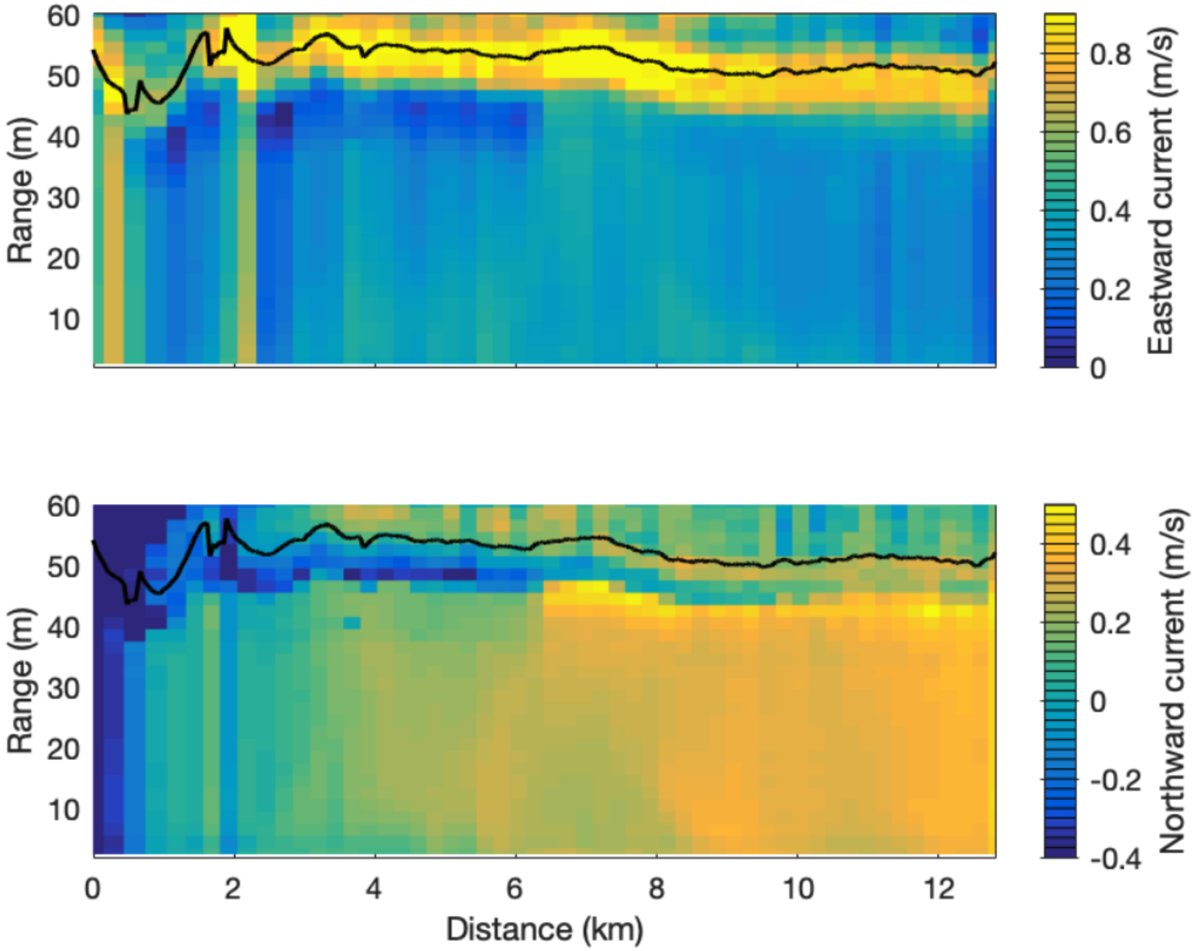


Figure 7.3: Current velocity from the Nortek Signature 500 upward-looking ADCP mounted in the V-Wing. The ship's motion has been subtracted using a 1 Hz GPS log. The raw 8 Hz velocities have been bin-averaged to 2 minutes to reduce the effect of the lateral motion of the V-Wing – along-track velocities appear to be uncontaminated at higher resolution. The artifacts near the beginning of the record are due to adjustments to the tow-cable winch and the height of the sheave, which were altered several times to obtain the desired depth of the uppermost sensor and a nice lead over the sheave. These adjustments are not measured or recorded, and so cannot be corrected for in the same manner as can the ship's motion. The pressure recorded by the V-Wing, in dbar, is plotted in each panel as a black line, corresponding to the location of the surface (the vertical coordinate is range from the V-Wing rather than depth). The upper 8-10 meters appear to be contaminated, most likely by side-lobe reflections from the surface.

# Chapter 8

# Wirewalker Operations

Ben Hodges (WHOI)

On April 4, the Wirewalker belonging to Melissa Omand (URI) was assembled on board the *N/O Pourquoi Pas?* The central instrument was an RBR Maestro CTD, which acted as a logger for the Rinko oxygen sensor, WetLabs chlorophyll fluorometer/backscatter meter, and C Star beam transmissometer. Separately logged sensors included PAR on both the Wirewalker body and the buoy, and a Nortek single-point acoustic current meter.

The vent plug for the external battery pack had been packed separately from the rest of the Wirewalker paraphernalia, and was not located immediately. A member of the crew made a brass plug to seal the hole. It was deemed too rough to attempt to ballast the instrument by overboarding, so, starting at 16:00Z, the procedure was attempted in the moon pool. The water level in the pool varied by several feet with the swell and the movement of the ship, so it was not feasible to observe the behavior of the Wirewalker on its test cable. Instead, it was lowered into the water without its cable, and repeatedly submerged so that the rise rate could be estimated. It was difficult to obtain an accurate estimate, but it seemed to be in the neighborhood of the specified 20 cm/s, and we decided not to adjust the buoyancy.

A test deployment was begun shortly after 17:00Z, and the buoy was released by 17:45Z. The squirt boom on the starboard side was used. Approximately 200 m of wire was loaded onto the winch at the end of the boom, and the lifelines beneath the boom were removed. Recovery started before 19:00Z, and was complete by 19:30Z. During the recovery, the wire angle was closer to horizontal than vertical, and at times far enough aft that the wire slipped off the edge of the guide roller, rubbing over a hard corner on the boom. This damaged the wire, and required it to be shortened to roughly 150 meters for future deployments. An additional problem is that all the wire stacked up on the outboard side of the drum, creating a jam. Also, the copious amount of grease on the winch drum and roller transferred to the cable and thence to the Wirewalker internal mechanism.

From the pressure record, it was apparent that, after having been pulled down to roughly 100 m depth during deployment by current (the wire departure angle was quite horizontal during deployment as well) the Wirewalker rose to the surface at a rate of 10 cm/s and remained just below the buoy for the rest of the test. The slow rise rate could have resulted from poor estimation during the moon pool test, or additional drag from the wire, or a combination. Two potential reasons for the failure to profile were identified: the Wirewalker was ballasted too heavy, and the greasy wire and camming mechanism allowed slippage. Both issues were addressed: the wire was reterminated, removing the damaged section, and the wire, Wirewalker, winch drum, and guide roller were cleaned of grease; and two internal foam blocks were added to increase the net buoyancy by roughly 1 kg. The brass plug in the battery case was replaced by the vent plug, which had been found. However, the temporary plug had cause several problems. First, it had been made with a different thread pitch than the original plug, causing the plastic internal threads to strip. Second, in order to make room for a beefy socket to turn the temporary plug, the crew member had drilled into the plastic endcap with a roughly 1-inch bit. In doing so, he drilled some distance into the sealing surface, preventing the inner boss o-ring from making contact. With stripped threads, neither plug formed a reliable seal, but the threads on the vent plug were full diameter, unlike those on the temporary plug, so it held a bit better, and in addition it had a secondary, face-sealing o-ring. The (in retrospect poor) decision was made to attempt a deployment with the vent plug.

The first science deployment began around 02:00Z on April 8. A carabiner on a rope was clipped around the cable during deployment to allow a crew member to control the feed of cable coming off the drum. Recovery was begun around 18:30Z the same day, again using the carabiner to guide the cable. This operation went smoothly, but the battery case had flooded, popping the upper cap off and destroying the batteries. The Wirewalker had completed 8 cycles to 150 m over the first 90 minutes or so, and had then gotten too heavy to turn around at the surface due to the water accumulating in the battery case. It had remained just below the float for an additional two hours, and then sunk to the bottom of the cable. A few hours later, the batteries fried, indicated in the data by a switch to internal power.

The vent hole was drilled and tapped for a new, larger diameter plug. New internal batteries were installed in the RBR Maestro. The battery case was cleared out, and the weight of its contents replaced by shackles.

The final deployment began at around 23:00Z on April 8. Thirty six hours later, at around 11:00Z on April 10, recovery began. The Wirewalker logged 205 cycles. At around 09:00, two hours before recovery, the optical sensors stopped reporting data, presumably due to dying batteries. The CTD appears to have continued to function normally.

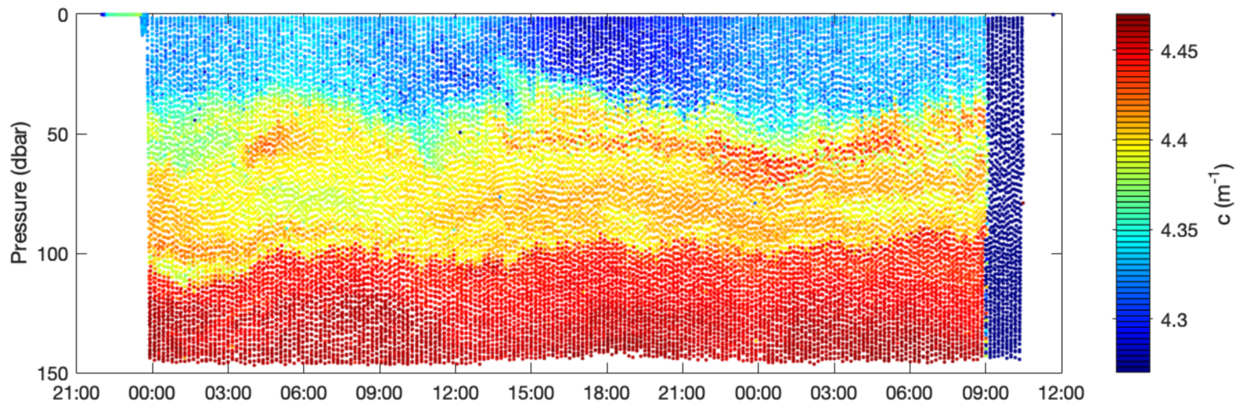


Figure 8.1: Raw data from the C Star beam transmissometer during the final Wirewalker deployment.

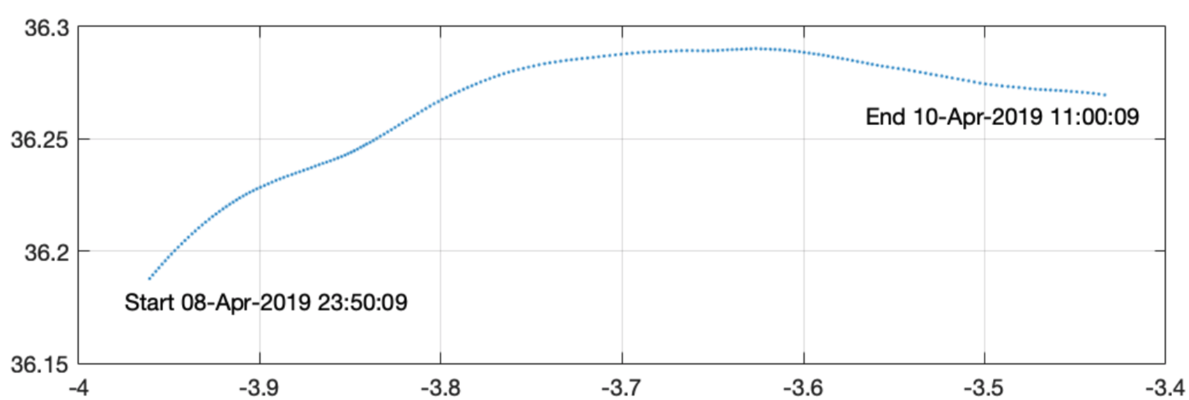


Figure 8.2: Wirewalker drift path for the final deployment (corresponding to the beam c section in Fig. 8.1).

# Chapter 9

# Lagrangian Float Deployments

ERIC D'ASARO (UW)

We brought three identical Lagrangian floats, numbers 81, 82 and 83. Floats 81 and 82 were deployed together once; 83 was a spare. These were standard Lagrangian floats measuring temperature and salinity at the top and bottom (1.4 m apart) and pressure at the top and center of the float. In addition, each carried a Nortek 1 MHz, 5 beam ADCP mounted on the side of the float and pointing upward. This measured 3 components of velocity using broadband pulses at 1 m resolution to about 20 m range and pulse-coherent pulses at 5 cm resolution to 6 m range.

The floats were deployed during the final operation of the cruise within a few minutes of each other on 08-Apr-2019 at 13:55 Z. Both missions ended within a few minutes of 10-Apr-2019 07:06 Z. Both floats were recovered by a boat from the *N/O Pourquoi Pas?*nd were onboard by 09:30 Z.

Float 81 was not ballasted well and most of the mission was spent adjusting the ballasting. This was achieved during the last 20 hours of the mission. During this time the float measured the turbulence in the mixed layer, with some interesting density changes. However, there was little other nearby data to help with the interpretation.

Float 82 was the most interesting record. It was well-ballasted from the previous cruise and operated very well. Figure 9.2 shows the approximate float track, computed by interpolating linearly between surface GPS fixes. The colors show the surface density measured from the *N/O Pourquoi Pas?*nderway system (lines) and the underway CTD (diamonds). The many sections crossing the float track provide good measurements of its environment. There is a clear front between denser Mediterranean mixed water to the north and lighter Atlantic water to the south. The floats were deployed on the dense side of this front and were carried eastward by the frontal current.

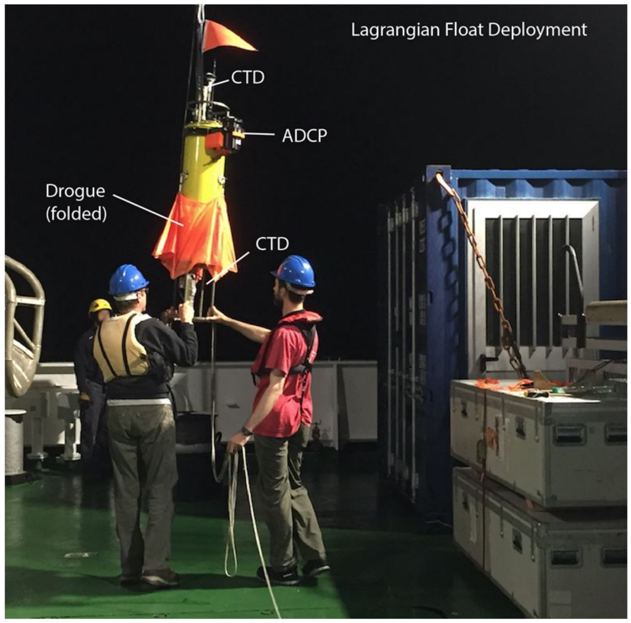


Figure 9.1: Photograph of Lagrangian float being deployed, with components labeled.

The float record is divided into two sections, Part 1 and Part 2, colored magenta and black in figure 9.2. In both, the float subducted beneath lighter water. Part 1 is a stronger subduction. The most interesting part of the record is shown in figure 9.3. During this deployment, wind speeds were close to 10 m/s. These speeds cause vigorous mixing within the mixed layer, as we have measured many times with these floats. The floats rapidly traverse the mixed layer, with their trajectories filling the mixed layer uniformly. An example appears from yearday 99.53 to 99.65 in the bottom panel of figure 9.3, which plots the float depth and the density on each of the two CTDs. From the beginning of its mission to time A, float 82 similarly repeatedly traverses the $\sim$50 m deep mixed layer. Matching its density and depth in the top left section, it is seen to be just north of the front. From point A to B, it descends again, but does not return to the surface. Instead, from points C to D, it stays at the bottom of the mixed layer, first in unstratified water and then in highly stratified water, as can be seen by the difference in density between the top and bottom CTDs near time D. When the float surfaces just after time D, it is seen to be in stratified water. The right top section shows that this has occurred as the front tilted. Matching these float features to the top right section, the float is seen to have been subducted under this sloping front. Float 82 thus subducted under a slumping front and measured the subduction of the dense mixed layer that occurred as the result of this slumping.

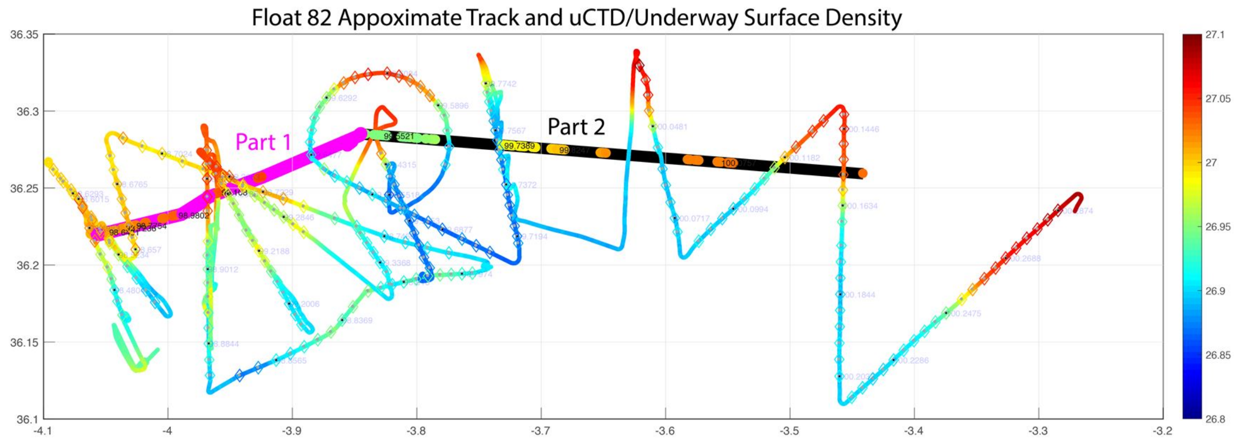


Figure 9.2: Approximate track of float 82, showing float location over time and ship location colored by surface density.

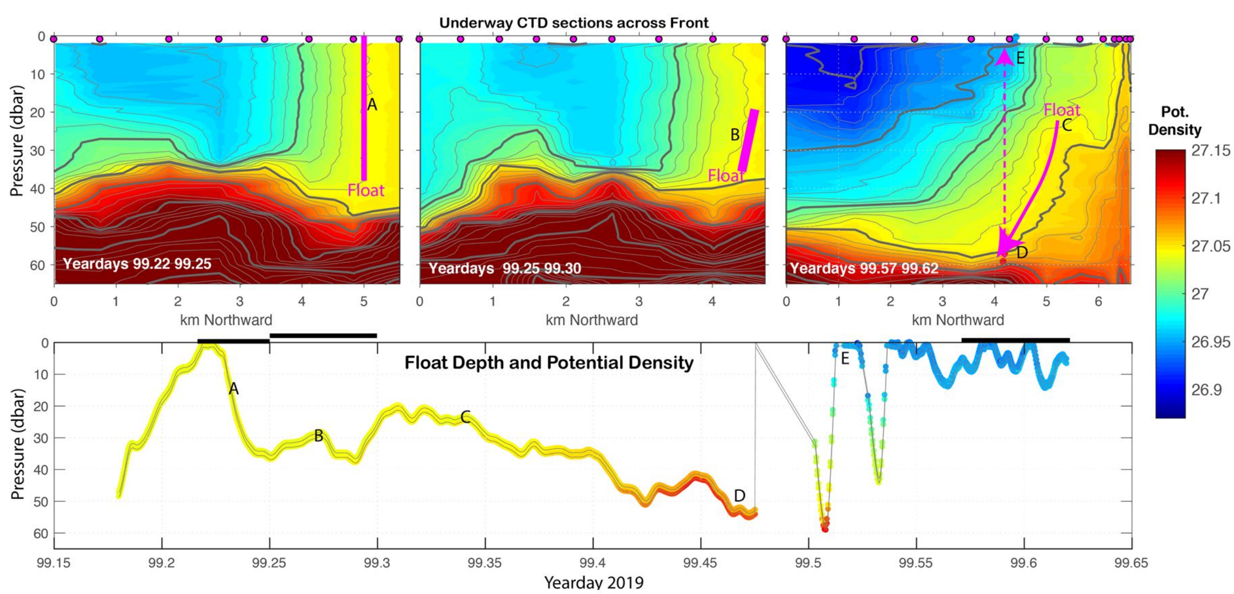


Figure 9.3: Float depth and density with corresponding underway CTD sections showing part of the deployment record of float 82.

# Chapter 10

# R/V SOCIB operational support

Shaun Johnston (SCRIPPS)
Uwe Send (SCRIPPS) and Matthias Lankhorst (SCRIPPS)
Dan Rudnick (SCRIPPS)

## 10.1 UCTD Operations

On 4 Apr 2019, R/V SOCIB carried out a UCTD survey (see Chapter 2) at the northern end of the confluent flow sampled earlier from *N/O Pourquoi Pas?* but operations were hampered by weather. Twenty-five UCTD profiles were obtained along two transects, measuring temperature and salinity (Figure 10.1).

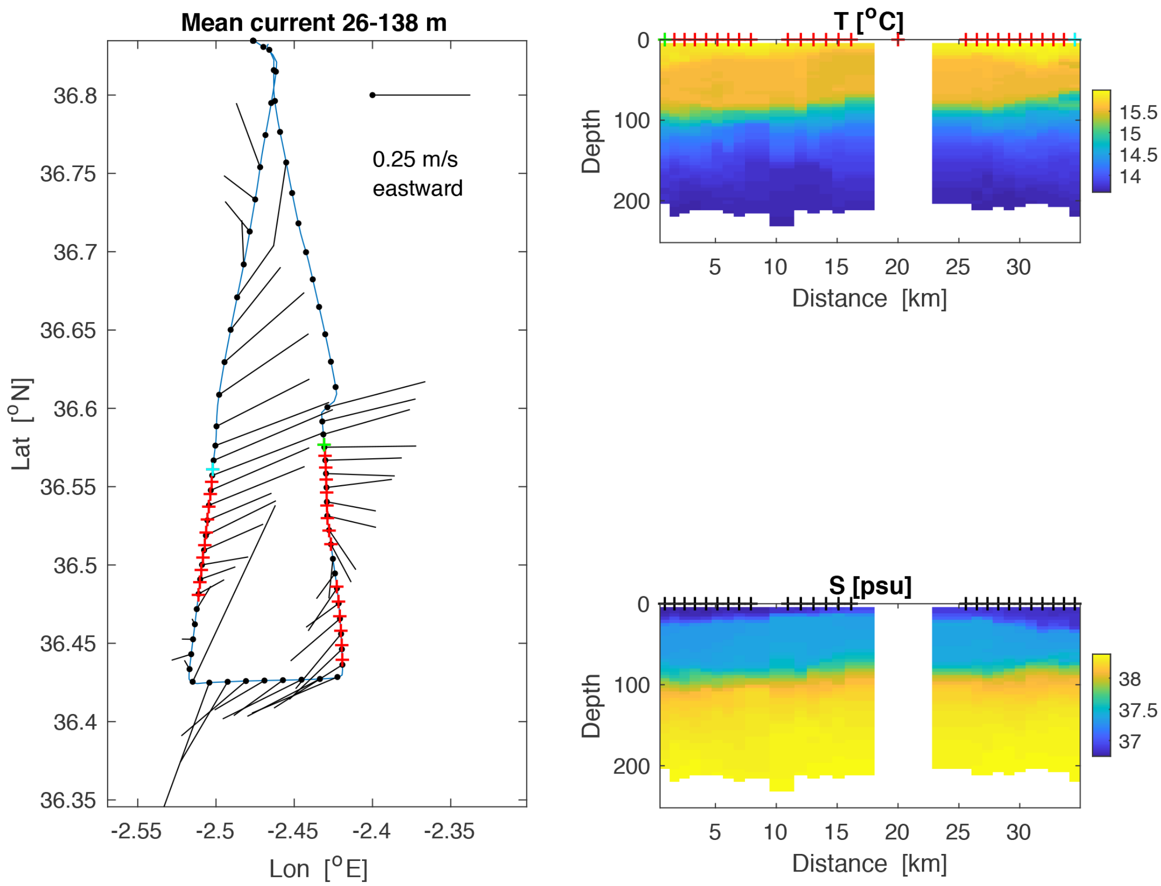


Figure 10.1: [left] Ship track of the R/V SOCIB during the UCTD survey. Locations of UCTD profiles are indicated (red crosses), along with the mean current averaged over the range 26-136 m, as measured by the shipboard ADCP. Transect of temperature [top right] and salinity [bottom right] obtained from the UCTD data are shown.

## 10.2 Mooring deployments

Three moorings were deployed by the R/V SOCIB southwest of Almería, Spain. Figure 10.2 shows a map of the locations. The principal investigator for these mooring deployments was Uwe Send from Scripps Institution of Oceanography (SIO). Each mooring was equipped with 7 instruments measuring temperature and salinity distributed over the top 500 m of the water column (Figure 10.3). The mooring locations were chosen at short notice to capture the confluence of currently existing flow branches, with the objective to provide subsurface and transport boundary conditions for numerical simulations (e.g. confluence forming/feeding a front). The data stream was set up to deliver real-time data to provide support to both the land-based modeling effort, as well as the field operations on board the *N/O Pourquoi Pas?* After mooring recovery, the full-resolution data was retrieved from internal memory within the instruments; this delayed-mode data supersedes the real-time data streams and should be the preferred dataset to use going forward. Deployments of the second and third moorings were delayed due to bad weather, but apart from this delay, all mooring instruments collected complete and scientifically valid data records. The deployment periods and locations for each mooring are listed in Table 10.1. Each deployment and recovery operation was done during a day trip out of Almería. Table 10.2 lists the members of the scientific parties, as well as the operations during each trip.

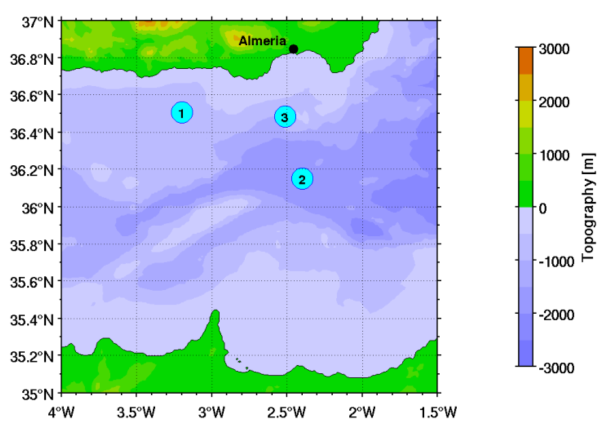


Figure 10.2: Locations of the three moorings deployed from the R/V SOCIB.

The instrument make and models on the moorings were Sea-Bird Scientific SBE37-IM, in varying configurations with and without pressure sensors. Figure 10.3 shows a schematic design drawing of the moorings. CTD casts with salinity water sampling were carried out at the times of the mooring operations, in order to calibrate/validate the mooring data. Salinity samples were processed at the SOCIB institution; there was a calibration issue with the salinometer that was ultimately resolved. Corrections applied to the mooring instruments were compared against the known histories of the instruments, and found to agree with corrections from previous deployments. This finding also validates the corrections made to the SOCIB salinometer. Processed mooring data from internal instrument memory was distributed within the project via the google cloud service in two different versions: one version consists of one file per mooring that holds all data at the native instrumental resolution in time, and the other version is a single file that contains data from all three moorings merged onto a common depth-time grid. Both versions were distributed as netCDF files with embedded CF-compliant metadata, with the intent that there be enough information for the data to be usable for all project partners.

As expected, the moorings found three different water mass regimes: mooring #1 captured the fresher and colder Atlantic water, mooring #2 sampled saltier and warmer Mediterranean water, while mooring #3 sampled through a mix of these two water masses. Time series of salinity as measured from the moorings are shown in Figure 10.4. Geostrophic currents and transports between moorings are computed and shown in Figure 10.5. Geostrophic velocities ranged from -0.3 to +0.3 m/s, while the geostrophic transport varied between -1.5 and 1.5 Sv. A reversal in the current direction and transport is observed between the mooring pairs 1-2 and 2-3, suggesting the passage of a front or mesoscale eddy through the site.

Table 10.1: Deployment times and locations for moorings deployed from the R/V SOCIB.

| Mooring number | Deployment dates | Locations (latitude, longitude) |
|---|---|---|
| 1 | 25 Mar - 13 Apr 2019 | 36.50783°N, 3.19991°W |
| 2 | 01 Apr - 12 Apr 2019 | 36.15007°N, 2.39929°W |
| 3 | 02 Apr - 11 Apr 2019 | 36.48470°N, 2.51339°W |

Table 10.2: Cruise participants and list of operations carried out during the mooring cruises on the R/V SOCIB. Each "cruise" was a day trip out of Almería on the R/V SOCIB.

| Date | Science party | Operations |
|---|---|---|
| 25/03/2019 | SIO: Uwe Send, Ethan Morris, Riley Baird. SOCIB: John Allen, Benjamin Casas, Irene Lizaran, Pau Balaguer. | Bathymetry survey of mooring 1 site. Deploy mooring 1. CTD cast at mooring 1 site. |
| 01/04/2019 | SIO: Jeff Sevadjian, Ethan Morris, Riley Baird. SOCIB: Irene Lizaran, Pau Balaguer. | Bathymetry survey of mooring 2 site. Deploy mooring 2. CTD cast at mooring 2 site. |
| 02/04/2019 | SIO: Jeff Sevadjian, Ethan Morris, Riley Baird. SOCIB: Irene Lizaran, Pau Balaguer. | Bathymetry surveys of 2 candidate sites for mooring 3. Picked flatter one based on surveys. Deploy mooring 3. CTD cast at mooring 3 site. |
| 11/04/2019 | SIO: Jeff Sevadjian, Drew Cole, Jessica Durette. SOCIB: Nikolaus Wirth, Carlos Castilla. | Recover mooring 3. Data retrieval from instruments. |
| 12/04/2019 | SIO: Jeff Sevadjian, Drew Cole, Jessica Durette. SOCIB: Nikolaus Wirth, Carlos Castilla. | Recover mooring 2. Data retrieval from instruments. |
| 13/04/2019 | SIO: Jeff Sevadjian, Drew Cole, Jessica Durette. SOCIB: Nikolaus Wirth, Carlos Castilla. | Recover mooring 1. Data retrieval from instruments. CTD cast with all 21 SBE37 instruments attached to rosette for cal/val. Salinity water samples. |

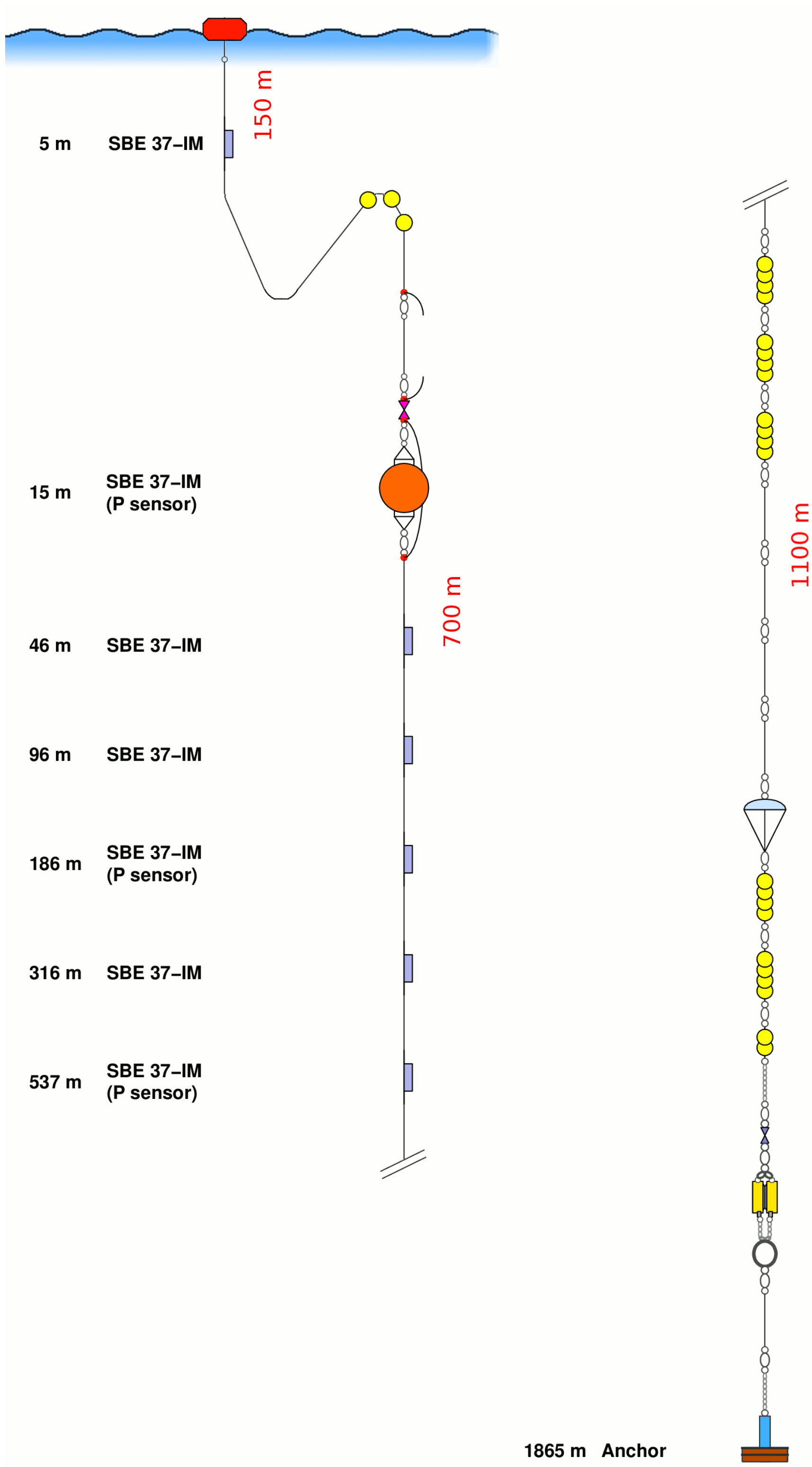


Figure 10.3: Schematic drawing of mooring #2, which is similar to the others except for different wire lengths to accommodate different water depths. Instrument depths below the sea surface are indicated in black on the left. Red numbers list approximate wire lengths. The top buoy sits on the surface and contains the satellite telemetry. Communication between the top buoy and all instruments occurs through the mooring wire.

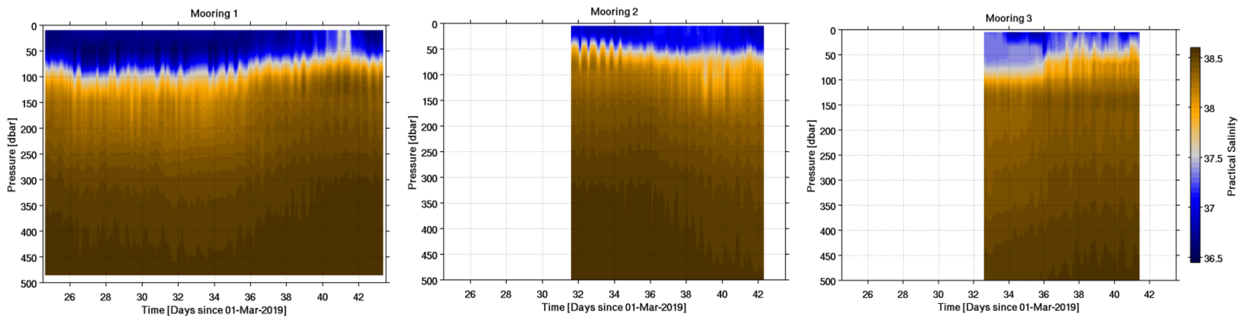


Figure 10.4: Salinity observations from moorings #1, 2, and 3. Mooring locations can be seen in Figure 10.2.

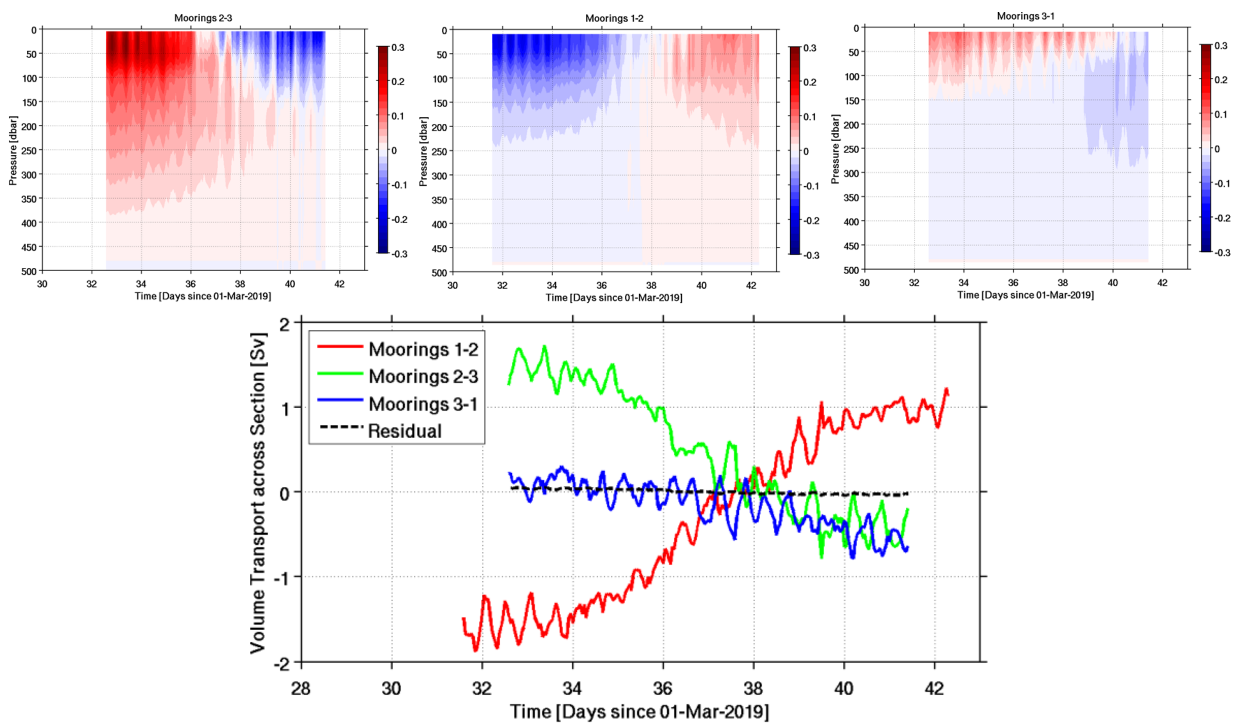


Figure 10.5: [Top] Geostrophic velocities [in m/s] and [bottom] geostrophic transport computed between each mooring pair. Positive velocity and transport denote a flow into the triangle formed by the moorings. Transport is integrated over the upper 500 m and is computed relative to the 500 m level.

## 10.3 Underwater glider deployment and recovery

A fleet of 8 underwater gliders was deployed on 20 March 2019 from the R/V SOCIB in an effort to resolve the evolving three-dimensional hydrography and flow (Figure X). The fleet included 6 Spray gliders from Scripps, one Slocum each from SOCIB and IMEDEA. The entirety of the operation lasted until 20 May 2019 when the Scripps gliders were recovered. The SOCIB glider stopped transmitting on 4 April, and is assumed lost. The IMEDEA glider was recovered on 14 April as the R/V SOCIB was returning to Palma. A total of 407 glider-days produced 2459 dives to 700 m covering 9300 km over ground. The gliders were deployed in 5 lanes oriented in the direction across the Almeria-Oran front, with the lanes separated by 8.75 km. The Scripps gliders measured temperature, salinity, velocity (using an ADCP), chlorophyll fluorescence, and acoustic backscatter. The SOCIB/IMEDEA gliders measured temperature, salinity, chlorophyll fluorescence, dissolved oxygen, turbidity, and photosynthetically active radiation. Over 60 sections across the front were collected, allowing investigation of the evolution of the front over the two months. The unusual wind forcing may have contributed to the front being west of the survey area for the first three weeks of operations, but on about April 10 the front propagated eastward into the survey region. The Spray gliders were programmed with the ability to follow subsurface isotherms, with the objective of following active subduction. One glider was used in this way, doing a series of one-day tracks while staying with a vertical root-mean-square distance of 5 m from the desired isotherm. The largest downward velocities observed by the displacement of the glider were roughly 50 m/day.

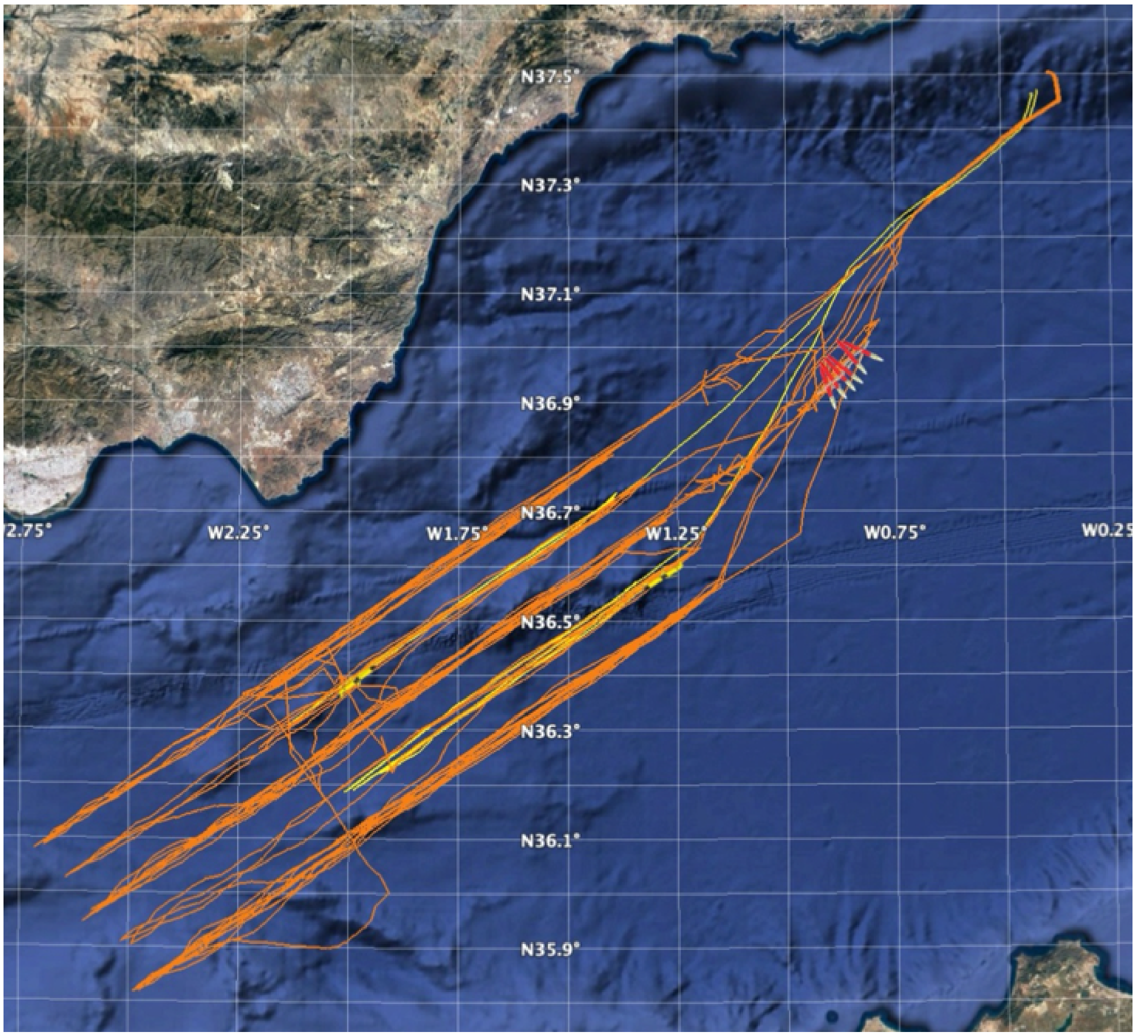


Figure 10.6: Tracks of underwater gliders during Calypso 2019. The six Scripps Spray glider tracks are orange, and the two SOCIB/IMEDEA Slocum track are yellow.

# Chapter 11

# Near Real-Time modeling support

Helga Huntley (University of Delaware)
Baptiste Mourre (SOCIB)
Pierre Lermusiaux (MIT) and Chris Mirabito (MIT)

## 11.1 Shore-Support for Dynamic Deployments Decisions

To support decisions by the scientists on board the ships as to what areas to target with sampling, modeling and remote-sensing data were analyzed daily. The resulting value-added products were gathered on a website, which was updated daily beginning three weeks prior to the cruise and ending a few days after the return of the ship to port. An example page is shown in Figure 11.1.

The list of the particular products generated and included was developed in collaboration with the chief scientists on the cruise to maximize utility. The model products were based on the forecasts from SOCIB's Western Mediterranean Operational system (WMOP; see Section 11.2) and included the following:

1. Snapshot of 1-day surface-trapped trajectories starting at midnight GMT of the current day. Used to illustrate transport.
2. Animation of surface-trapped trajectories for 3 days, with color-coding by initial latitude. Used to visualize horizontal mixing.
3. Snapshot of Direct Lyapunov Exponents (DLE, also known as Finite-Time Lyapunov Exponents or FTLE) at the surface for the current day at midnight GMT based on

3-day trajectory integrations. Used to find predicted transport barriers in the surface flow.

4. Forecast residence time of surface drifters in the Spanish economic exclusion zone (EEZ), i.e. in the waters where the ship had permission to operate, and forecast residence time in the combined Spanish and Moroccan EEZs, i.e. in the waters where the ship was expected to receive permission to operate. Used to assess feasibility of retrieval for drifter releases.

5. Predicted cluster density after three days for initially uniformly released virtual particles. Used to show regions from where deployed surface drifters are likely to converge, as forecast by the model.

6. Dilation (path-integrated divergence) over the past three days. Used to show current accumulation regions, i.e. where one would expect to find previously released surface drifters.

7. 24-hour mean sea surface salinity and surface currents, as well as an animation of the forecast sea surface salinity and surface currents for the next 24 hours. Used to provide a synoptic Eulerian view of the flow conditions.

Except for the animations, the results were made available as .png file for quick display and as .kmz files for easy simultaneous, layered display in tools such as Google Earth.

Images of satellite-derived sea surface temperature, sea surface height, and chlorophyll concentration were generated by colleagues at IMEDEA and added to the website for a direct comparison with the model forecasts.

## 11.2 WMOP model

The 2-km resolution Western Mediterranean Operational system (WMOP) run at SOCIB was used to provide support to the cruise planning. WMOP [*Juza et al.*, 2016; *Mourre et al.*, 2018, `http://socib.es/?seccion=modelling&facility=forecast`] uses a regional configuration of the ROMS model [*Shchepetkin and McWilliams*, 2005] implemented over the Western Mediterranean Sea to produce daily 3-day forecasts of ocean temperature, salinity, sea level and currents. The model is nested in the larger scale CMEMS Mediterranean model and is forced by high-resolution atmospheric forcing from the Spanish Meteorological Agency (AEMET-Harmonie model with a resolution of 2.5 km and 1 hour). Data assimilation is implemented in this system through a local multi-model Ensemble Optimal Interpolation scheme [*Hernandez-Lasheras and Mourre*, 2018] using a 3-day cycle (i.e. an analysis is computed every 3 days). The system routinely assimilates satellite along-track sea level anomalies, satellite SST from the CMEMS-Med ultra-high resolution L4 product, Argo temperature and salinity profiles as well as surface currents from HF radar observations

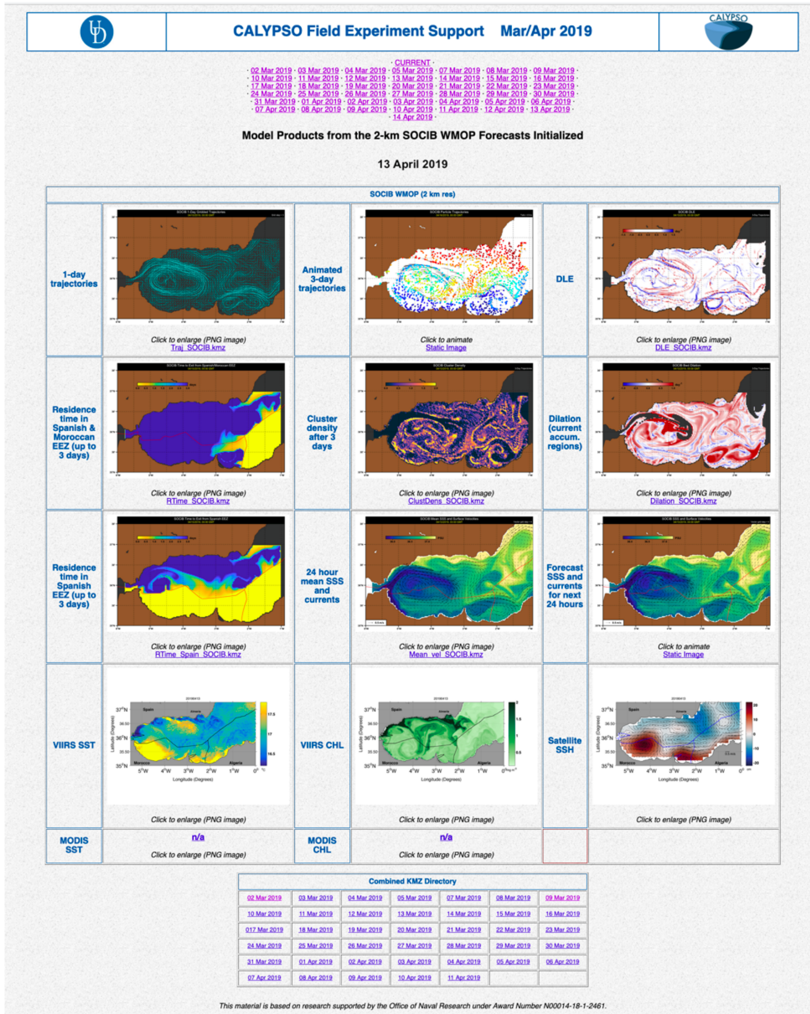


Figure 11.1: Sample webpage with real-time model and satellite products for dynamic deployment decision support during the spring 2019 CALYPSO cruise.

in the Ibiza Channel. During this experiment, real-time CTD observations from the *N/O Pourquoi Pas?*ere also assimilated in the system. A 5-day assimilation window is considered for satellite along-track, Argo and CTD observations.

An ad-hoc web-based visualization of the model results was implemented for the CALYPSO project: `http://socib.es/?seccion=modelling&facility=calypso_assim`. This visualization interface displays maps of surface temperature, salinity, height, currents, temperature and salinity gradients, relative vorticity, horizontal divergence and vertical velocities, focused on the Alboran Sea. It also includes model comparisons to altimetry and satellite SST, as well as illustrations of the latest assimilated data. Morover, dynamic visualization tools are also available on SOCIB website (`http://thredds.socib.es/lw4nc2/index.html?m=wmop`).

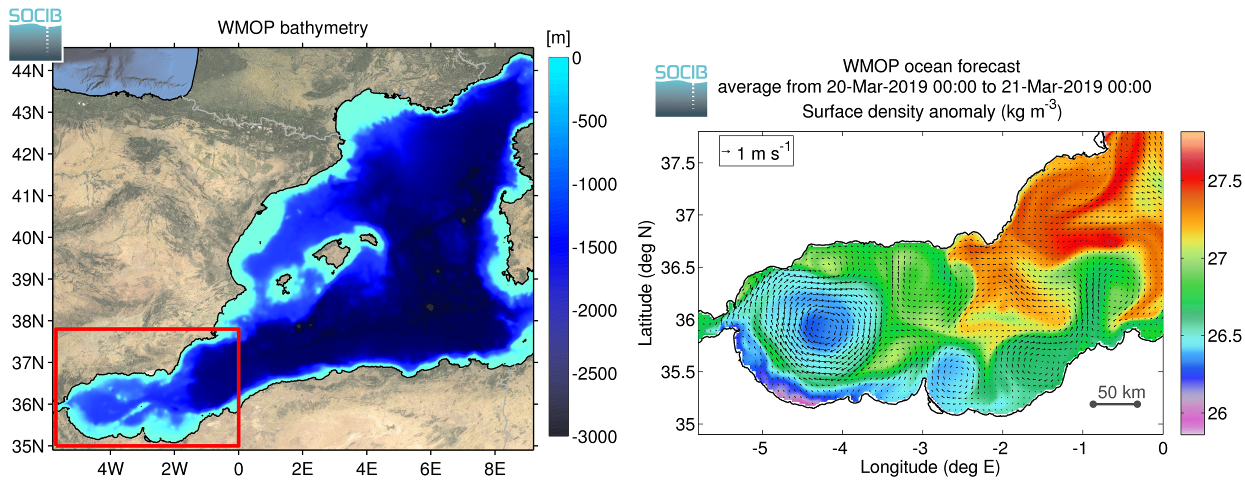


Figure 11.2: Left:WMOP model bathymetry over the Western Mediterranean Sea. The area of interest for the CALYPSO 2019 experiment is indicated by the red rectangle. Right: WMOP sea surface density anomaly and currents in the Alboran Sea on 20 March 2019.

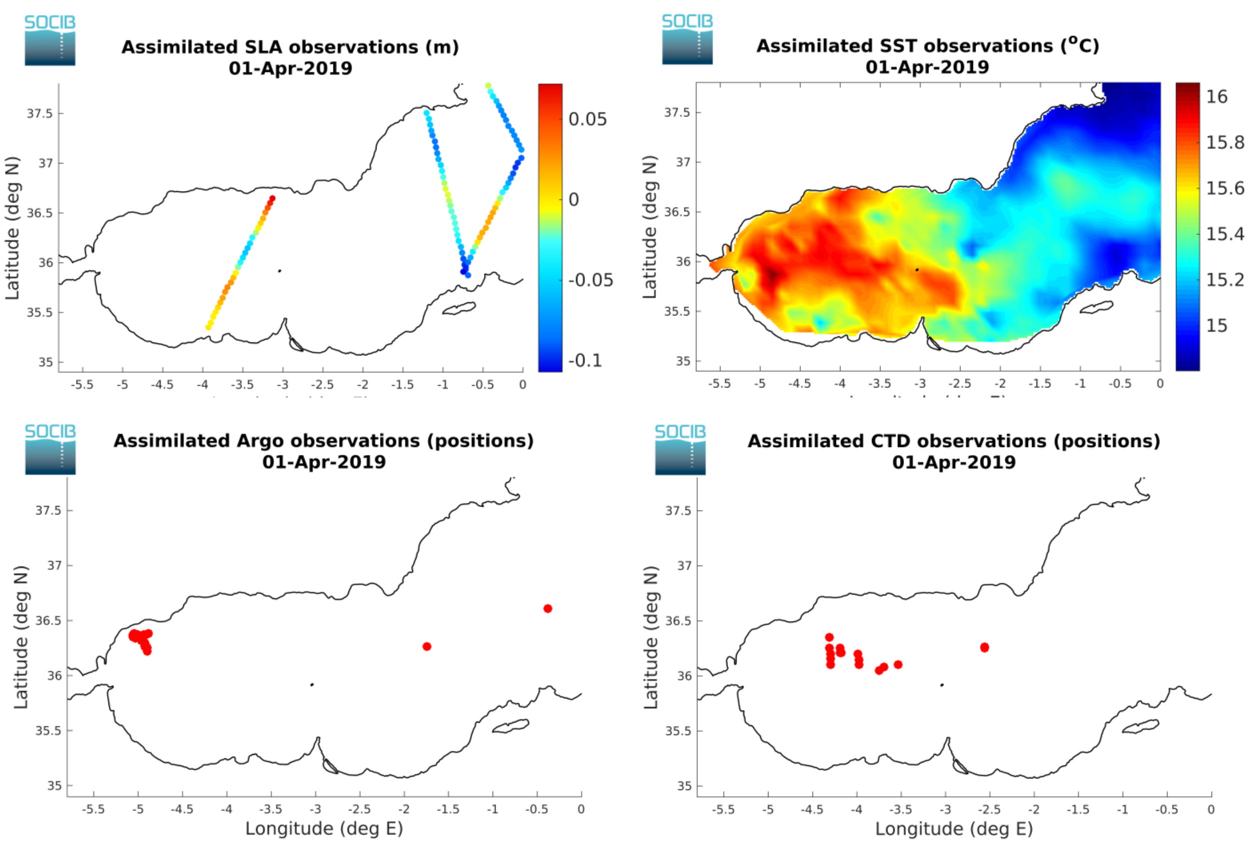


Figure 11.3: Assimilated observations on 1 April 2019: along-track SLA, SST and position of Argo floats and CTDs profiles.

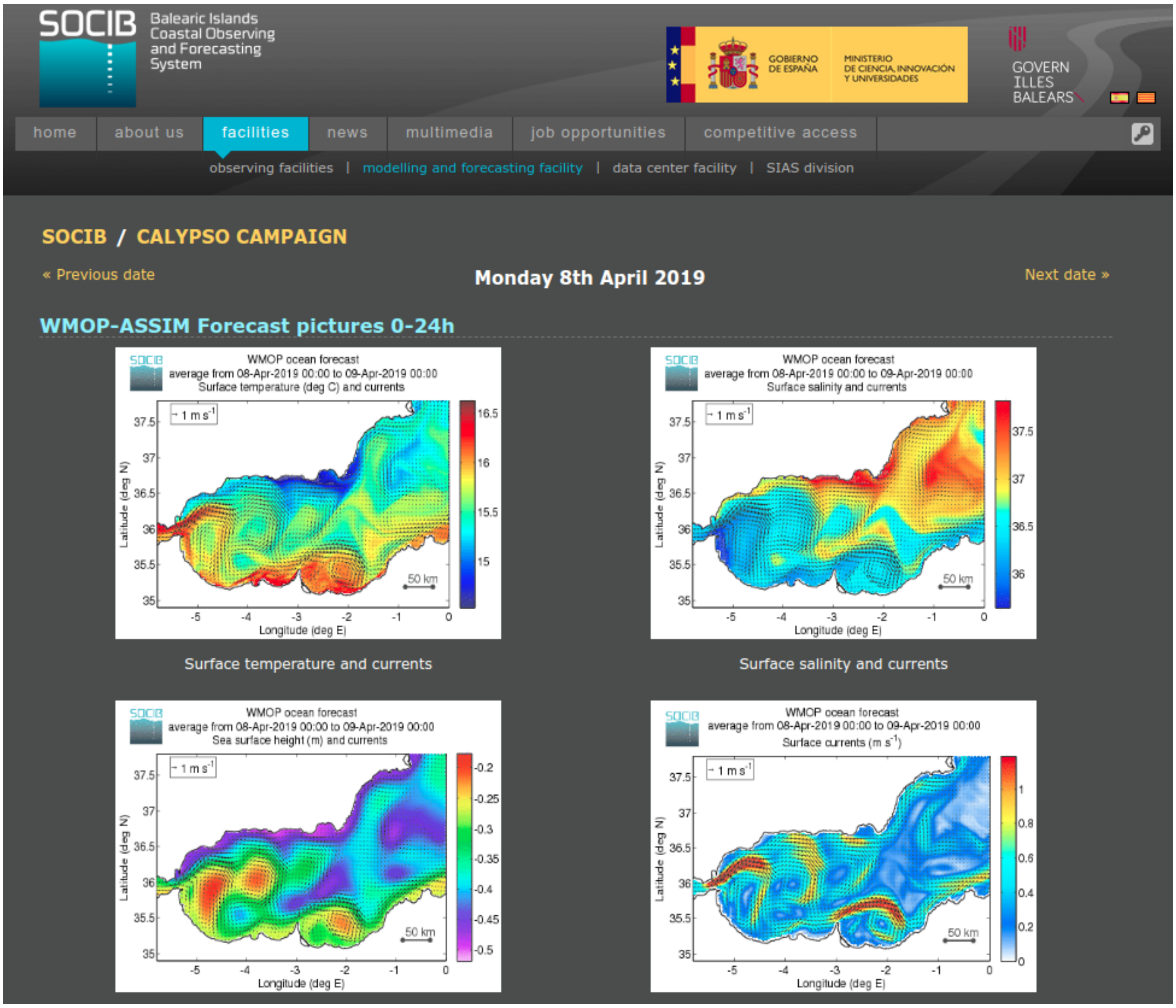


Figure 11.4: Web-based visualization interface displaying WMOP predictions in the Alboran Sea.

Three-hourly surface netcdf files are available on SOCIB thredds server (`http://thredds.socib.es/thredds/catalog/operational_models/oceanographical/hydrodynamics/wmop_surface/catalog.html`). In particular, these were used at the University of Delaware to generate a series of added-value products including advanced Lagrangian analysis (`http://lagrange.ceoe.udel.edu/CALYPSO/`). Moreover, customized netcdf files were also created and distributed through ftp to provide initial and boundary conditions to the MIT-MSEAS very high-resolution model (`http://mseas.mit.edu/Sea_exercises/CALYPSO/2019/index.html`).

## 11.3 Real-Time Four-Dimensional Ocean and Lagrangian Forecasting and Analysis (MSEAS Group - MIT)

### 11.3.1 Real-Time Multi-resolution Ocean Modeling and Dynamics Analyses

For our CALYPSO real-time forecasts, we set up a domain spanning approximately 430 km $\times$ 267 km at a horizontal resolution of $1/200°$ ($\sim 500$ m) with 70 optimized terrain-following vertical levels. Our bathymetry was based on the 15 arcsecond SRTM15+ bathymetry from Scripps. Our simulations were forced with atmospheric fluxes from the $1/4°$ NCEP GFS product and tidal forcing from the high-resolution TPXO8-Atlas tides from OSU. These tides were reprocessed for our higher resolution bathymetry/coastline and for our quadratic bottom drag formulation. Initial conditions were downscaled from 3 different models: $1/12°$ HYCOM, $1/24°$ CMEMS, and $\sim 1/50°$ WMOP. The downscaled initial conditions were continuously corrected using ARGO data and, on April 10, using also Uwe Send moorings. The velocities were optimized for our high-resolution coasts and bathymetry [*Haley et al.*, 2015]. These simulations were used to forecast real-time physics, Lagrangian flowmaps, 2D and 3D LCSs, surface drifter trajectories, and 3D subduction forecasts. We refer to our real-time web page for most of real-time products:
`http://mseas.mit.edu/Sea_exercises/CALYPSO/2019/`.
Overall, during the March-April experiment, 43 sets of forecast surface velocity fields (spanning the period March 23 – April 15) were provided in real-time to CALYPSO collaborators.

These downscaled forecasts also served as the central forecasts in our novel real-time three-model ensemble forecasting method and initialize using ESSE initialization schemes [*Lermusiaux*, 2002]. The initial 3D perturbations were constructed from a combination of vertical EOFs of historical March CTD data along with an eigendecomposition of a horizontal correlation matrix computed using a 12.5km decay scale and a 31.25km zero-crossing. A 3D PE balance was applied to the perturbed velocities.

**Real-Time Forecasts and Descriptive Analyses.** The ocean surface circulation was forecast to be strongly affected by three these distinct wind forcing periods. In the first (March 25–31), the prevailing winds are towards the west. Then, there is a transition period with variable winds and a final period (April 4–16) with the prevailing winds toward the east. There were a number of very strong wind events including 2 gales (March 26–27 and April 5–7). An example of a high-resolution real-time forecast downscaled from WMOP is presented in fig. 11.5. Here the surface vorticity on April 12 is shown. The generation of vorticity can be seen off capes, at islands, and along jets. Our real-time forecasts also show internal tides/internal waves being generated along the bathymetry (shelfbreak and above the Alboran Ridge) by the tidal forcing. These waves propagate offshore (or away from the Alboran Ridge) (not shown). During the third wind regime, relatively strong winds to the east lead to the re-establishment of the AO front by about April 15–17. This was visible both in our physical forecasts and our surface trajectory forecasts (not shown). Examples of our uncertainty forecasts are presented in fig. 11.6. The uncertainty forecasts show that the uncertainty grows in frontal shear region south of Cabo del Gata. In addition, the surface uncertainty is transferred to deeper regions.

**Real-Time Evaluation of Real-Time Forecasts.** Numerous comparisons were made of our forecasts to data in real-time. For example, fig. 11.7 shows the MSEAS-PE real-time forecast skill seen in forecasts for April 6 versus independent April 6 ARGO data. The main improvements are to thermocline/halocline. These can come from both resolution and corrections from earlier ARGO data. Overall, the temperature RMSE improves 64% of the time, and the salinity RMSE improves 62% of the time. On average, the improvement in RMSE is about 4% for both $T$ and $S$. This average improvement was calculated over all cases, including those in which the PE does worse. Similar comparisons were also made to the Uwe Send mooring data (not shown). Main improvements were to the thermocline/halocline and in the mixed layer. No mooring data was used to correct the ICs. Corrections can come from resolution and/or previous ARGO corrections that may have advected to the mooring site. Comparisons to persistence (not shown) also demonstrated corrections in the thermocline/halocline and the mixed layer. No additional data were assimilated into the forecasts beyond the IC corrections.

Additional real-time skill evaluations were also completed by comparing our simulated drifter trajectories to the actual trajectories. We simulated the CARTHE SPOT drifters (from RSMAS, co-PI Tamay Özgökmen), with a drogue depth of 0.65 m. Fig. 11.8 shows the comparisons made for drifters starting from 12Z on April 8, 9, and 10. All tracks were simulated for 4 days. Qualitatively, the forecast initialized from downscaled WMOP does the best on April 10, but most drifters miss a U-turn by the African coast. But quantitatively (using the Fréchet distance), the forecast downscaled from WMOP has the highest mean Fréchet distance likely because of the large cluster of drifters that miss the U-turn near the coast of Africa. Additional definitions of distances between curves will also be utilized in the future.

**Real-Time Evaluation of Real-Time Ensemble Forecasts.** Skill evaluations were also made of the ensemble MSEAS-PE forecasts to independent data. The comparison for the ensemble on April 9 to independent ARGO data is shown in fig. 11.9. The data (red profiles) are entirely contained in the envelop of the ensemble (black profiles). In addition the standard deviation of the ensemble is seen to be a reasonable estimator of the RMS error of the ensemble (green and blue curves in the smaller inset plots) indicating that the forecast ensemble spread is a reasonable estimate of the uncertainty.

### 11.3.2 Real-time Four-dimensional Lagrangian Forecasts and Subduction Analyses

Using the MSEAS-PE forecasts, Lagrangian flow maps were computed in real-time using our composition-based advection method [*Kulkarni and Lermusiaux*, 2019], forced by the MSEAS forecast of the 3D ocean currents ($u$, $v$, and $w$). The forecast flow maps were then used to forecast Lagrangian Coherent Structures (LCSs). They were also employed to find and identify water volumes that started near the surface and ended at a significant depth. These (PE) forecasts were also used to numerically compute drifter trajectories which were later compared to the real drifter trajectories.

There were 3 distinct subduction regimes reflecting the 3 distinct wind regimes. One examples of this is shown in fig. 11.10. In the subduction panels, the blue water volumes are the initial positions of the waters that start within 0-to-10 m depths and reach 50m after 4 days. These waters were selected directly from our flow map forecasts. The green water volumes represent the location of the same parcels but after two days while the red water volumes represent the final location of the parcels after 4 days. There is a direct relation between this 3D subduction (from above 10m depth to deeper than 50m depth) and the 3D attracting Lagrangian Coherent Structures that we forecast (see the maps of the forecast 3D backward FTLE fields).

During the period of March 28 to April 3, there was a weakening winds after the March 27 gale. The winds through March 31 are towards the west and become variable afterward. The release of kinetic energy input by the strong winds has however created new (sub)-mesoscale eddies and frontal structures, especially south of the Spanish coastline (downwelling). Subduction now also takes place along these eddies and fronts ($\sim$ 15 to 40 m/day). Subduction was subsiding during the end of the period (e.g., Apr 1).

During the period of April 3–7 (shown in fig. 11.10), the winds build back up through April 7 gale. The winds reverse and are on average towards the east. There is increased subduction along the African coastline. Subduction still occurs along (sub)-mesoscale eddies and frontal structures in the middle of the Alboran Sea, especially around the weakened WAG and south of Cabo de Gata (e.g., sinking in thin sheets along convergent/attracting fronts and edges of interacting eddies).

Finally, during the period of April 8–14, the winds weaken following the April 7 gale (especially after April 11). The winds are on average towards the east. Subduction weakens along the African coastline. Some 3D subduction also occurs along (sub)-mesoscale eddies and frontal structures south of Almeria and Cabo de Gata, as well as on the edges of a weak WAG and of the Atlantic jet (e.g., sinking in thin sheets along convergent/attracting fronts and edges of interacting eddies).

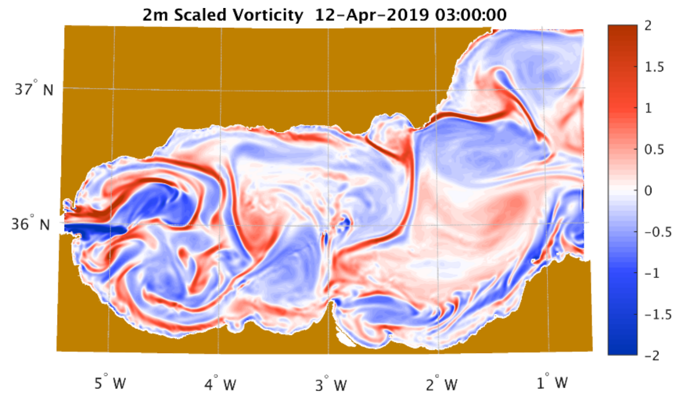


Figure 11.5: Example of MIT MSEAS-PE real-time relative vorticity forecast, issued for 12 April 2019 at 03Z, from a high-resolution (500m) simulation downscaled from WMOP. Surface vorticity is generated off capes, at islands, and along jets.

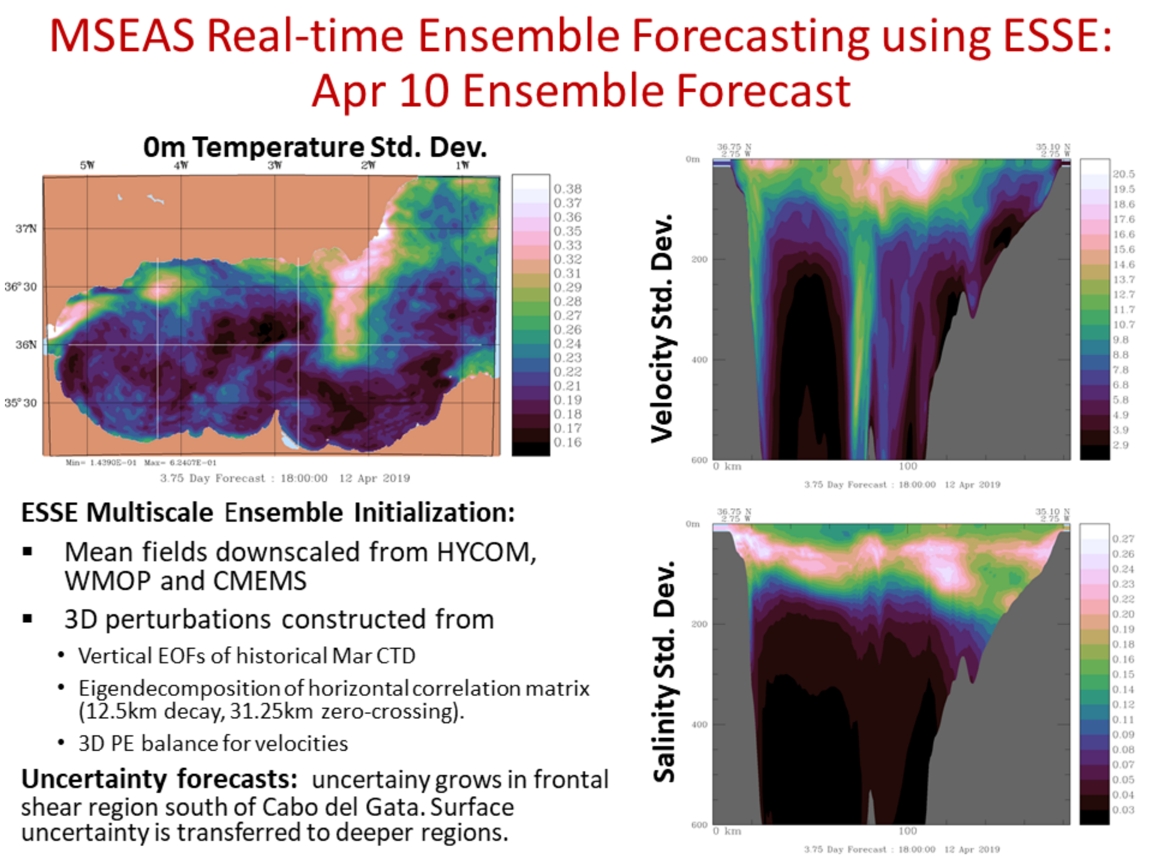


Figure 11.6: Our MIT MSEAS-PE real-time uncertainty forecasts for April 12 at 18Z, issued on April 10. The realistic ensemble forecasts were initialized using our ESSE initialization methods.

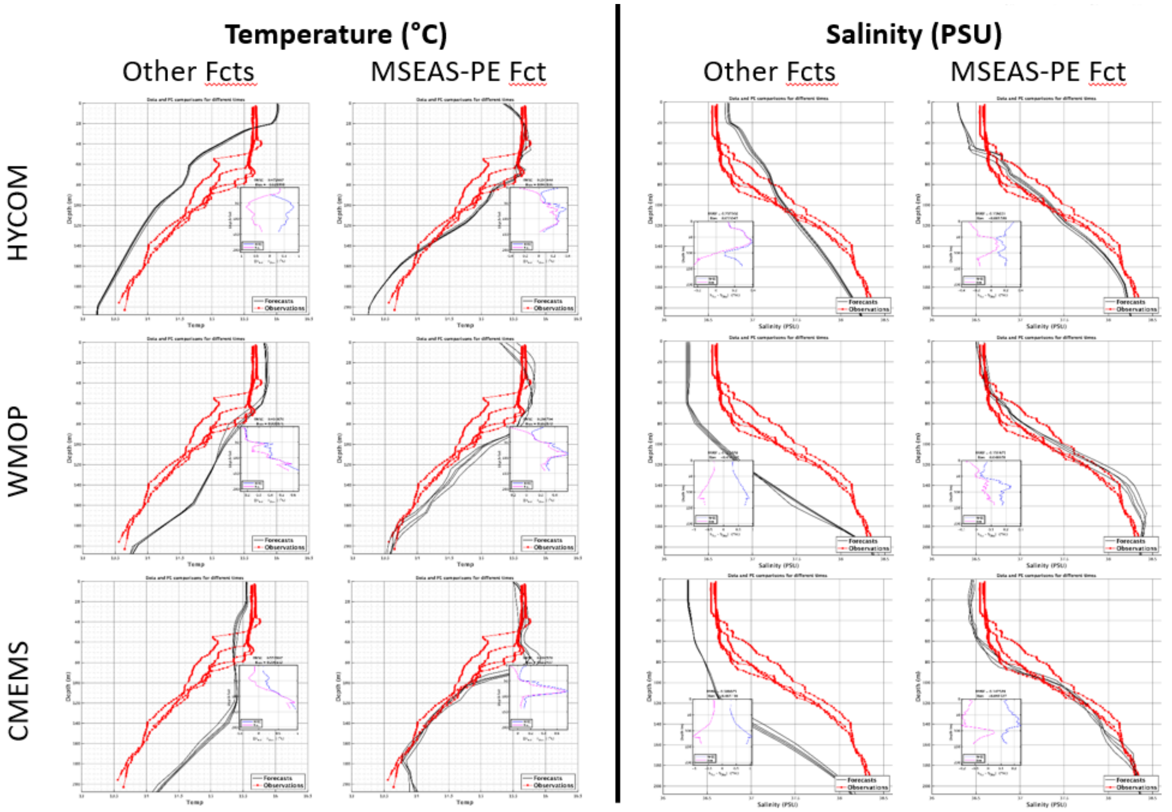


Figure 11.7: Our MIT MSEAS-PE real-time forecasts for April 6 compared with independent April 6 ARGO data.

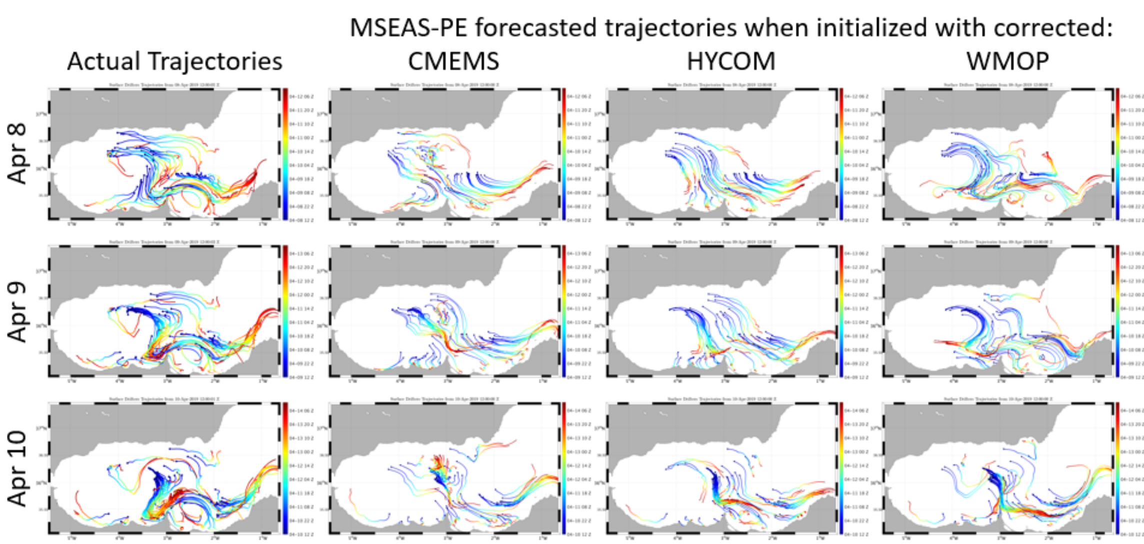


Figure 11.8: Simulated vs. actual drifter trajectories for drifters released at 12Z on April 8, 9, and 10. Qualitatively, MSEAS forecasts initialized with WMOP produce tracks most alike the actual tracks on April 10, but most drifters miss the U-turn by the African coast; quantitatively, forecasts initialized with WMOP produce the most dissimilar tracks, as measured by Fréchet distance.

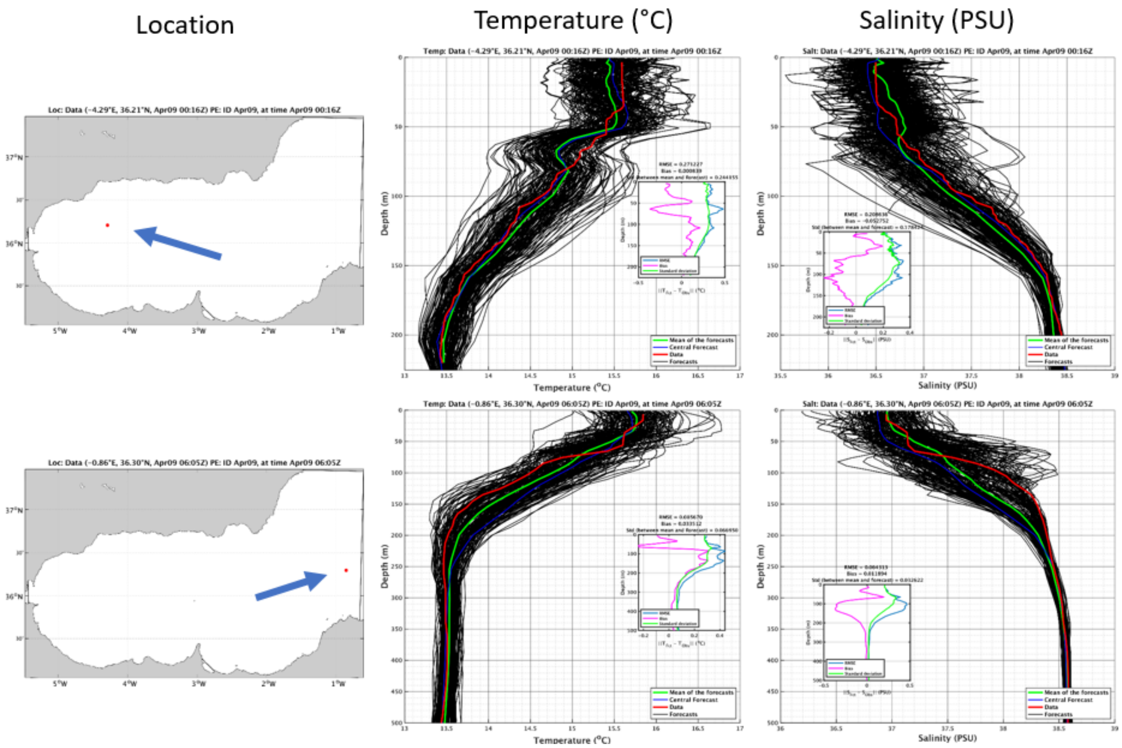


Figure 11.9: Our MIT MSEAS-PE ensemble forecast skill evaluation by comparison with independent ARGO data on April 9. Our ensemble consisted of 300 members and was initialized using ESSE.

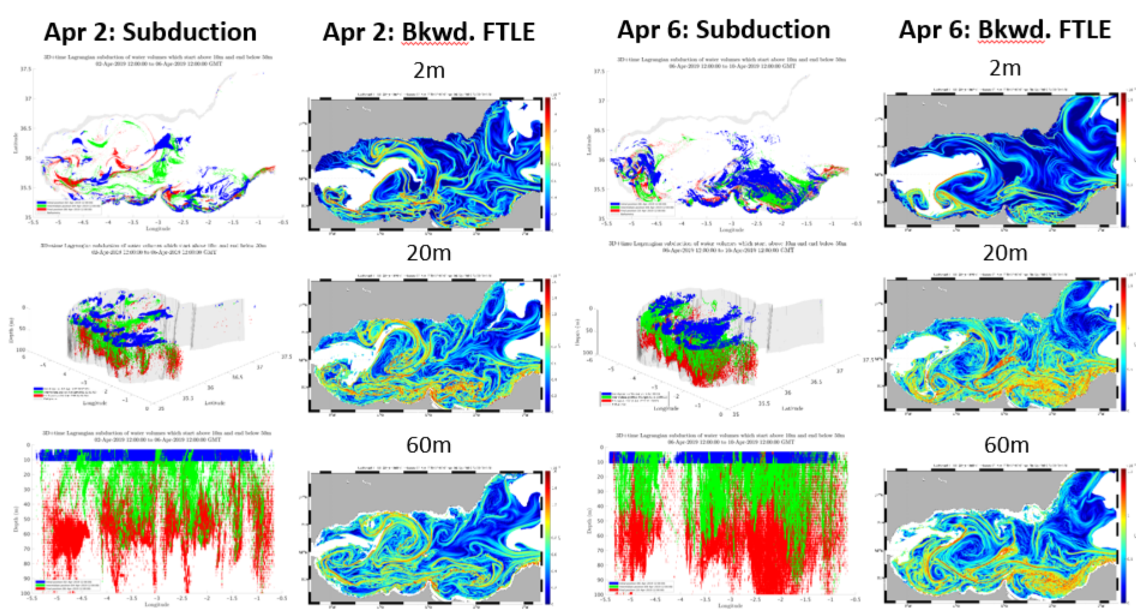


Figure 11.10: Our MIT-MSEAS 3D Lagrangian subduction forecast from April 3 to April 7. The blue water volumes are the initial positions of these waters that start within 0-to-10 m depths and reach 50m after 4 days.

# Chapter 12

# Real Time Tools and Satellite Imagery analysis

Simón Ruiz (IMEDEA) and Ananda Pascual (IMEDEA)
Isabel Caballero (ICMAN-CSIC), Gabriel Navarro (ICMAN-CSIC)
and Nikolaos Zarokanellos (SOCIB)

## 12.1 Shore-based satellite data analysis

### 12.1.1 Introduction

This document describes the satellite data (Altimetry, Sea Surface Temperature and Chlorophyll-a) used during the Calypso 2019 experiment performed in the Alboran Sea between March 28 and April 11 2019. IMEDEA-CSIC was in charge of providing near-real time satellite data. Absolute Dynamic Topography (ADT) data were daily downloaded from Copernicus Marine Services[1] while Sea Surface Temperature (SST), and chlorophyll-a (Chl-a) data were downloaded from NASA website[2]. Images were generated at IMEDEA and together with nc files were daily available at Google drive[3] for researchers onboard *N/O Pourquoi Pas?*nd other Calypso teams at land. Additionally, images of ADT, SST and chl-a were also displayed at the website[4] created by H. Huntley.

[1]http://marine.copernicus.eu/services-portfolio/access-to-products/
[2]https://oceancolor.gsfc.nasa.gov/cgi/browse.pl
[3]https://drive.google.com/drive/u/0/folders/1l44TqJUx8O69VG820mIjsUyTXb9GpIYH
[4] http://lagrange.ceoe.udel.edu/CALYPSO/

During the field experiment, IMEDEA staff (Noemí Calafat, Benjamín Casas, Eugenio Cutolo and Daniel Rodríguez-Tarry) onboard *N/O Pourquoi Pas?*as also involved in different sampling operations (see other sections of the general Cruise 2019 report for details):

- CTD sampling and processing.
- Water sampling.
- uCTD samplings operations
- Drifters deployment operations.
- Wirewalker operations.

### 12.1.2 Oceanographic context from satellite

In the next pages the oceanographic context from satellite data is presented to contextualize in-situ observations collected during the Calypso 2019 field experiment. The study area (Figure 12.1) is the Alboran Sea (Western Mediterranean).
SST, Chl-a and ADT from remote sensing provided a synoptic view of meso- and submesoscale features at the Alboran Sea, and helped together with real-time in-situ ship's data (uCTD and VM-ADCP), to determine the location of main features of interest (meanders, eddies, and fronts).

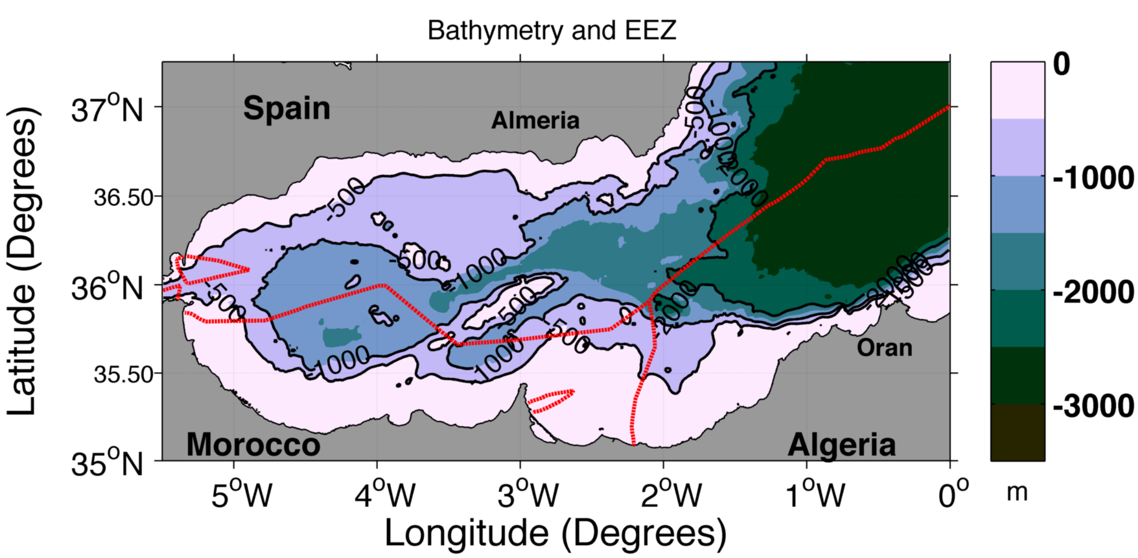


Figure 12.1: Alborán Sea (Western Mediterranean) bathymetry. Red line corresponds to EEZ between three countries (Spain, Morocco and Algeria). Calypso 2019 experiment took place in Spain and Moroccan waters between March 28 and April 11, 2019.

### Altimetry

Near-Real time gridded altimeter product specific for the Mediterranean Sea and delivered by the Copernicus Marine Service (CMEMS)[5] was downloaded on a daily basis. The variables included in this product are Sea Level Anomaly (SLA) and the corresponding geostrophic velocity anomaly, ADT, which is obtained adding a mean dynamic topography *Rio et al.* [2014] to the SLA and absolute geostrophic currents. See Table 12.1.2 for further details about this product.

| | |
|---|---|
| file name format | nrt-med-allsat-phy-l4-yyyymmdd-yyyymmdd.nc |
| URL | http://marine.copernicus.eu/services-portfolio/access-to-products/ |
| Processing Level | L4 |
| Spatial resolution | 1/8° |
| Temporal resolution | 1 day |
| Geophysical data used | Absolute Dynamic Topography (ADT)<br>and absolute geostrohpic current |

Table 12.1.2 Specifications of altimetry product used during Calypso cruise 2019.

Altimetry images (Figure 12.2) reveal the presence of the quasi-permanent Western Alboran Gyre (WAG) with associated velocities of about 1 m/s. Further east, between Almería and Orán, data reveal a cyclonic eddy with velocities of about 0.7 m/s. The signal of a smaller anticyclonic eddy is also observed near Almeria coast. Daily ADT images for the complete period of the Calypso 2019 cruise are available in Section 12.1.3. These images (0.125°x0.125° resolution) provided a general context of the position and intensity of the WAG and associated fronts in the study area. Other instruments onboard *N/O Pourquoi Pas?*s the VM-ADCP and uCTD sampling allowed a more precise identification of small features, such as meanders associated with the main flow identified in altimetry maps. Relative vorticity has been estimated from altimetry, revealing values of about $0.5f$ in the study area (Figure 12.3).

### Sea Surface Temperature and Chlorophyll-a

SST and Chl-a data were downloaded from NASA's Ocean Colour website[6]. SST images used in this study are at 1-km spatial resolution and correspond to Level-2 SST acquired by the Moderate-Resolution Imaging Spectroradiometer (MODIS) sensor onboard the Aqua and Terra satellites. The Ocean Colour data come from MODIS Level-2 single swaths. SST images (Figure 12.4) show the presence of a filament around 36.1° N Latitude, 4° W Longitude, in the eastern edge of the western Alboran Gyre that was sampled during the first phase of the Calypso 2019 experiment.

[5] http://marine.copernicus.eu/services-portfolio/access-to-products/
[6] https://oceancolor.gsfc.nasa.gov/cgi/browse.pl

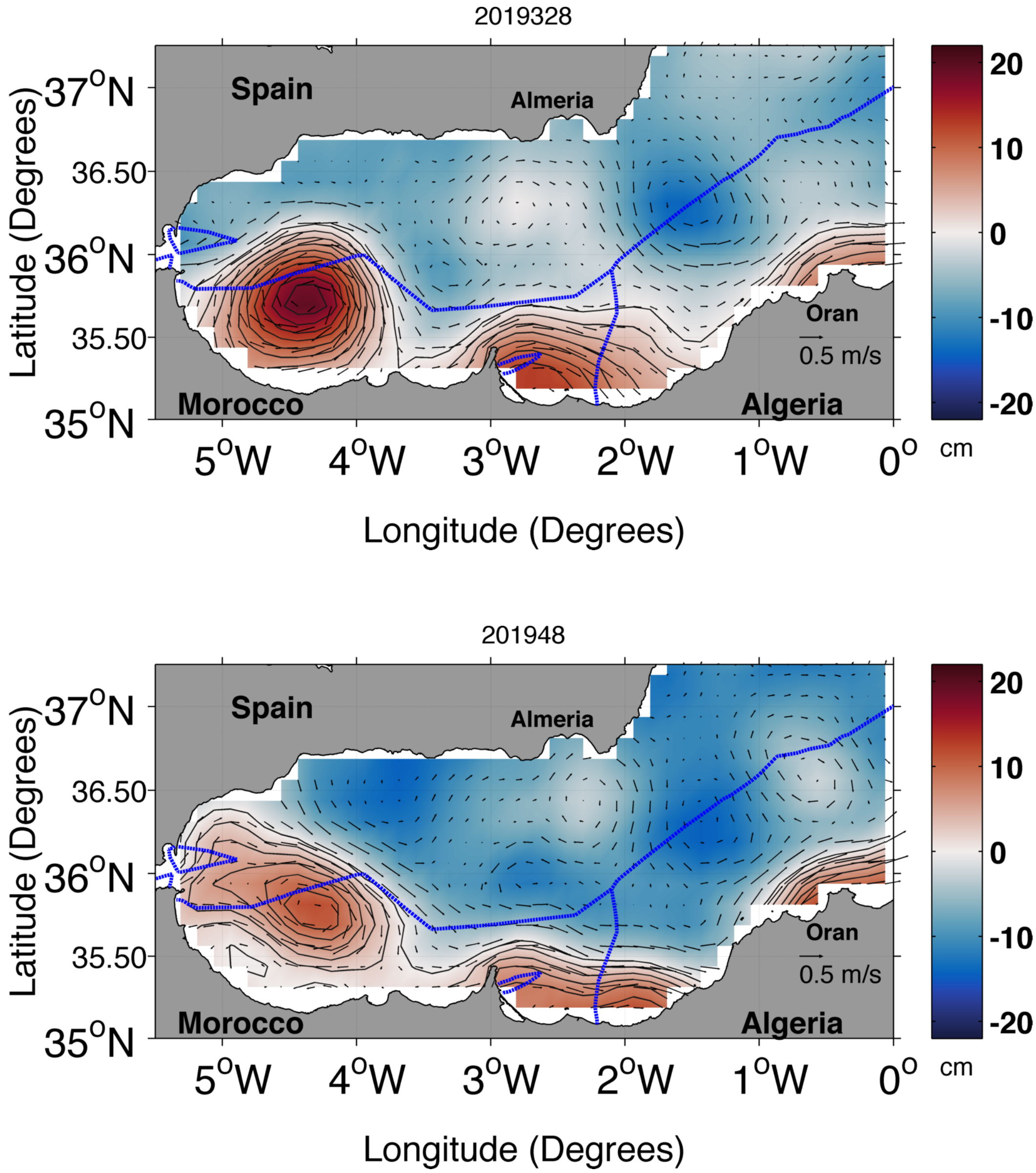


Figure 12.2: ADT and associated velocity for March 28 and April 10. Data from Copernicus Marine Service (CMEMS). Blue dashed line corresponds to the EEZ.

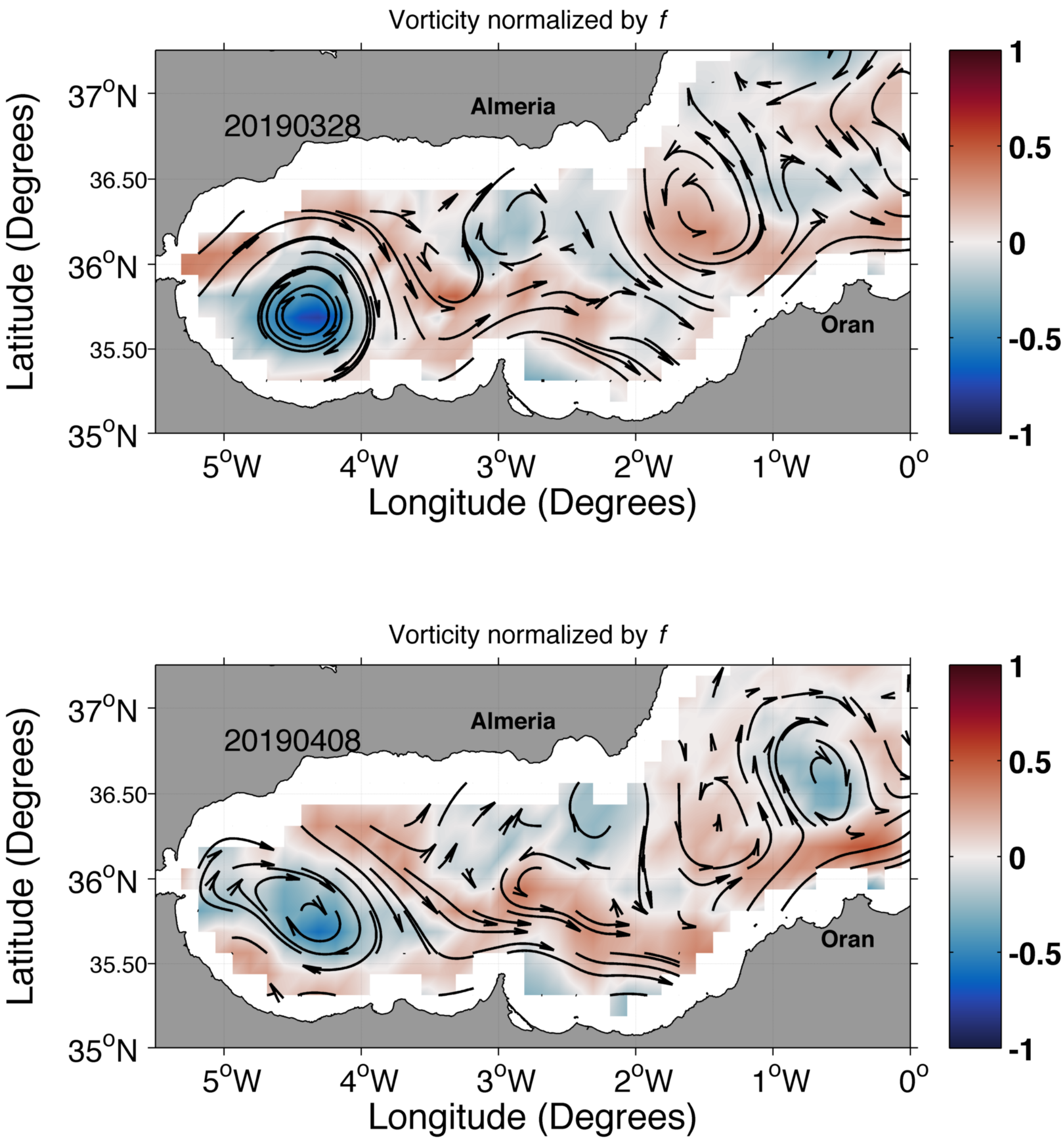


Figure 12.3: Relative vorticity (normalized by f) estimated from Absolute Geostrophic Velocity (altimetry product).

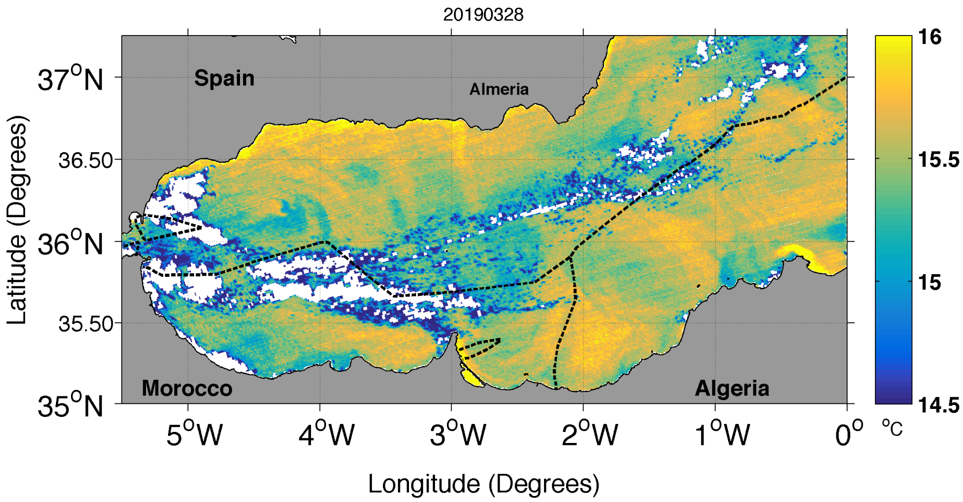


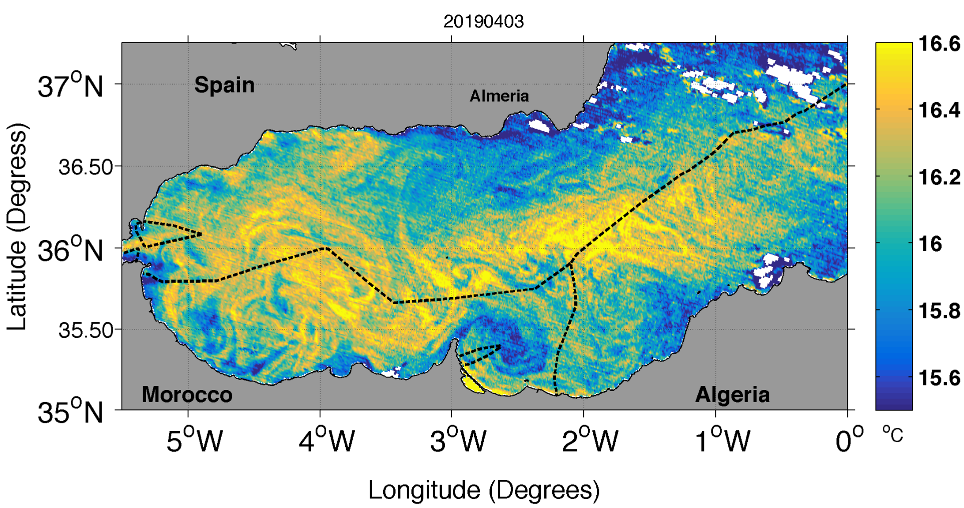


Figure 12.4: Examples of SST images for March 28 and April 3 2019.

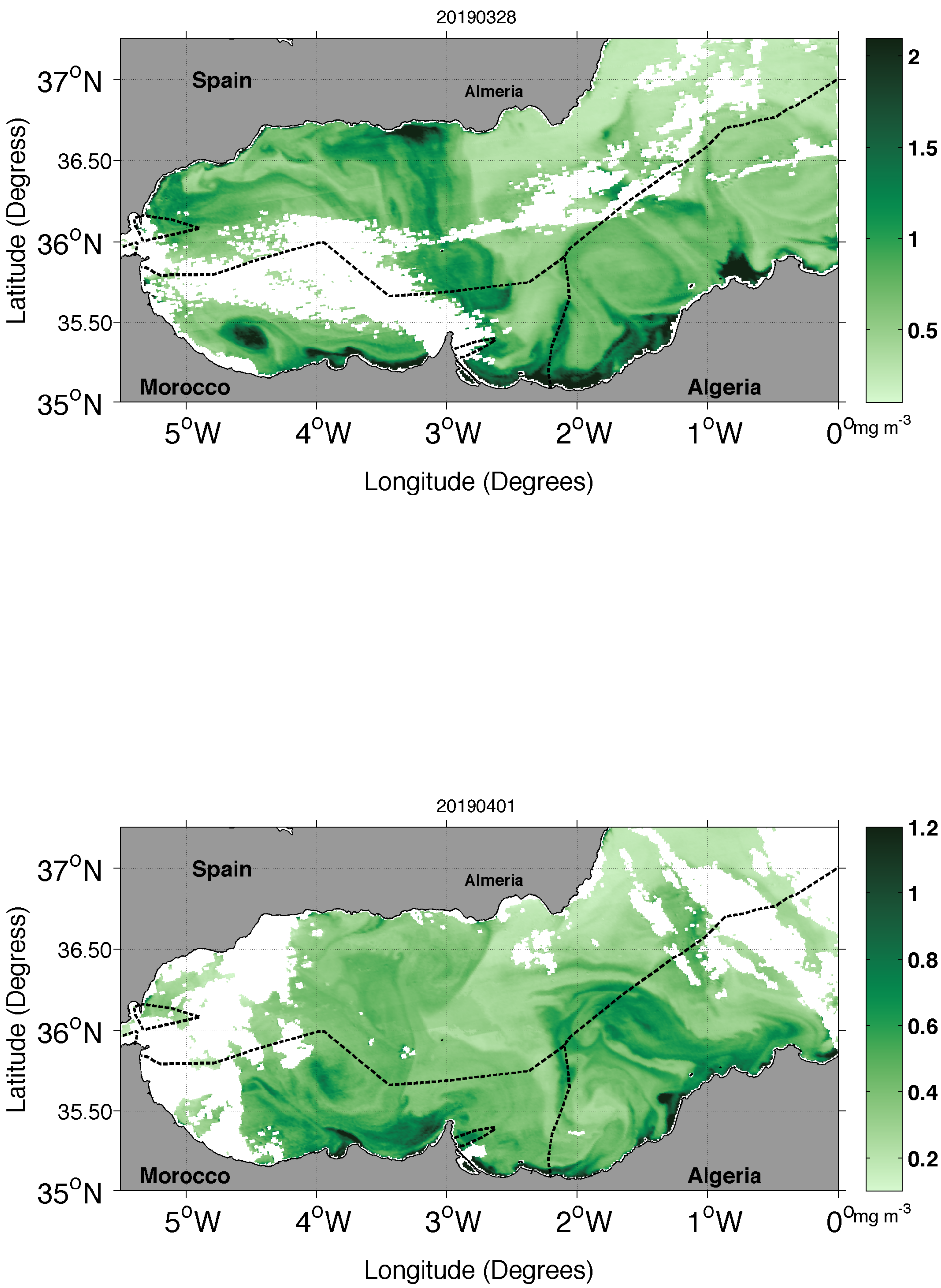


Figure 12.5: Examples of Chl-a images from MODIS for March 28 and April 1st 2019.

Figure 5 shows two examples of the Chl-a images in the Alboran Sea, suggesting the presence of filaments in the eastern part of the western Alboran Gyre and the presence of a small eddy near the cost of Almería that was also sampled during the second phase of the experiment.

Sections 12.1.4 and 12.1.5 compile SST and Chl-a daily images for the entire period of the experiment, respectively. Unfortunately, during the cruise period, there were a few days with high percentage of cloud cover and consequently, good quality images were not available.

### 12.1.3 ADT daily images

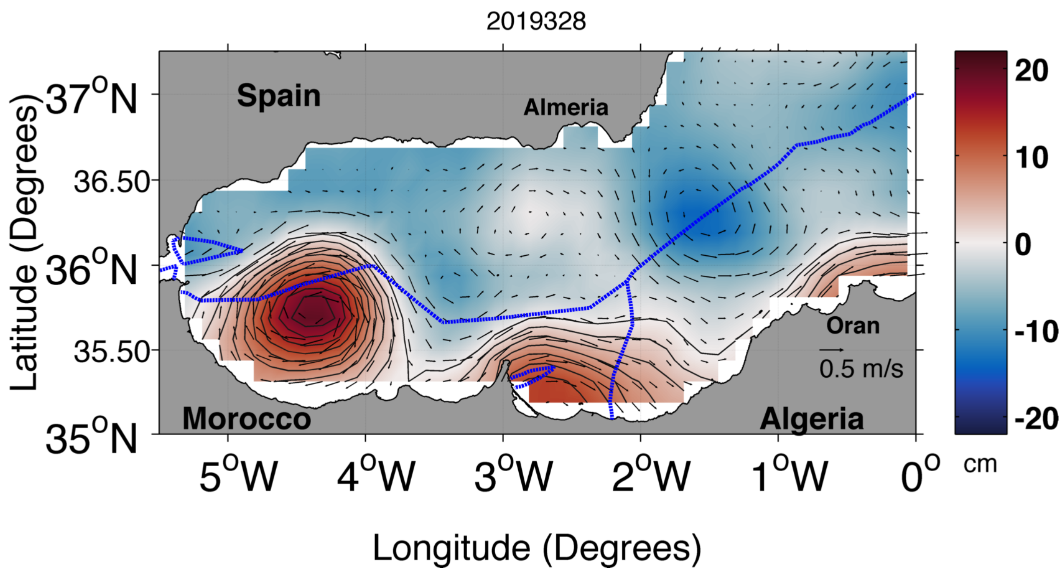


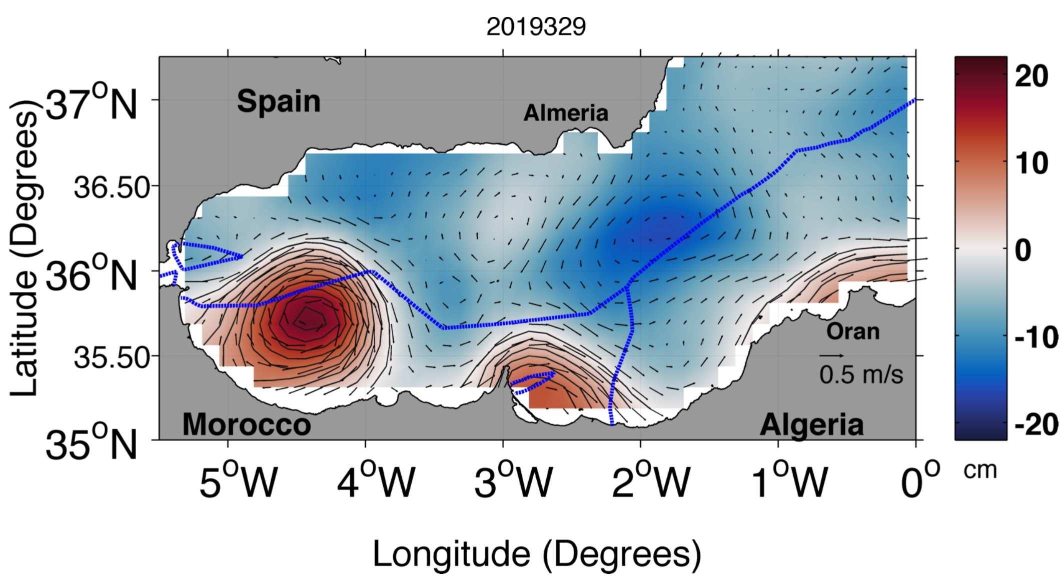

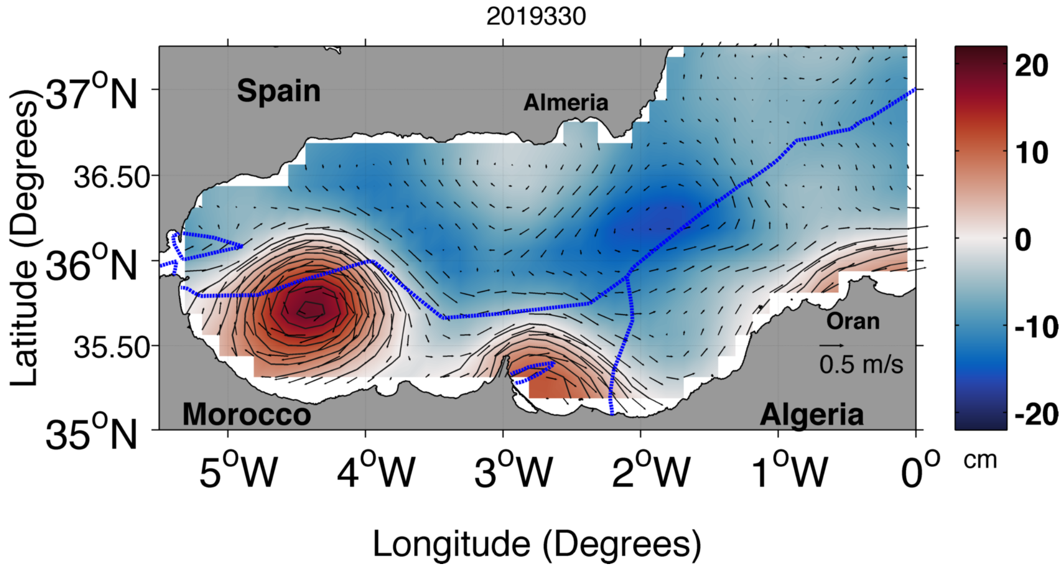
2019330
Spain
Almeria
Morocco
Algeria
Oran
0.5 m/s
37°N
36.50
36°N
35.50
35°N
5°W
4°W
3°W
2°W
1°W
0°
Latitude (Degrees)
Longitude (Degrees)
20
10
0
-10
-20
cm

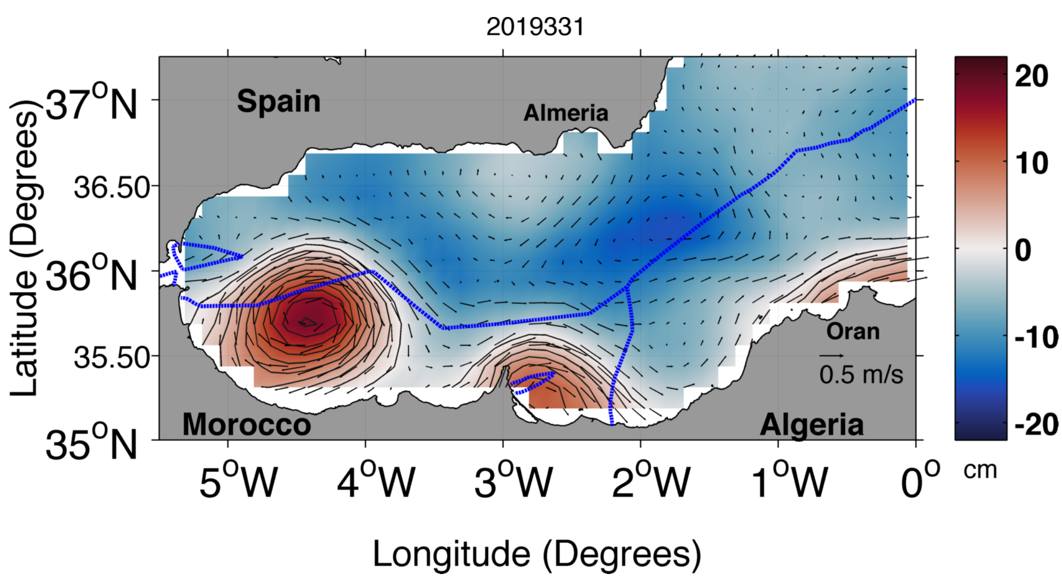
2019331
Spain
Almeria
Morocco
Algeria
Oran
0.5 m/s
37°N
36.50
36°N
35.50
35°N
5°W
4°W
3°W
2°W
1°W
0°
Latitude (Degrees)
Longitude (Degrees)
20
10
0
-10
-20
cm

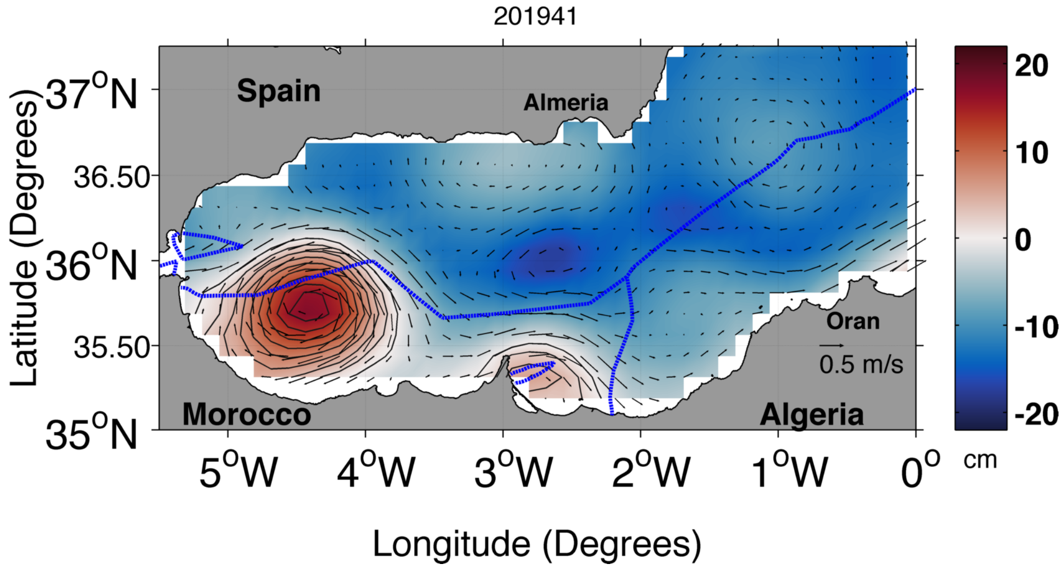
201941
Spain
Almeria
Morocco
Algeria
Oran
0.5 m/s
37°N
36.50
36°N
35.50
35°N
5°W
4°W
3°W
2°W
1°W
0°
Latitude (Degrees)
Longitude (Degrees)
20
10
0
-10
-20
cm

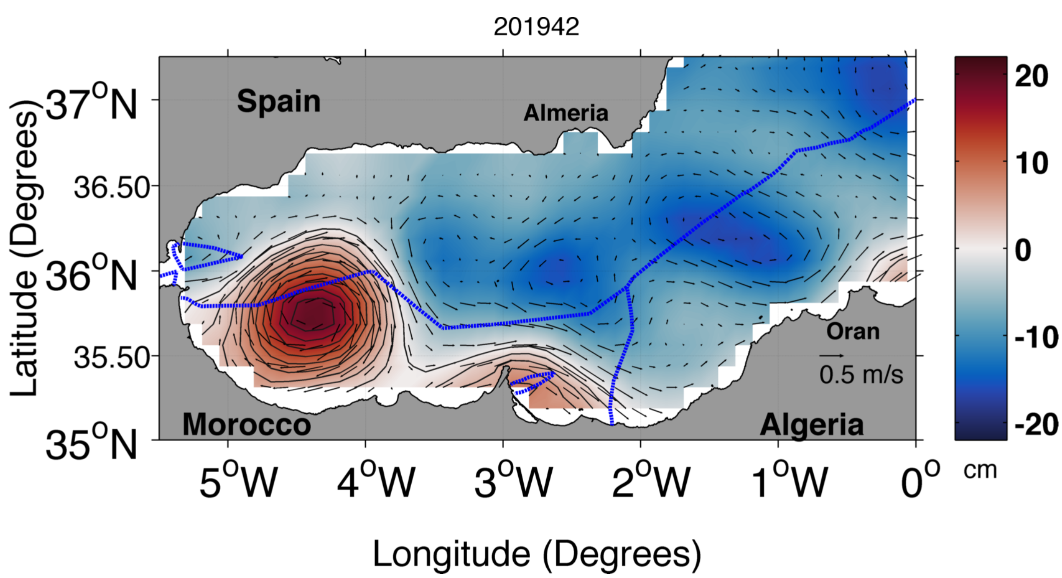
201942
Spain
Almeria
Morocco
Algeria
Oran
0.5 m/s
37°N
36.50
36°N
35.50
35°N
5°W
4°W
3°W
2°W
1°W
0°
Latitude (Degrees)
Longitude (Degrees)
20
10
0
-10
-20
cm

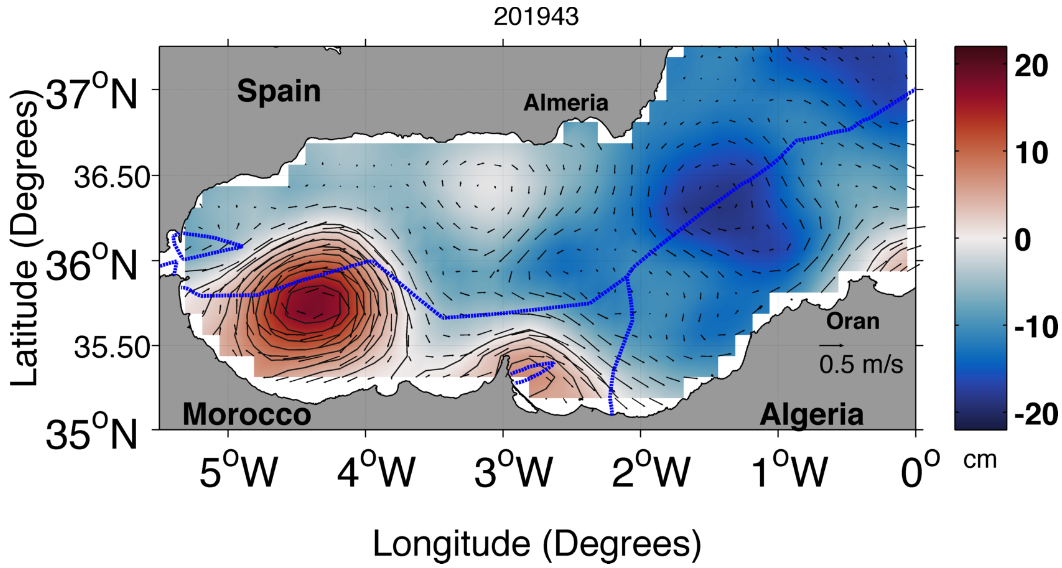
201943
Spain
Almeria
Oran
0.5 m/s
Morocco
Algeria
37°N
36.50
36°N
35.50
35°N
5°W
4°W
3°W
2°W
1°W
0°
Latitude (Degrees)
Longitude (Degrees)
20
10
0
-10
-20
cm

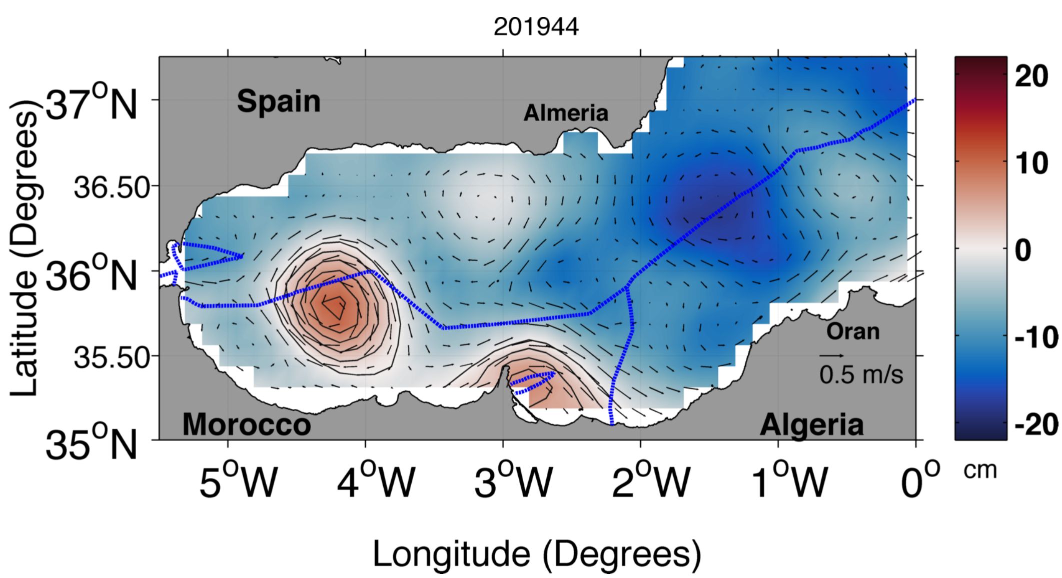
201944
Spain
Almeria
Oran
0.5 m/s
Morocco
Algeria
37°N
36.50
36°N
35.50
35°N
5°W
4°W
3°W
2°W
1°W
0°
Latitude (Degrees)
Longitude (Degrees)
20
10
0
-10
-20
cm

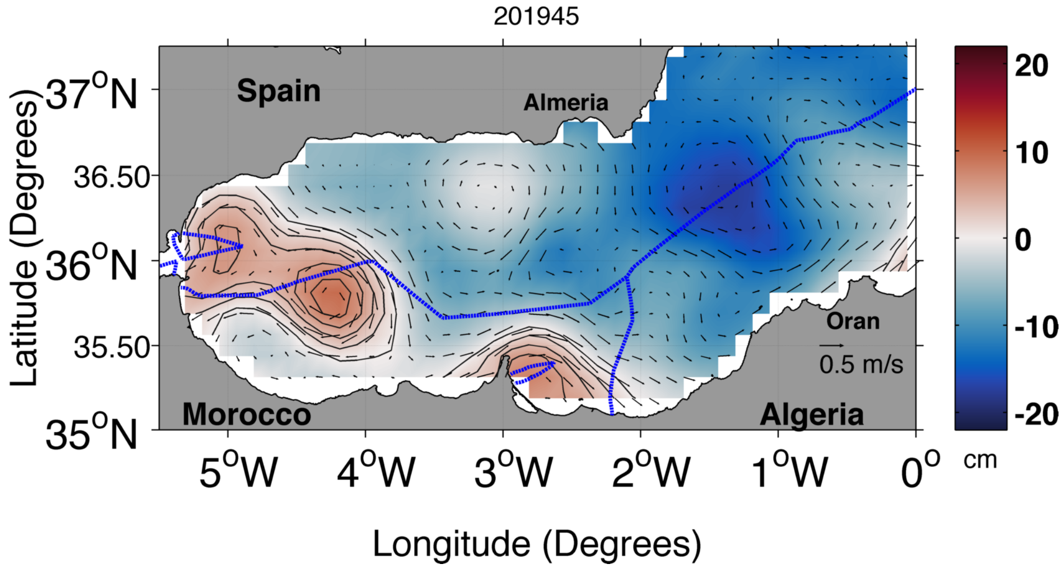
201945
Spain
Almeria
Oran
0.5 m/s
Morocco
Algeria
37°N
36.50
36°N
35.50
35°N
5°W
4°W
3°W
2°W
1°W
0°
Latitude (Degrees)
Longitude (Degrees)
20
10
0
-10
-20
cm

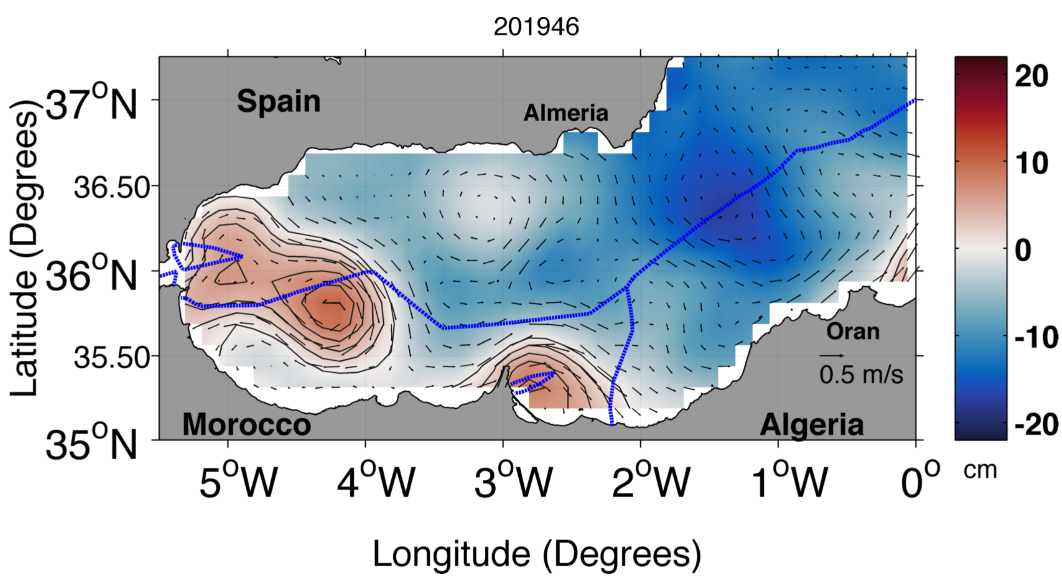
201946
Spain
Almeria
Oran
0.5 m/s
Morocco
Algeria
37°N
36.50
36°N
35.50
35°N
5°W
4°W
3°W
2°W
1°W
0°
Latitude (Degrees)
Longitude (Degrees)
20
10
0
-10
-20
cm

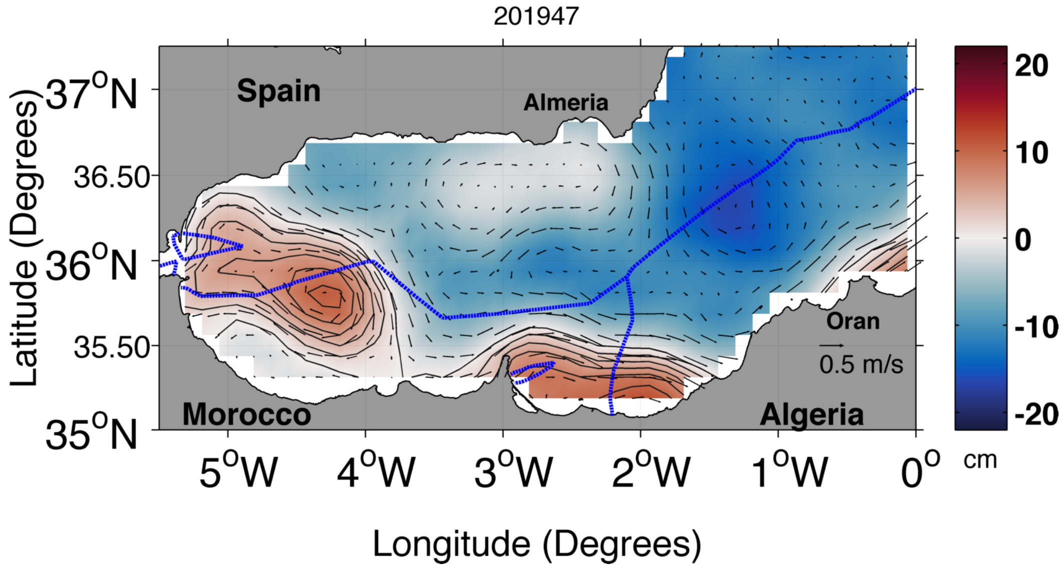
201947
Spain
Almeria
Oran
0.5 m/s
Morocco
Algeria
37°N
36.50
36°N
35.50
35°N
5°W
4°W
3°W
2°W
1°W
0°
Latitude (Degrees)
Longitude (Degrees)
20
10
0
-10
-20
cm

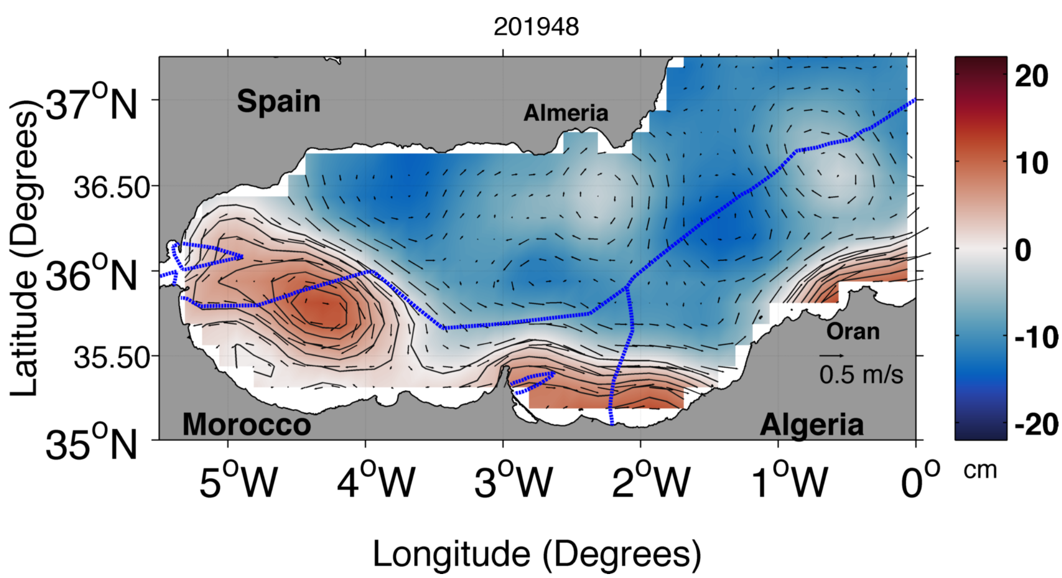
201948
Spain
Almeria
Oran
0.5 m/s
Morocco
Algeria
37°N
36.50
36°N
35.50
35°N
5°W
4°W
3°W
2°W
1°W
0°
Latitude (Degrees)
Longitude (Degrees)
20
10
0
-10
-20
cm

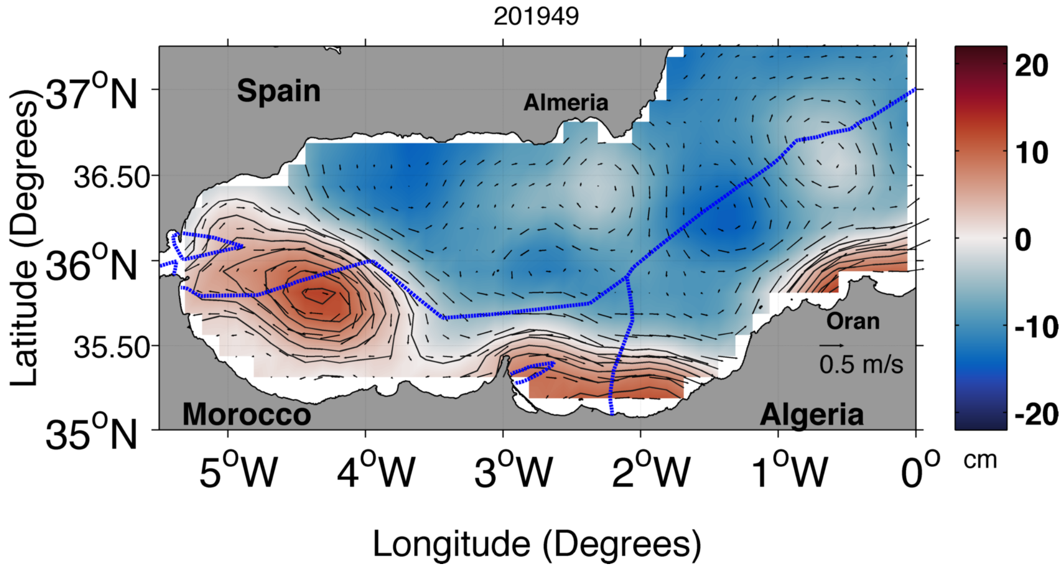
201949
Spain
Almeria
Morocco
Algeria
Oran
0.5 m/s
37°N
36.50
36°N
35.50
35°N
5°W
4°W
3°W
2°W
1°W
0°
Latitude (Degrees)
Longitude (Degrees)
20
10
0
-10
-20
cm

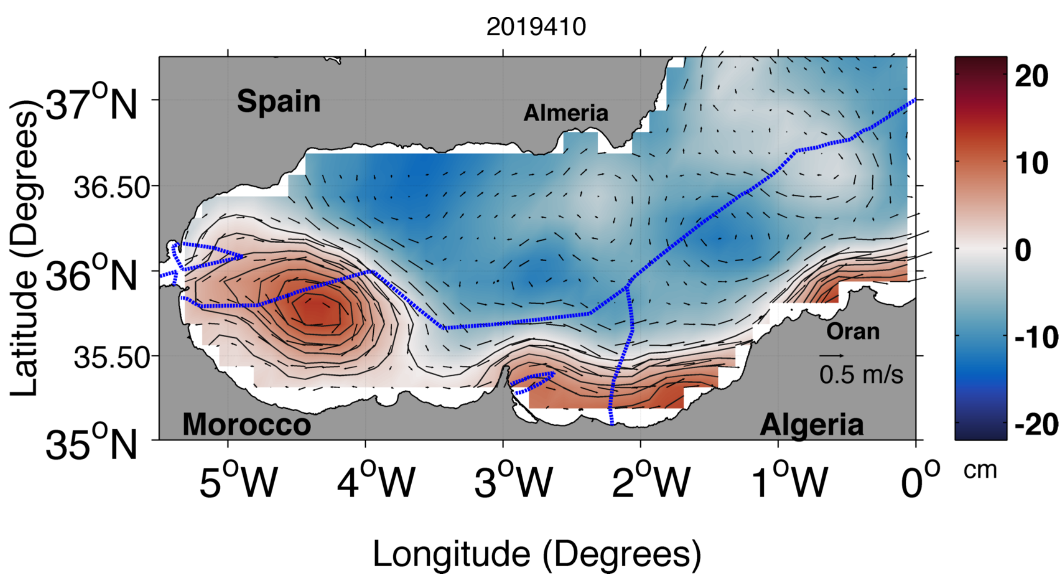
2019410
Spain
Almeria
Morocco
Algeria
Oran
0.5 m/s
37°N
36.50
36°N
35.50
35°N
5°W
4°W
3°W
2°W
1°W
0°
Latitude (Degrees)
Longitude (Degrees)
20
10
0
-10
-20
cm

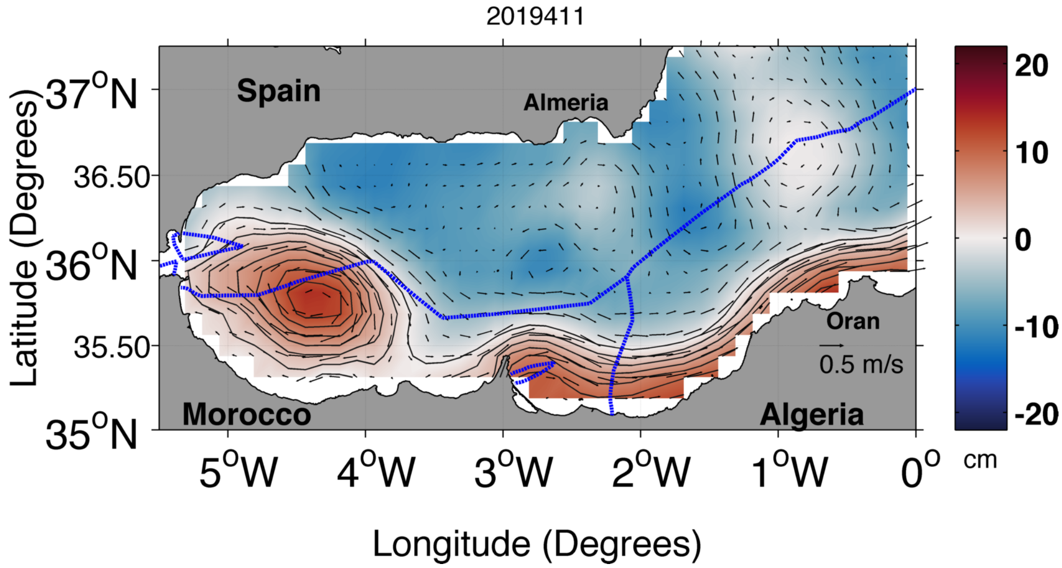


### 12.1.4 SST daily images

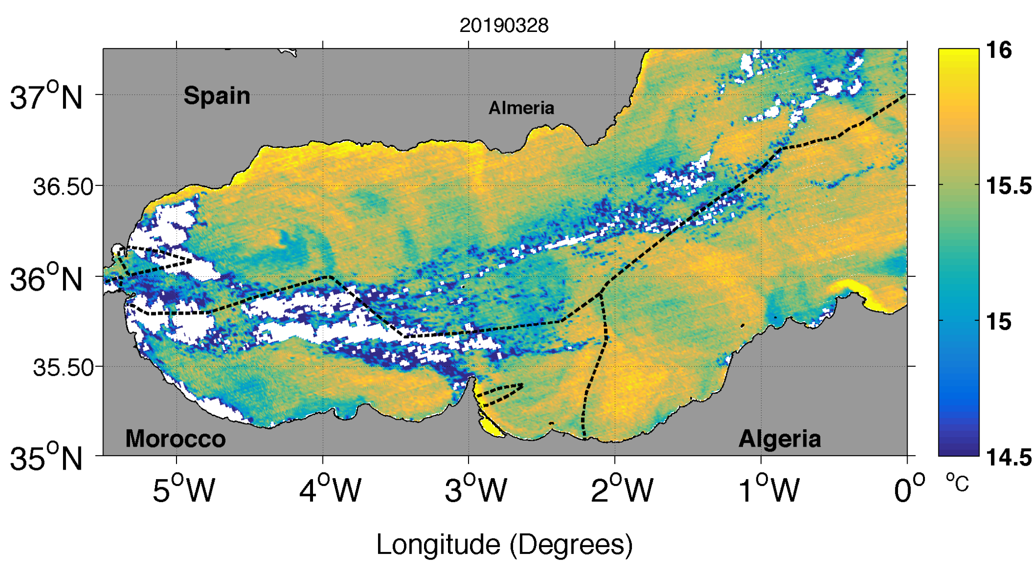

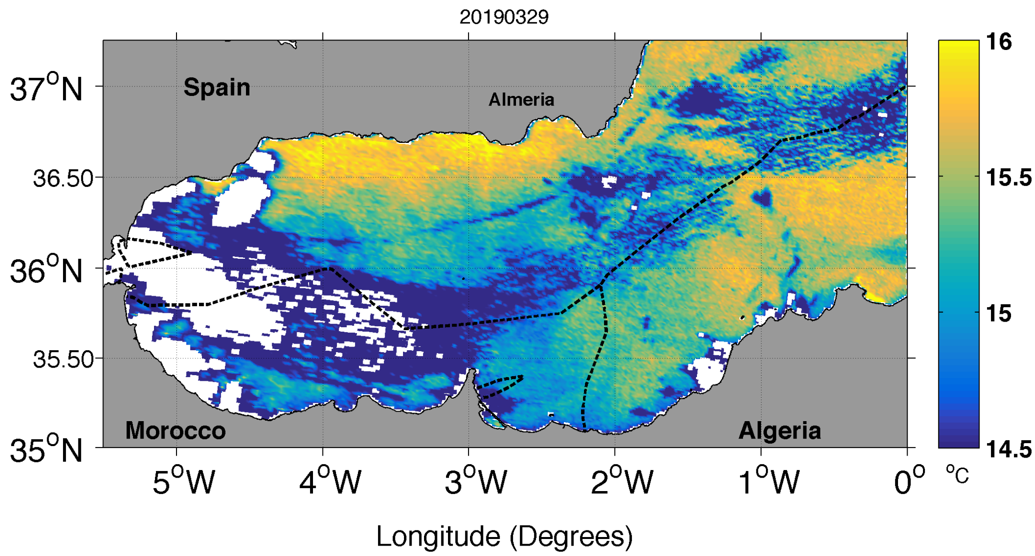
20190329
Spain
Almeria
Morocco
Algeria
37°N
36.50
36°N
35.50
35°N
5°W
4°W
3°W
2°W
1°W
0°
Longitude (Degrees)
16
15.5
15
14.5
°C

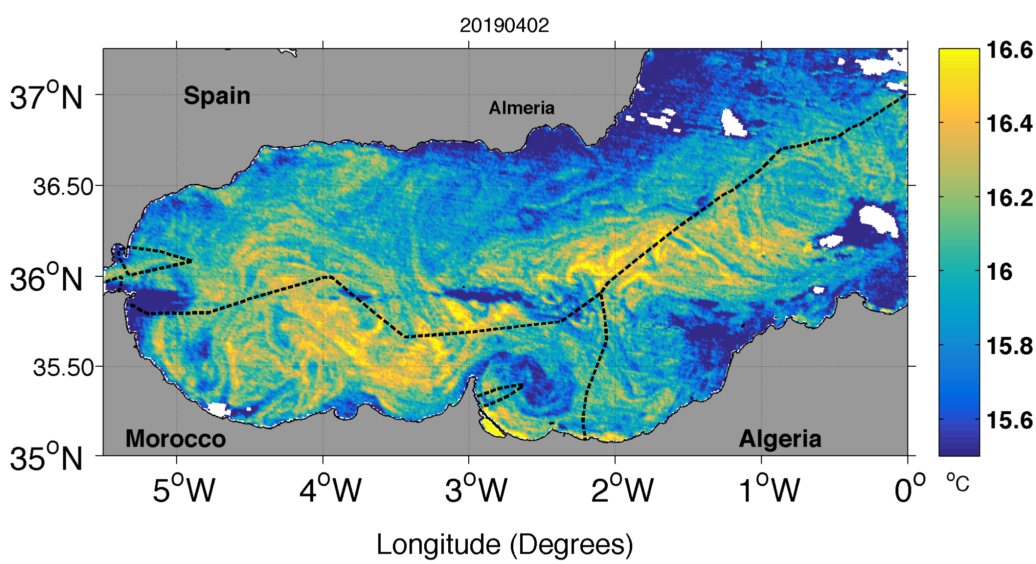
20190402
Spain
Almeria
Morocco
Algeria
37°N
36.50
36°N
35.50
35°N
5°W
4°W
3°W
2°W
1°W
0°
Longitude (Degrees)
16.6
16.4
16.2
16
15.8
15.6
°C

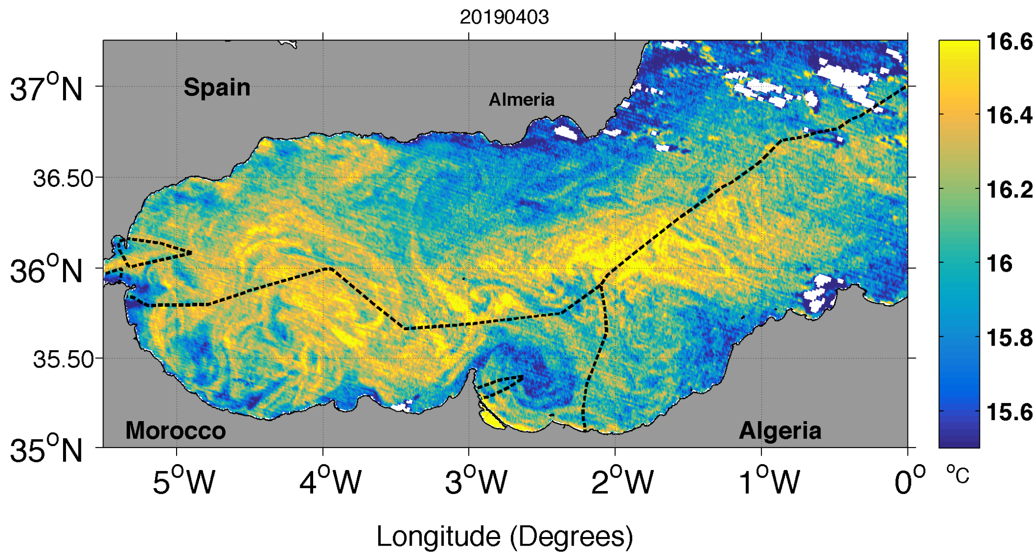
20190403
37°N
36.50
36°N
35.50
35°N
Spain
Almeria
Morocco
Algeria
5°W
4°W
3°W
2°W
1°W
0°
Longitude (Degrees)
16.6
16.4
16.2
16
15.8
15.6
°C

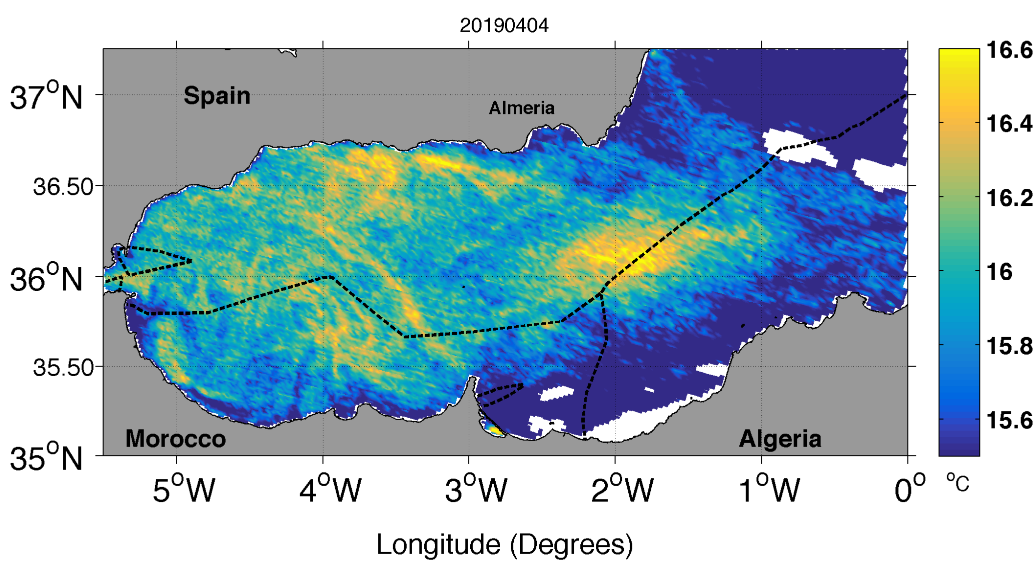
20190404
37°N
36.50
36°N
35.50
35°N
Spain
Almeria
Morocco
Algeria
5°W
4°W
3°W
2°W
1°W
0°
Longitude (Degrees)
16.6
16.4
16.2
16
15.8
15.6
°C

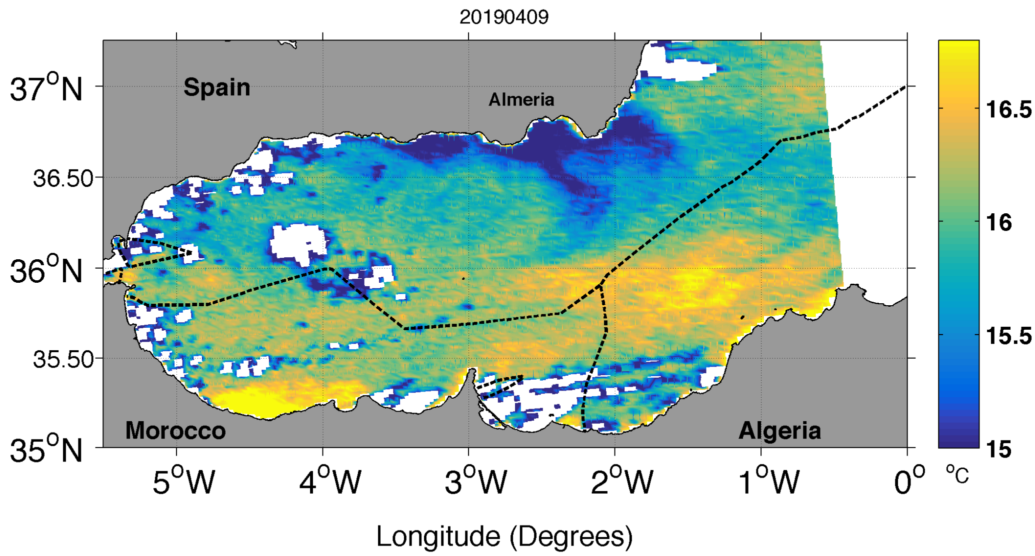
20190409
Spain
Almeria
Morocco
Algeria
37°N
36.50
36°N
35.50
35°N
5°W
4°W
3°W
2°W
1°W
0°
Longitude (Degrees)
16.5
16
15.5
15
°C

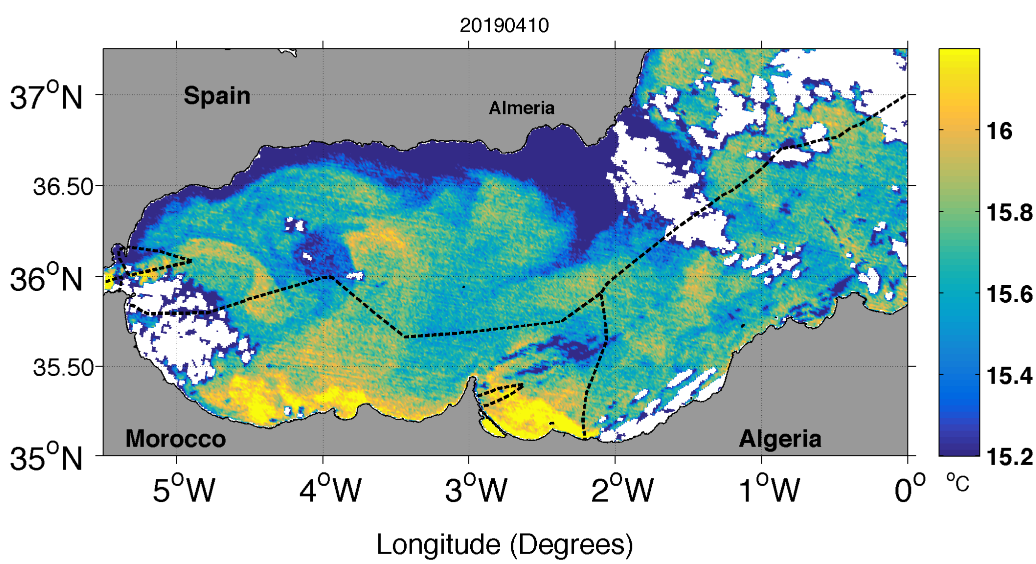
20190410
Spain
Almeria
Morocco
Algeria
37°N
36.50
36°N
35.50
35°N
5°W
4°W
3°W
2°W
1°W
0°
Longitude (Degrees)
16
15.8
15.6
15.4
15.2
°C

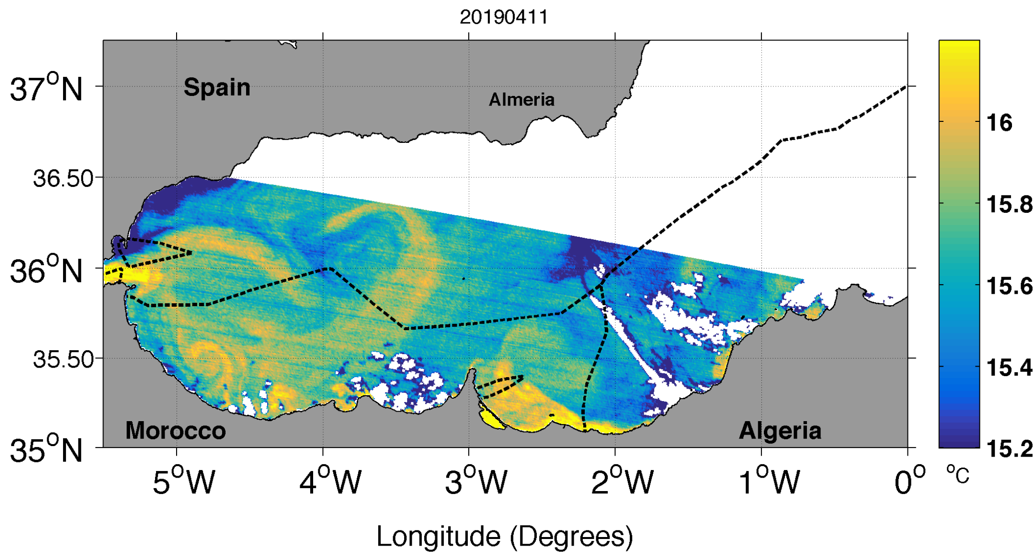


### 12.1.5 Chl-a daily images

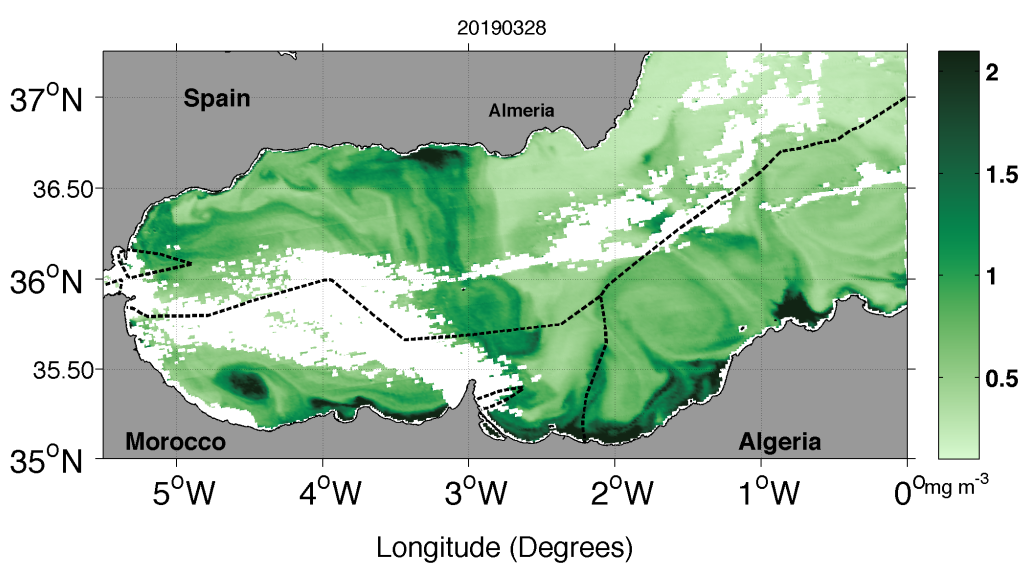

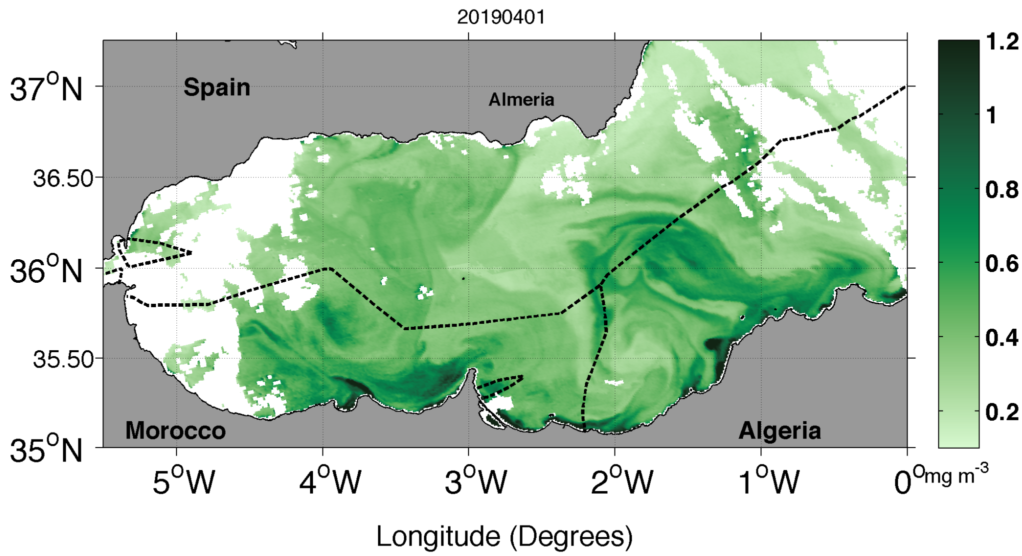
20190401
Spain
Almeria
Morocco
Algeria
37°N
36.50
36°N
35.50
35°N
5°W
4°W
3°W
2°W
1°W
0°
Longitude (Degrees)
mg m$^{-3}$
1.2
1
0.8
0.6
0.4
0.2

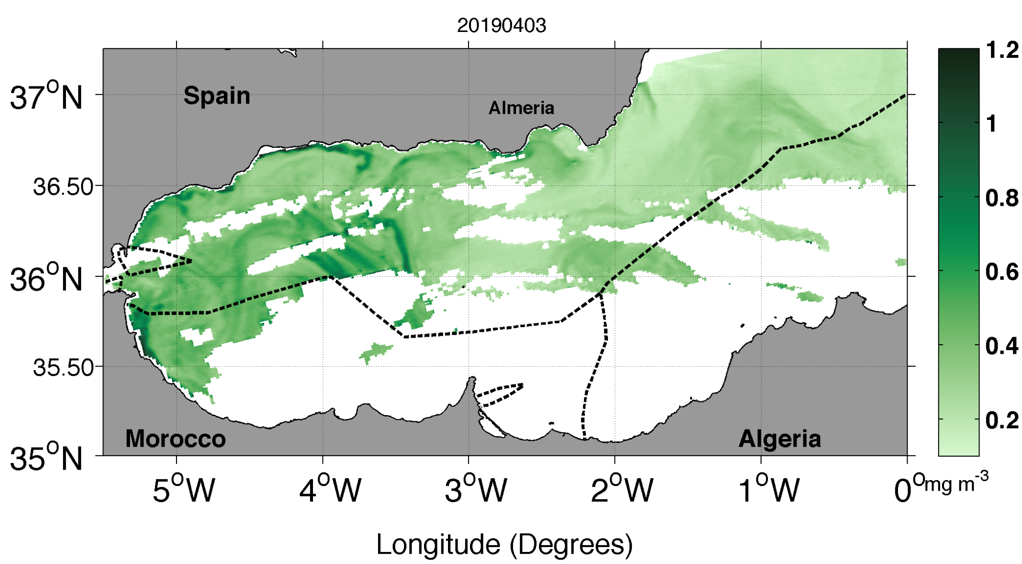
20190403
Spain
Almeria
Morocco
Algeria
37°N
36.50
36°N
35.50
35°N
5°W
4°W
3°W
2°W
1°W
0°
Longitude (Degrees)
mg m$^{-3}$
1.2
1
0.8
0.6
0.4
0.2

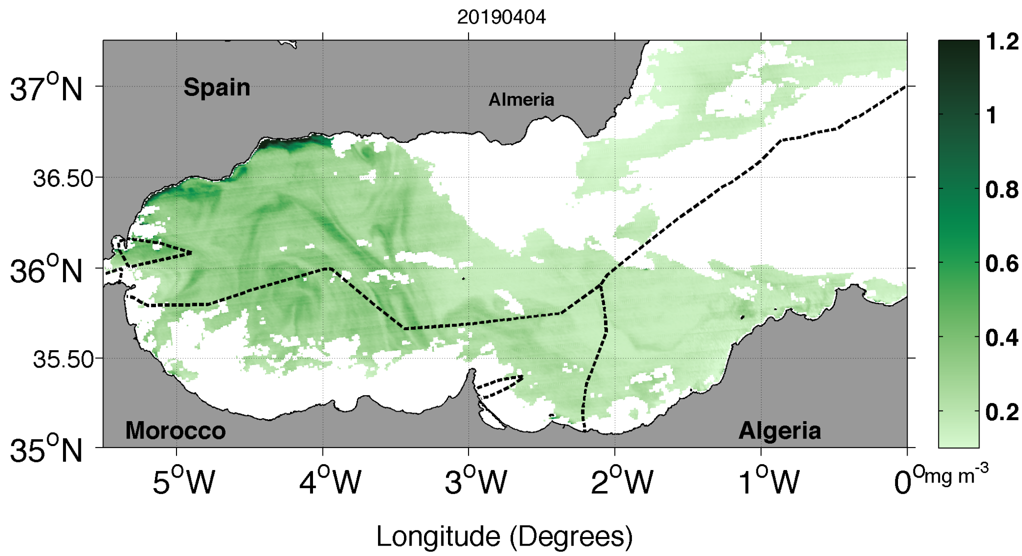
20190404
Spain
Almeria
Morocco
Algeria
37°N
36.50
36°N
35.50
35°N
5°W
4°W
3°W
2°W
1°W
0°
Longitude (Degrees)
1.2
1
0.8
0.6
0.4
0.2
mg m-3

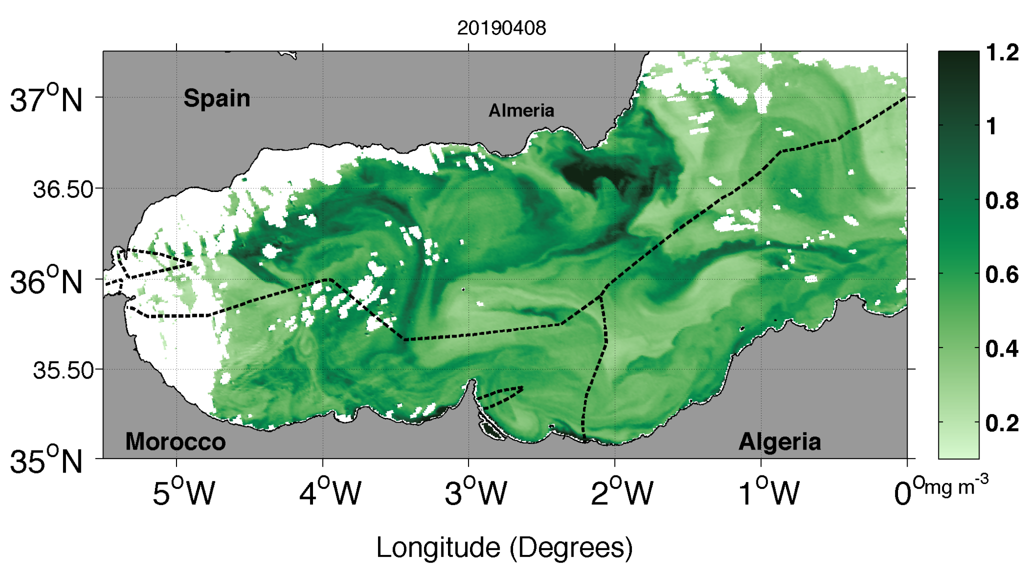
20190408
Spain
Almeria
Morocco
Algeria
37°N
36.50
36°N
35.50
35°N
5°W
4°W
3°W
2°W
1°W
0°
Longitude (Degrees)
1.2
1
0.8
0.6
0.4
0.2
mg m-3

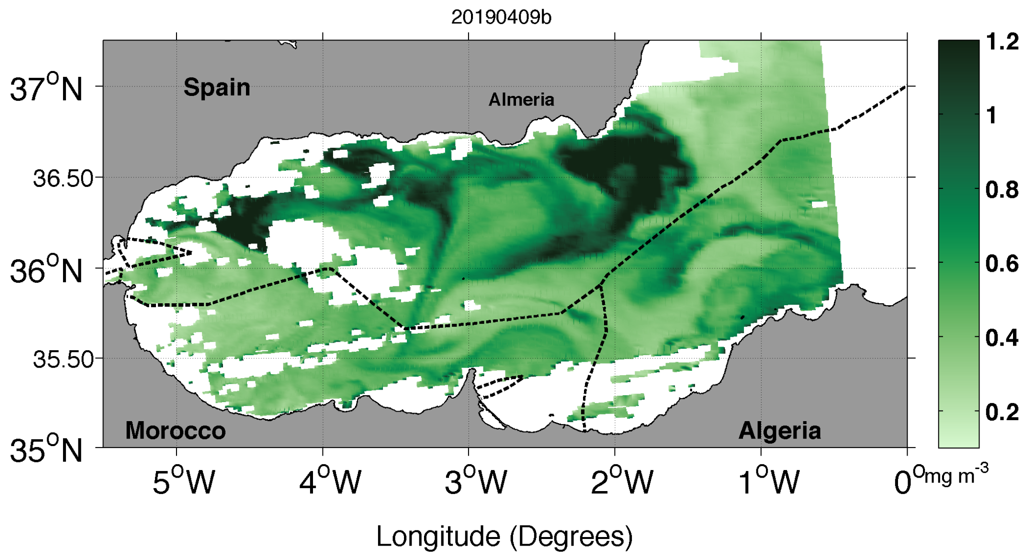
20190409b
Spain
Almeria
Morocco
Algeria
37°N
36.50
36°N
35.50
35°N
5°W
4°W
3°W
2°W
1°W
0°
Longitude (Degrees)
1.2
1
0.8
0.6
0.4
0.2
mg m-3

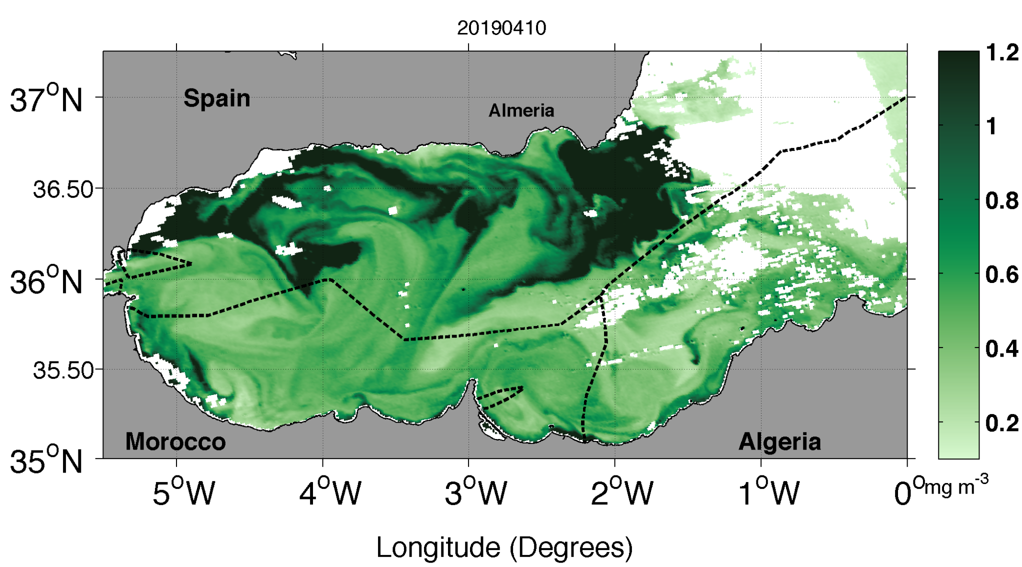
20190410
Spain
Almeria
Morocco
Algeria
37°N
36.50
36°N
35.50
35°N
5°W
4°W
3°W
2°W
1°W
0°
Longitude (Degrees)
1.2
1
0.8
0.6
0.4
0.2
mg m-3

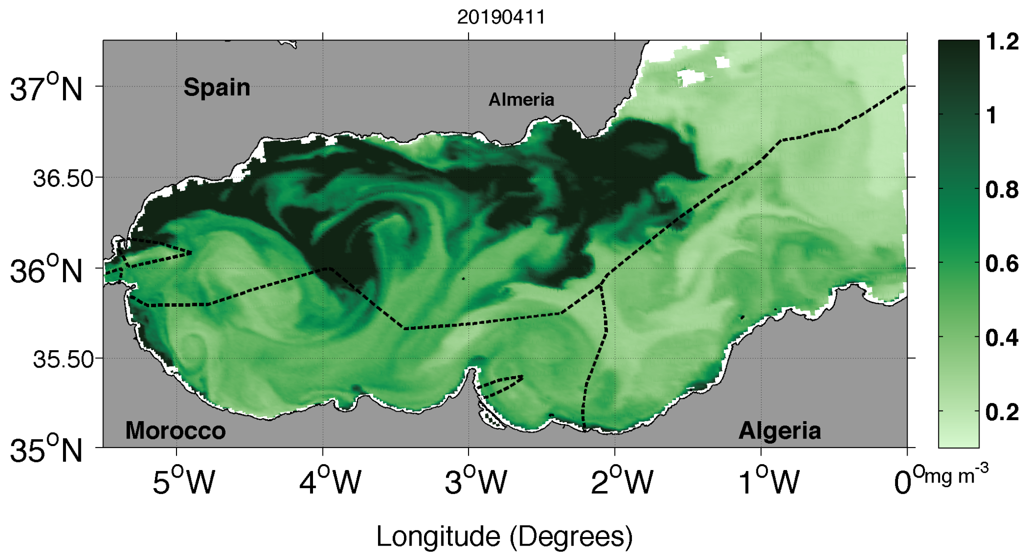


## 12.2 Ship-based satellite data analysis

### 12.2.1 Introduction

In the framework of the CALYPSO initiative, the main objective of the remote sensing CSIC and SOCIB activity, that was initiated in November 2018 and is briefly presented here, was to develop decision support tools for the detailed near-real time planning of the CALYPSO 2019 cruise (March 28-April 10, 2019) and further study of the spatial and temporal variability the surface signatures of frontal features and meso- and submesoscale structures in the Alborán Sea. A multi-sensor (multi-resolution) approach was used, taking profit of several standard satellites of medium resolution such as MODIS at 1 km and VIIRS at 750 m but also new satellites with higher resolution such as Sentinel-3 at 300 m and Sentinel-2 at 10 m, from the Copernicus Earth Observation program. This approach allowed optimal definition of sampling strategies before and during at sea operations and provided technical support to the different phases of the cruises and post cruises detailed analysis. A database was created and updated with all available daily satellite images at different spatial scales before and during the field experiment. Main variables included in this analysis are chlorophyll-a concentration (Chl) and sea surface temperature (SST). Chl was found to be especially useful to characterize the surface biogeochemical patterns and offer a synoptic view of the study region in quasi-real time, helping determine the positions of the gyres, fronts, and filaments and improving the coordinated sampling strategy.

### 12.2.2 Methodology during the CALYPSO campaign

Specifically, during the CALYPSO 2019 cruise, a satellite database with daily images at Level 2 was generated and uploaded by Isabel Caballero in the CALYPSO/satellite_data/ folder. Given the limited internet connection during the cruise, the electronic team of the *N/O Pourquoi Pas?*as able to manage a computer in Deck 7 to download daily imagery. Only the first scene per day corresponding to **Sentinel-3A and Sentinel-3B** (overpass at 10 am UTC, download at 3 pm UTC) was selected to give support in near-real time to the CALYPSO decisions. The source data is ESA-Copernicus program and CODA EUMESAT. A quality-assurance procedure was performed on the Chl data based on the Sentinel-3 Ocean and Land Colour Instrument (OLCI) technical information. The cloud coverage during the study period from 28 March to 10 April was severe ∼70% (Table 12.1). Figure 12.6 and Figure 12.7 indicate an example of the images generated for Chl at Full Resolution (FR, 300 m) and SST Reduced Resolution (RR, 1 km) on 1st April 2019, respectively. The ocean colour imagery was used to assist the surveying as shown in Figure 12.8 over an operating area close to Almeria. The imagery was also converted into KML format for visualization in GoogleEarth overlapped with all the CALYPSO instruments (Figure 12.9).

We conducted an evaluation of the multi-sensor approach (1km-10m) to inspect and quantify the sub-mesoscale patterns before and during the CALYPSO 2019 cruise adding the information from MODIS, VIIRS, and Sentinel-2 optical sensors. All datasets were saved in calypso_2019_cruise/Satellite_data/SOCIB_ICMAN_Remote_Sensing/. The sensors corresponded to MODIS, VIIRS, and MSI.

1. CHL and SST **Moderate Resolution Imaging Spectroradiometer (MODIS)**: 1 km spatial resolution (daily revisit). Source: NASA, Level 2. Figure **??** shows a chl image on 1st April 2019 at 1km spatial resolution.

2. CHL and SST **Visible Infrared Imaging Radiometer Suite (VIIRS)**: 750 m spatial resolution (daily revisit). Source: NOAA, Level 2. Figure 6 shows a chl image on 1st April 2019 at 750 m spatial resolution.

3. CHL **Sentinel-2A and Sentinel-2B Multispectral Instrument (MSI)**: 10 m spatial resolution (5-day revisit). Source: ESA-Copernicus programme, Level 1.

For the CALYPSO 2019 campaign, we found extremely severe cloud contamination at these latitudes for Sentinel-2 due to its high spatial resolution. However, we have developed the procedure to generate Level 2 imagery and inspect the spatio-temporal patterns upscaling to 10 m using the MSI onboard the Sentinel-2A/B satellites. The methodology is already performing accurately for clear scenes in February and March 2019 (Figure 12.12 through 12.15), and the atmospheric and sun glint correction implemented with ACOLITE processor seems to be optimal (minimum striping). Detailed features can be more precisely analyzed and quantified with MSI compared to MODIS or VIIRS. The proposed approach could be employed to better define fronts, filaments, and their spatial coverage at surface. MSI processing is time-consuming and it was not used for real-time analysis during the field trip.

Worth mention is the work carried out before the field trip in order to assist the sampling stations and offer a synoptic view of the Alborán Sea study region in the weeks and days prior to the 2019 cruise. Figures 12.16 and 12.17 display the spatio-temporal variability of Chl surface features by means of the multi-sensor approach with MODIS, VIIRS, and OLCI.

### 12.2.3 Ongoing and future work initially planned by the RS team:

- Multi-platform cross-validation: Comparison of satellite chlorophyll (validation of Sentinel-2 and Sentinel-3 satellites, Figure 12.18), in vivo water sampling, EcoCTD (Figure 12.19) and glider observations. We found consistency between OC standard observations from OLCI and MSI matchups, demonstrating the potential of Sentinel-2A/B to derive chl in coastal and offshore waters (Figure 12.18). This task will be accomplished by Isabel Caballero.

- Evaluation of regional climatology features and characterization of the biogeochemical mesoscale variability (monthly to inter-annual) and the potential mechanisms contributing to this variability in the Alborán Sea. Implementation of the Canny algorithm in order to automate the identification of the position and the intensity of ocean fronts. The weekly ocean color imagery with Chl and SST (Marine Copernicus, merged product of SeaWiFS, MODIS, MERIS and VIIRS) with spatial resolution of 1km is being used (Figure 12.20). This task will be accomplished by Gabriel Navarro.

- A study focused on characterizing the mesoscale of the Almeria-Oran Front (AOF) in space and time using remote sensing imagery and glider observations will be accomplished. In this work, we take advantage of the new technologies and tools combining glider observations with a large set of high-resolution (700 m) satellite-observed variables. The latter will help us to understand how mesoscale and sub-mesoscale features control the biochemistry of the AOF and identify the role/contribution in the abundance of the phytoplankton biomass. Additionally, relationships between Chl, Zeu and turbidity will be evaluated in order to provide information about the optical variability in time and space. This task will be accomplished by Nikolaos Zarokanellos.

Table 12.1: List of available imagery during the CALYPSO campaign 2019 for MODIS, VIIRS, OLCI and MSI sensors (V = low cloud coverage, % = severe cloud coverage, – =totally cloudy).

| SENSOR | MODIS | VIIRS | OLCI | MSI |
|---|---|---|---|---|
| 28 March | V | V | % | V |
| 29 March | – | – | % | |
| 30 March | – | – | – | |
| 31 March | – | – | – | |
| 1 April | V | V | V | V |
| 2 April | – | % | % | |
| 3 April | % | % | % | |
| 4 April | % | % | % | V |
| 5 April | – | – | – | |
| 6 April | – | % | – | V |
| 7 April | % | % | % | |
| 8 April | V | % | V | |
| 9 April | V | V | V | V |
| 10 April | V | V | % | |

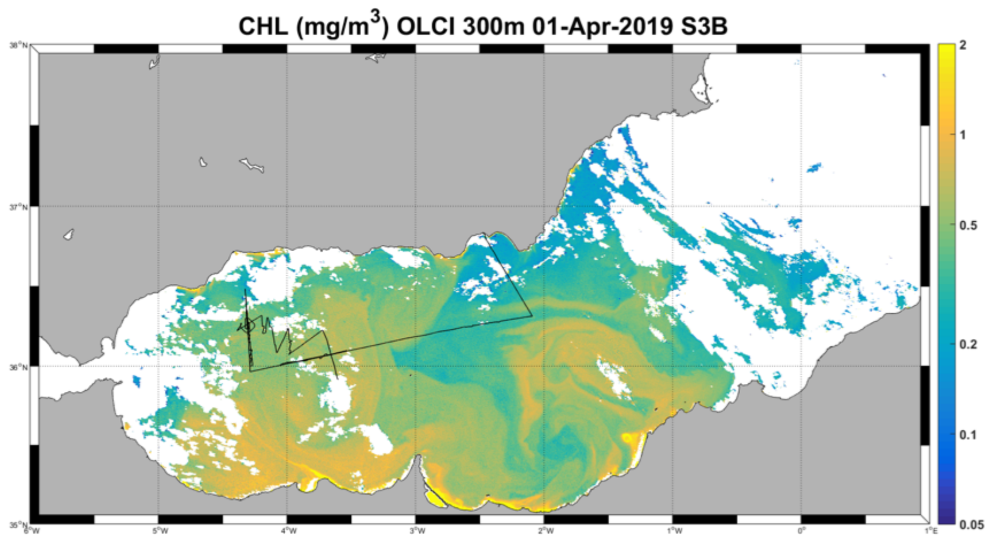


Figure 12.6: Chlorophyll (CHL) from the Ocean and Land Colour Instrument (OLCI) at Full Resolution (FR) 300 m on 1 April 2019. The black line is the track of *N/O Pourquoi Pas?*

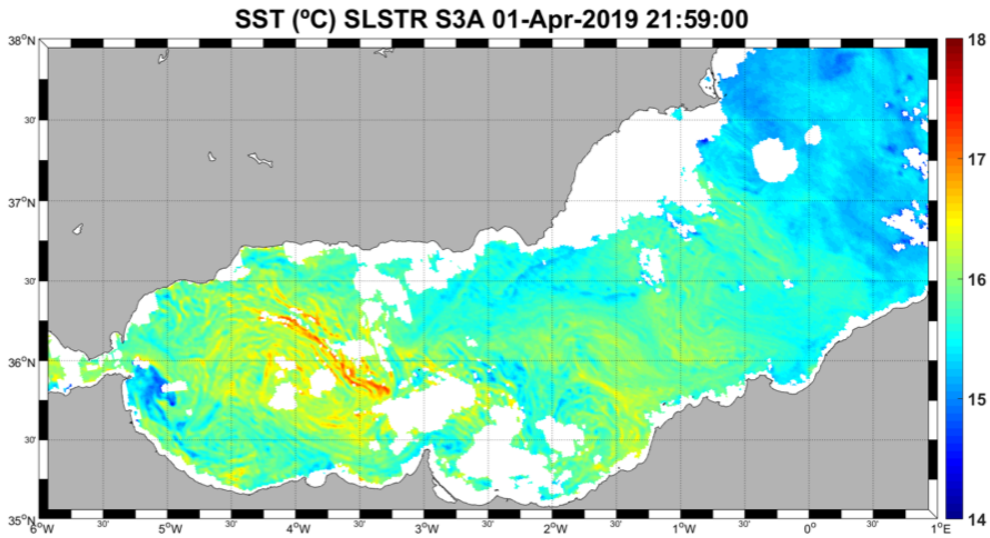


Figure 12.7: Sea surface temperature (SST) from the SLSTR instrument onboard Sentinel-3. Reduced Resolution (RR) 1km on 1 April 2019.

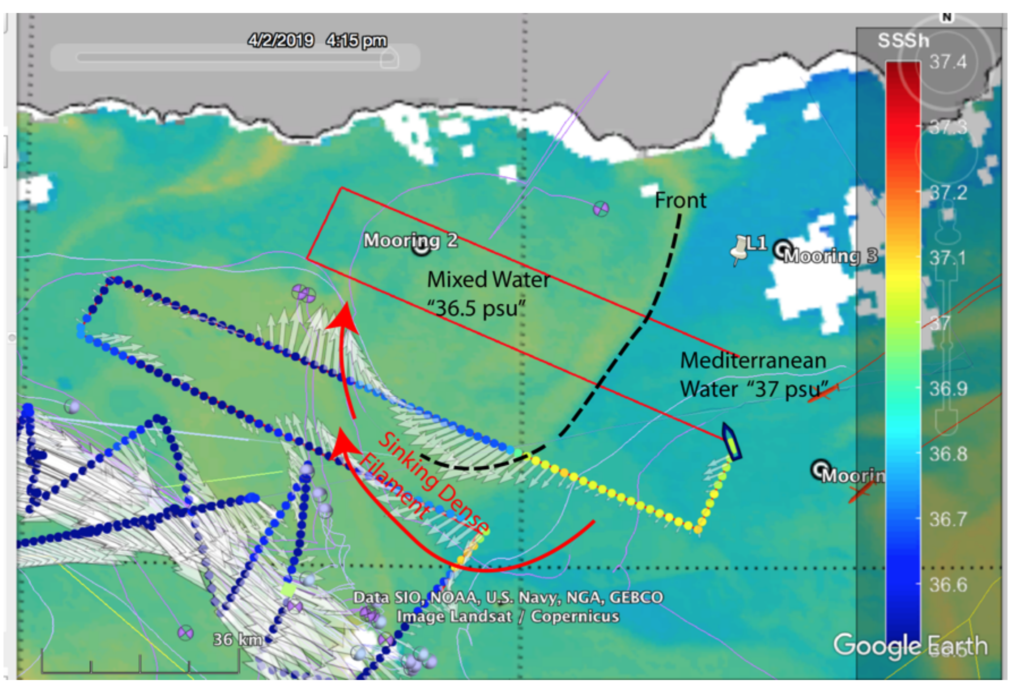


Figure 12.8: Plans for Second Leg.

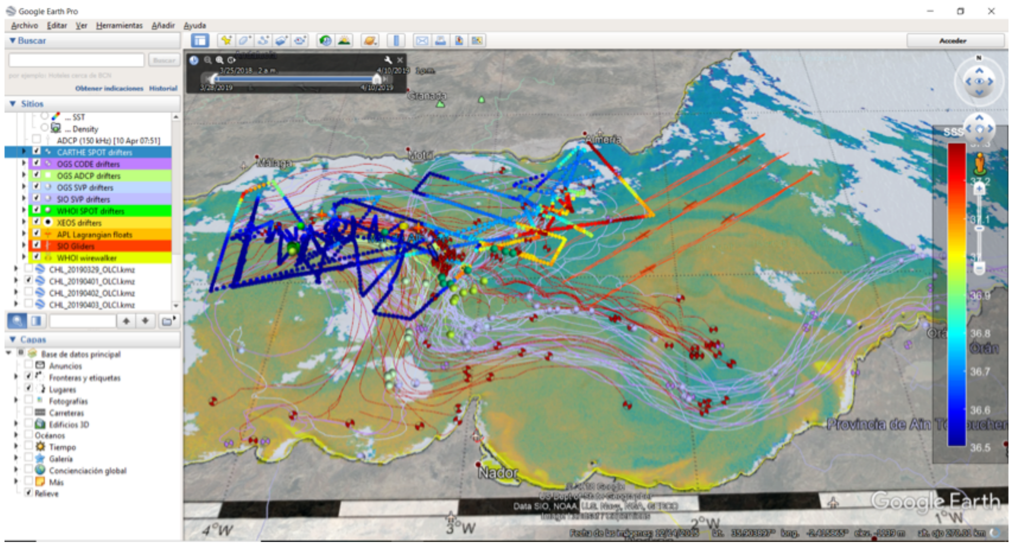


Figure 12.9: Google Earth tool with satellite data and CALYPSO instrumentation.

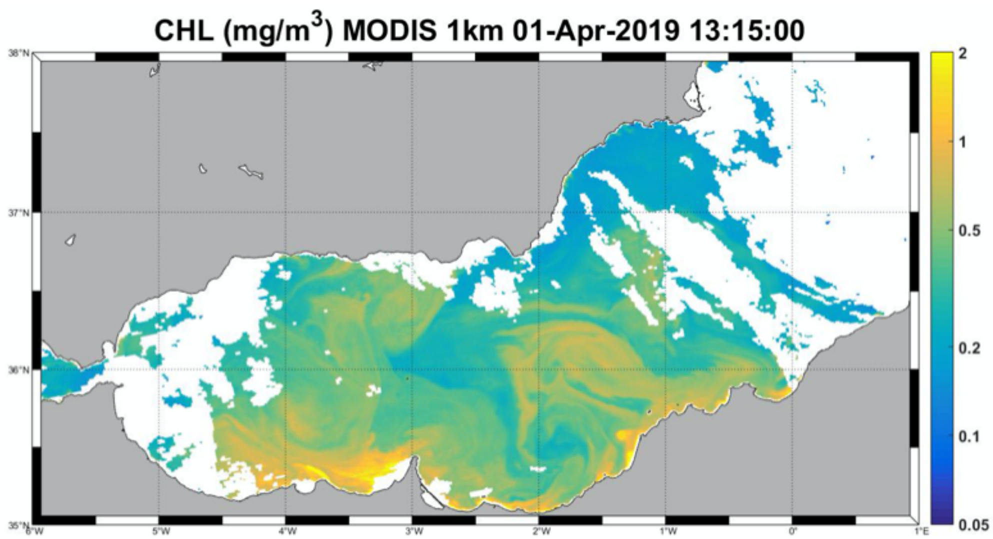


Figure 12.10: Chlorophyll (CHL) from MODIS at 1km on 1 April 2019.

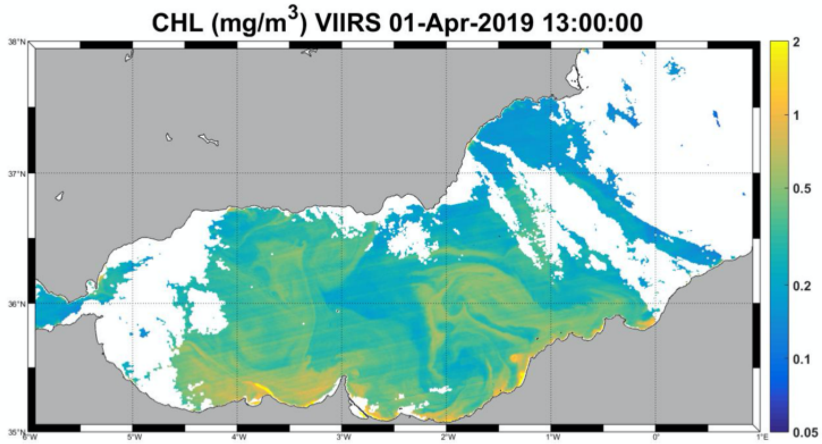


Figure 12.11: Chlorophyll (CHL) from VIIRS at 750 m on 1 April 2019.

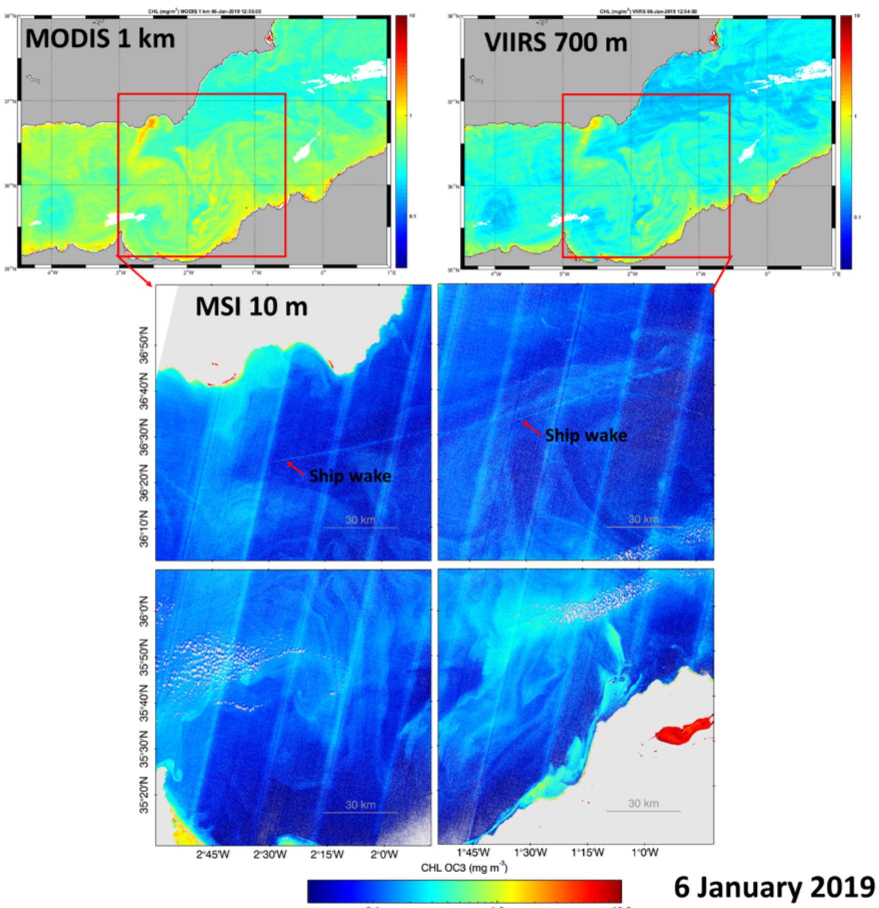


Figure 12.12: Example of chlorophyll concentration (chl) from MODIS at 1 km, VIIRS at 700 m, and MSI at 10 m on 6 January 2019.

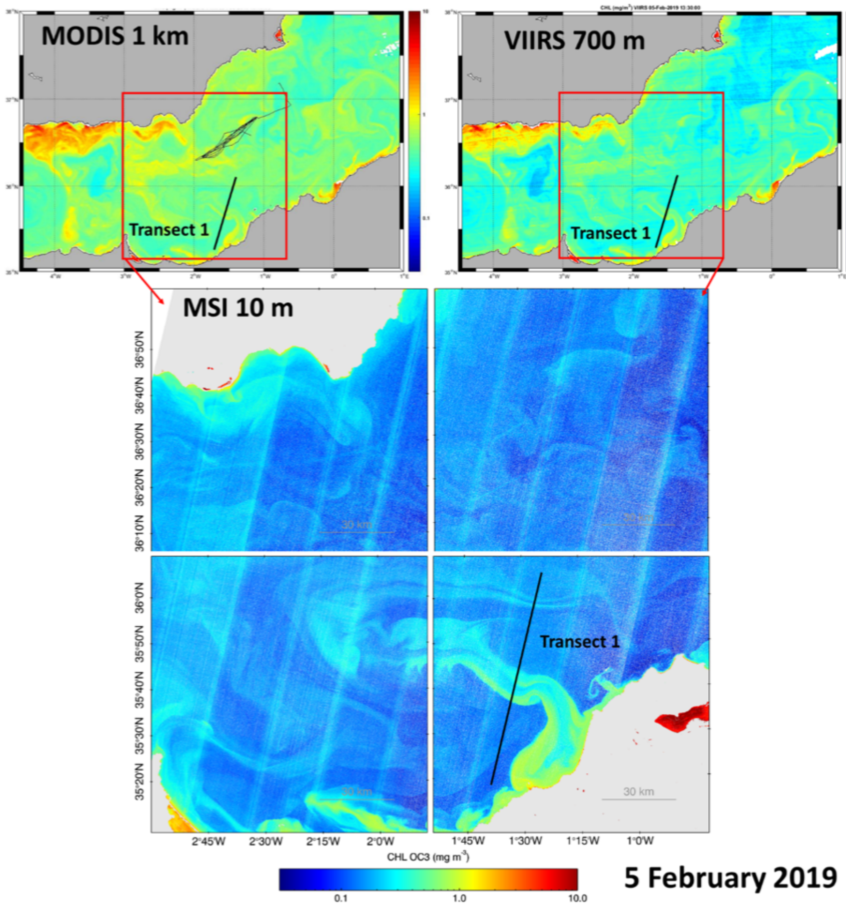


Figure 12.13: Example of chlorophyll concentration (chl) from MODIS at 1 km, VIIRS at 700 m and MSI at 10 m on 5 February 2019.

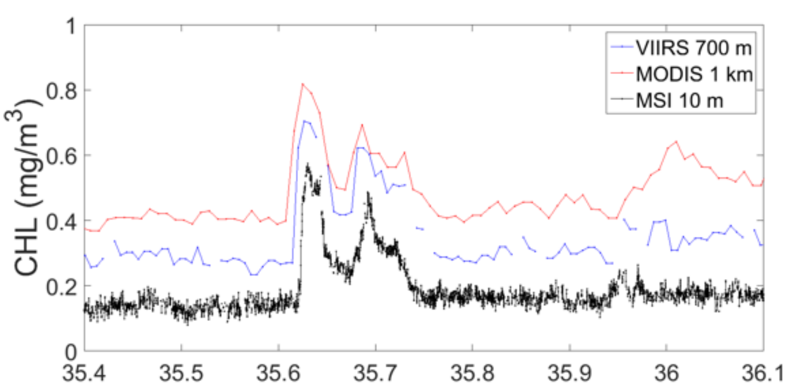


Figure 12.14: Transect of chlorophyll concentration from MODIS at 1 km, VIIRS at 700 m and MSI at 10 m on 5 February 2019 (see Transect location in Figure 12.13).

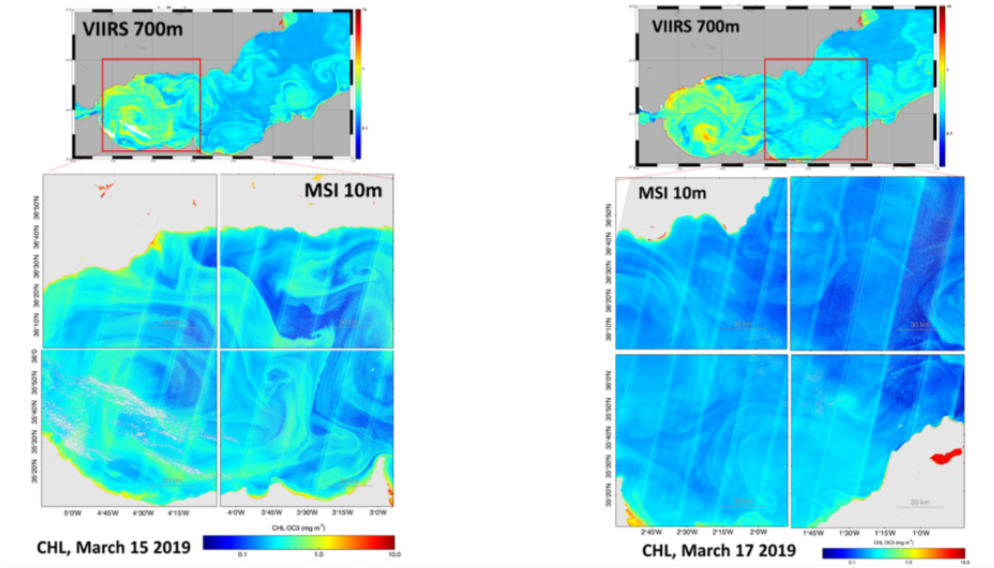


Figure 12.15: Example of chlorophyll concentration (chl) from VIIRS at 700 m and MSI at 10 m on 15 and 17 March 2019.

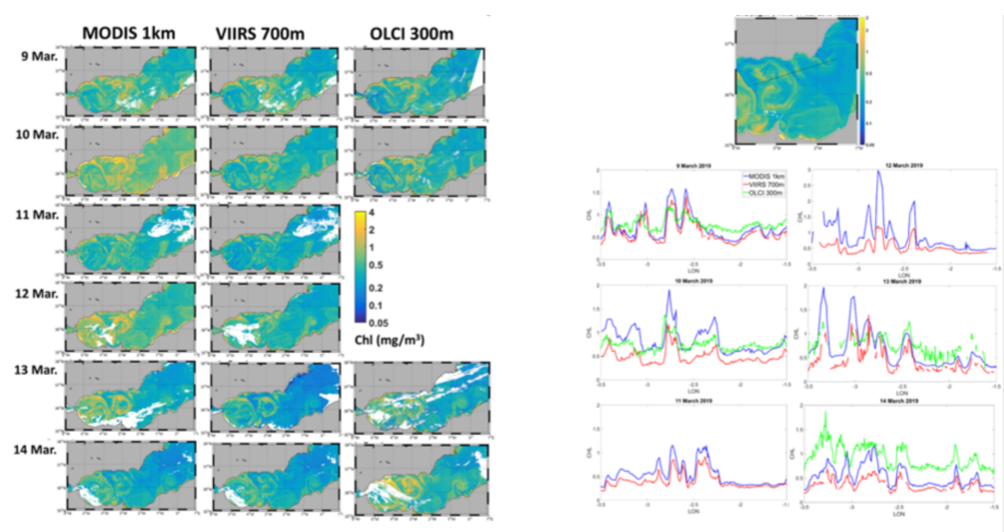


Figure 12.16: Spatio-temporal variability of the chl features in the Alboran Sea from 9 till 14 March 2019 using the multi-sensor methodology with MODIS, VIIRS, and OLCI.

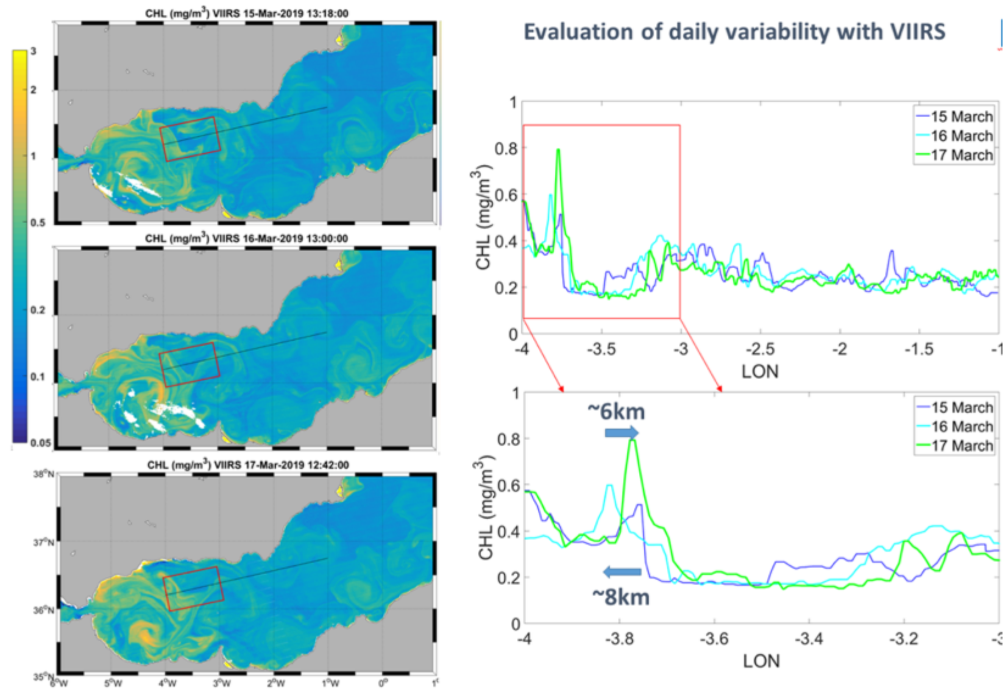


Figure 12.17: Spatio-temporal variability of the chl features in the Alboran Sea from 15 til 17 March 2019 with VIIRS datasets.

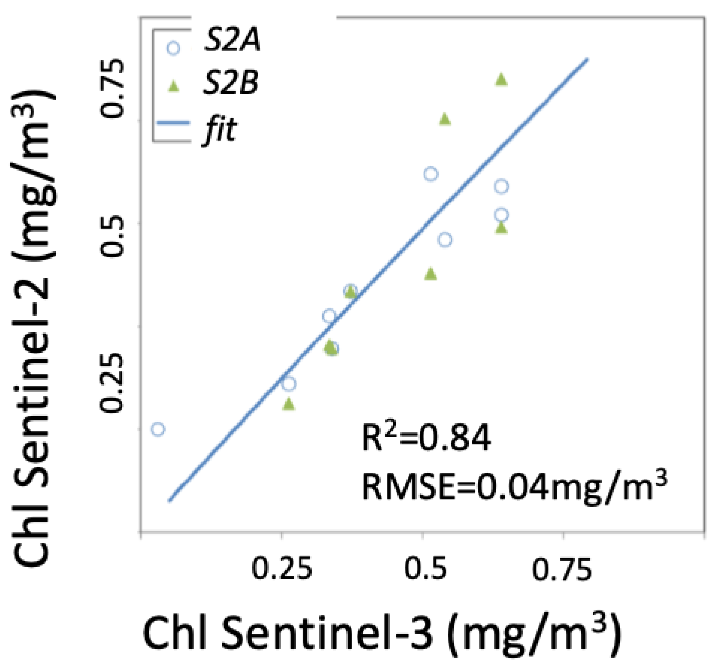


Figure 12.18: Cross-validation of chl from Sentinel-3 against Sentinel-2 during the CALYPSO 2019 campaign.

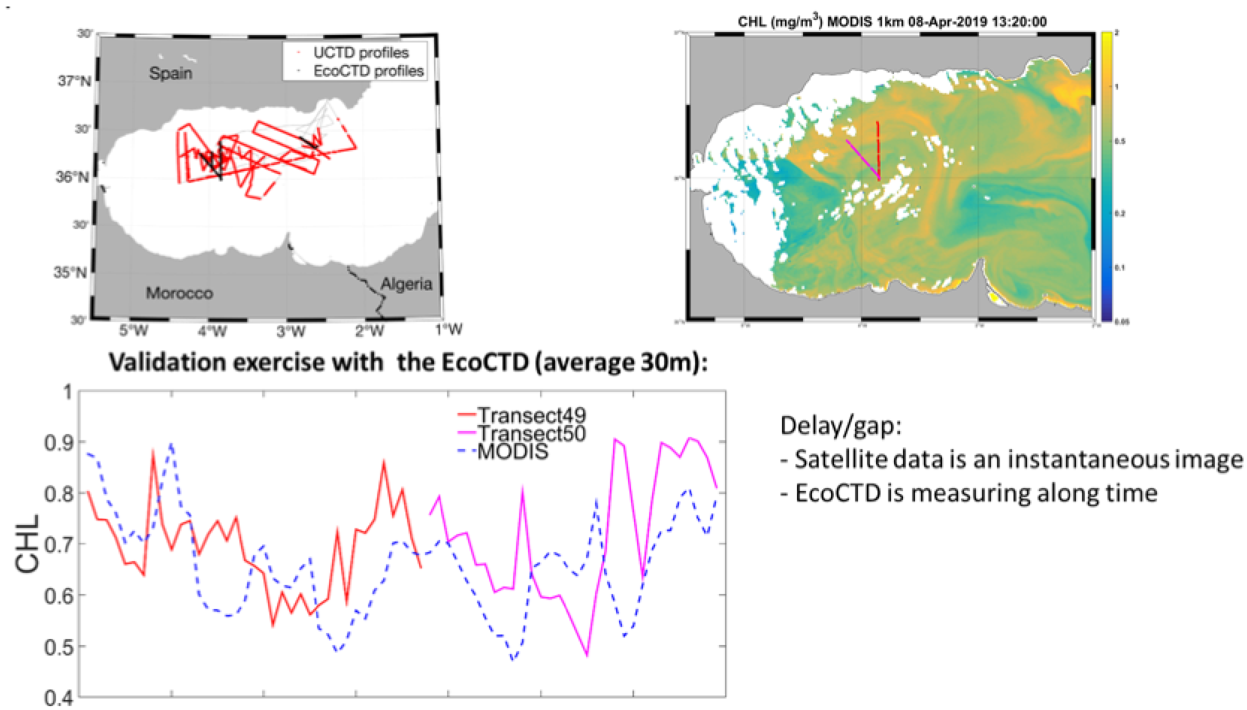


Figure 12.19: Comparison of chl from Level-3 EcoCTD and from MODIS during the CALYPSO 2019.

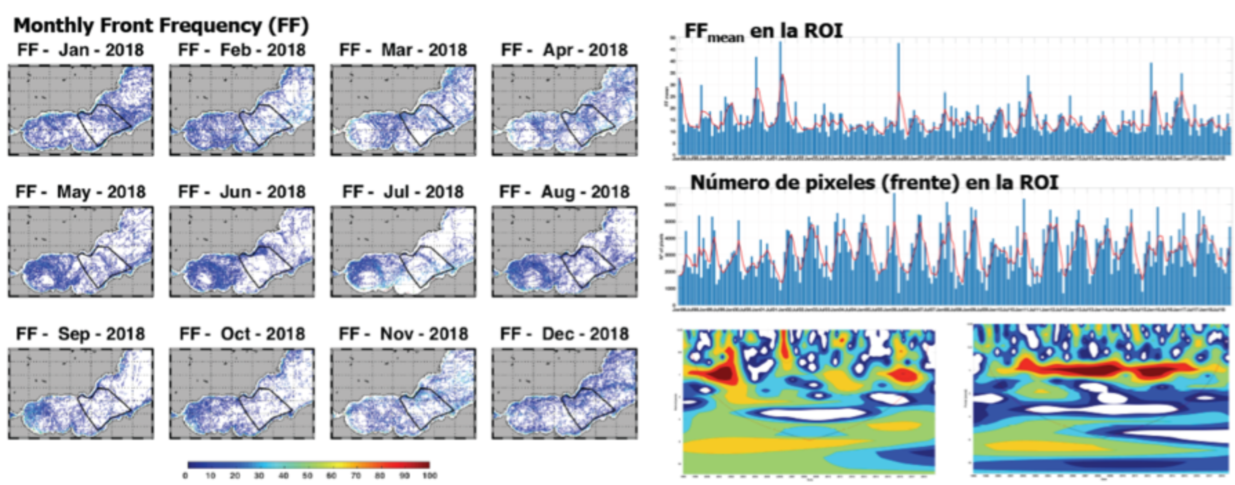


Figure 12.20: Preliminary results of the Canny algorithm in the Alborán Sea.

# Bibliography

Collins, J. R., P. D. Fucile, G. McDonald, J. E. Ossolinski, R. G. Keil, J. R. Valdes, S. C. Doney, and B. A. S. Van Mooy, An autonomous, in situ light-dark bottle device for determining community respiration and net community production, *Limnology and Oceanography: Methods*, *16*(6), 323–338, doi:10.1002/lom3.10247, 2018.

Haley, P. J., Jr., A. Agarwal, and P. F. J. Lermusiaux, Optimizing velocities and transports for complex coastal regions and archipelagos, *Ocean Modeling*, *89*, 1–28, doi:10.1016/j.ocemod.2015.02.005, 2015.

Hernandez-Lasheras, J., and B. Mourre, Dense ctd survey versus glider fleet sampling : comparing data assimilation performance in a regional ocean model west of sardinia, *Ocean Sci.*, *14*, 1069–1084, doi:10.5194/os-14-1069-2018, 2018.

Juza, M., et al., Socib operational ocean forecasting system and multi-platform validation in the western mediterranean sea, *Journal of Operational Oceanography*, *9*, s155–s166, 2016.

Kulkarni, C. S., and P. F. J. Lermusiaux, Advection without compounding errors through flow map composition, *Journal of Computational Physics*, *398*, 108,859, doi:10.1016/j.jcp.2019.108859, 2019.

Langdon, C., Determination of dissolved oxygen in seawater by Winkler titration using the amperometric technique, in *GO-SHIP repeat hydrography manual: A collection of expert reports and guidelines*, edited by E. M. Hood, C. L. Sabine, and B. M. Sloyan, IOCCP Report Number 14, ICPO Publication Series Number 134. Available online at: *http://www.go-ship.org/HydroMan.html*, 2010.

Lermusiaux, P. F. J., On the mapping of multivariate geophysical fields: Sensitivities to size, scales, and dynamics, *Journal of Atmospheric and Oceanic Technology*, *19*(10), 1602–1637, doi:10.1175/1520-0426(2002)019⟨1602:OTMOMG⟩2.0.CO;2, 2002.

Mourre, B., et al., *Assessment of high-resolution regional ocean prediction systems using muli-platform observations: illustrations in the Western Mediterranean Sea*, chap. 24, pp. 663–694, GODAE Ocean View, doi:10.17125/gov2018.ch24, 2018.

Poulain, P.-M., T. Ozgokmen, C. Guigand, G. Cristofano, and L. Centurioni, CALYPSO 2019 Experiment 28 March – 10 April 2019 R/V Pourquoi Pas? Lagrangian drifter and float deployments, *Tech. rep.*, OGS Tech. Report 2019/28 Sez. OCE 10 MAOS, 23 pp, 2019.

Prandke, H., K. Holtsch, and A. Stips, MITEC Report *Technical Note No.* ***I.96.87***, *Tech. rep.*, European Commission, Joint Research Centre, Space Applications Institute, Ispra/Italy, 2000.

Rio, M.-H., A. Pascual, P.-M. Poulain, M. Menna, B. Barceló, and J. Tintoré, Computation of a new mean dynamic topography for the mediterranean sea from model outputs, altimeter measurements and oceanographic in situ data, *Ocean Science*, *10*(4), 731–744, doi:10.5194/os-10-731-2014, 2014.

Rudnick, D. L., and J. Klinke, The Underway Conductivity–Temperature–Depth Instrument, *Journal of Atmospheric and Oceanic Technology*, *24*, 1910–1923, 2007.

Shchepetkin, A. F., and J. McWilliams, The regional oceanic modeling system (roms): a split explicit, free-surface, topography-following-coordinate oceanic model, *Ocean Modelling*, *9*, 347–404, 2005.

Utermöhl, H., Zur Vervollkommnung der quantitativen Phytoplankton-Methodik, *Mitteilungen der Internationalen Vereinigung für Theoretische und Angewandte Limnologie*, *9*, 1–38, 1958.

50272-101

| REPORT DOCUMENTATION PAGE | 1. REPORT NO. WHOI-2020-02 | 2. | 3. Recipient's Accession No. |
|---|---|---|---|

**4. Title and Subtitle**
CALYPSO 2019 Cruise Report:
Field Campaign in the Mediterranean

**5. Report Date** January 2020

**6.**

**7. Author(s)**
A. Mahadevan, E. D'Asaro, J. Allen, P. Almaraz García, E. Alou-Font, H. M. Aravind, P. Balaguer, I. Caballero, N. Calafat, A. Carbornero, B. Casas, C. Castilla, L. Centurioni, M. Conley, G. Cristofano, E. Cutolo, M. Dever, A. Enrique Navarro, F. Falcieri, M. Freilich, E. Goodwin, R. Graham, C. Guigand, B. Hodges, H. Huntley, S. Johnston, M. Lankhorst, P. Lermusiaux, I. Lizaran, C. Mirabito, A. Miralles, B. Mourre, G. Navarro, M. Ohmart, S. Ouala, T. Ozgokmen, A. Pascual, J-M. H. Pou, P.M. Poulain, A. Ren, D. Rodriguez Tarry, D. Rudnick, M. Rubio, S. Ruiz, I. Rypina, J. Tintore, U. Send, A. Shcherbina, M. Torner, G. S. Vieira, N. Wirth, and N. Zarokanellos

**8. Performing Organization Rept. No.**

**9. Performing Organization Name and Address**
Woods Hole Oceanographic Institution
Woods Hole, Massachusetts 02543

**10. Project/Task/Work Unit No.**

**11. Contract(C) or Grant(G) No.**
(C) N000141613130
(G)

**12. Sponsoring Organization Name and Address**
Office of Naval Research

**13. Type of Report & Period Covered**
Technical Report

**14.**

**15. Supplementary Notes**
This report should be cited as: Woods Hole Oceanographic Institution Technical Report, WHOI-2020-02.

**16. Abstract (Limit: 200 words)**
*This report describes a field campaign conducted in the Western Mediterranean Sea in the early Spring of 2019 as part of the ONR Departmental Research Initiative "CALYPSO" — Coherent Lagrangian Structures from the Surface Ocean to Interior. The objective of the campaign was to observe, gather evidence for, and gain a dynamical understanding of the three-dimensional transport of water from the surface to interior ocean through coherent pathways. The observations targeted density fronts as these are sites for enhanced vertical motion, but are also where the horizontal velocity is largest. Fronts formed by the salinity contrast between Atlantic, Mediterranean, and mixed waters, were identified and sampled along the edge of the Western Alboran gyre and at the periphery of a northern coastal eddy. Two research vessels were used — the N/O Pourquoi Pas?, a global class vessel, and the RV SOCIB, a research catamaran. Several autonomous platforms and ship-based instruments were deployed, including a fleet of gliders that sampled for several weeks, the ship's CTD with water sample collection for biogeochemistry, the ship's ADCP, underway, towed profiling instruments (uCTD and EcoCTD), a towed chain with CTDs, hundreds of drifters, water tracking Lagrangian floats, profiling floats, a Wirewalker, and 3 moorings. Satellite data and numerical modeling were used for guidance. The international research team consisted of scientists from multiple institutions in the United States, Spain and Italy. Measurements were facilitated by the captain and crew of the N/O Pourquoi Pas? and RV SOCIB, as well as support from the entire CALYPSO team.*

**17. Document Analysis** **a. Descriptors**

CALYPSO
Submesoscale dynamics
Western Mediterranean

**b. Identifiers/Open-Ended Terms**

**c. COSATI Field/Group**

| 18. Availability Statement | 19. Security Class (This Report) | 21. No. of Pages |
|---|---|---|
| Approved for public release; distribution unlimited. | | 120 |
| | 20. Security Class (This Page) | 22. Price |

(See ANSI-Z39.18) *See Instructions on Reverse* OPTIONAL FORM 272 (4
(Formerly NTIS-35)
Department of Commerce